Université de Montréal

Functional and Cellular studies of the form II Rubisco in the marine dinoflagellate *Gonyaulax polyedra*

par:

Nasha Nassoury

Département sciences biologiques

Faculté des arts et des sciences

Thèse présentée à la Faculté des études supérieures en vue de l'obtention du grade de doctorat en sciences biologiques

Août 2005

Université de Montréal

Faculté des études supérieures

Cette thèse intitulée:

Functional and Cellular studies of the form II Rubisco in the marine dinoflagellate *Gonyaulax polyedra*

Présentée par:

Nasha Nassoury

a été evaluée par un jury compose des personnes suivantes:

……..Jean Rivoal……..

président rapporteur

……David Morse……..……..

directeur de recherche

……Annie Angers……..

membre du jury

……Steven Schwartzbach……..

examinateur externe

…… Jean Rivoal ……..

représentant du doyen de la FES

Résumé
Études fonctionnelle et cellulaire de la forme II Rubisco chez le dinoflagellé marin *Gonyaulax polyedra*

Les dinoflagellés sont des organismes unicellulaires très particuliers. Ils représentent l'un des membres les plus importants du phytoplancton dans l'écosystème marin puisqu'ils sont à la base de la chaîne alimentaire. La plupart d'entre eux possèdent des plastes constitués par trois membranes, contrairement à ceux d'autres espèces qui n'en possèdent que deux. De plus, ils contiennent une forme II de Rubisco, une protéine clef dans la fixation du CO_2. La Rubisco dite de forme II, comme son homologue, la forme I, catalyse la première réaction de carboxylation dans le cycle de Calvin ainsi que la première réaction d'oxygénation dans la photorespiration. En conséquence, l'oxygène (O_2) est un inhibiteur compétitif de la liaison du CO_2 aux deux formes de Rubisco. À l'origine la Rubisco forme II fut décrite uniquement chez les bactéries anaérobies, d'où la nécessité d'investiguer le rôle de cette dernière dans les organelles génératrices d'oxygène. Chez *Gonyaulax* l'évolution de l'oxygène et la fixation du carbone varient selon des rythmes circadiens. La détermination des niveaux protéiques de Rubisco, de l'évolution de l'O_2 ainsi que de la fixation du CO_2 durant 48 heures indique que la fixation du carbone n'est pas due à un changement du niveau de Rubisco. Par contre, des analyses d'immunocytochimie montrent que l'activité rythmique de Rubisco se traduit par un changement de localisation à l'intérieur de l'organelle. Ces observations suggèrent que les plastes des cellules diurnes contiennent des régions de compléments protéiques différentes des cellules nocturnes. C'était la première évidence que l'activité circadienne d'une enzyme pouvait être corrélée à sa distribution dans l'organelle.

La classe des dinoflagellés à elle seule est responsable d'une grande fraction de la production primaire des océans. Il est donc crucial de comprendre comment l'organelle photosynthétique est générée et maintenue dans ces organismes. Les précurseurs protéiques des plastes sont des peptides de transit bipartites. Ils contiennent deux domaines distincts: (i) une séquence N-terminale hydrophobe, similaire aux peptides signals des protéines ciblées au réticulum endoplasmique, (ii) une région caractéristique des peptides de transition des plantes supérieures. Ainsi, le ciblage des protéines aux plastes des dinoflagellés se fait via des voies de sécrétion. J'ai démontré que le

mécanisme de ciblage protéique à la membrane tripartite des plastes dépend de leur structure et non de leur phylogénie.

Finalement, j'ai découvert une étape sensible à la Brefeldin-A (BFA) dans le rythme de fixation du carbone chez *Gonyaulax*. La BFA bloque le transport protéique à partir du Golgi et dans le cas des dinoflagellés, le transport protéique vers les plastes. Les expériences d'immunocytochimie sur des cellules traitées ou non à la BFA ont permis de démontrer que le blocage de l'importation de Rubisco nouvellement synthétisée vers les plastes perturbe la séquestration de celle-ci et par conséquent la fixation de CO_2 . Les résultats présentés dans cette thèse montrent pour la première fois l'effet de la BFA sur les dinoflagellés et soulignent l'importance de la localisation d'une enzyme dans la régulation du rythme circadien.

Abstract

Dinoflagellates are unicellular organisms with many peculiar characteristics. They are considered one of the most important members of the phytoplankton in our marine ecosystems and represent a major constituent of the food web. Most of them have plastids surrounded by three membranes (unlike other plastids normally bounded by two membranes) and posses a nuclear encoded form II Rubisco as their primary enzyme for the fixation of CO_2. The form II Rubisco, like its form I homolog, catalyzes both the first carboxylation step in the Calvin cycle and the first oxygenation step in photorespiration, and thus oxygen is a competitive inhibitor of CO_2 binding to both forms of Rubisco. The form II Rubisco has previously been reported only in anaerobic bacteria hence it was interesting to see how this so called anaerobic enzyme actually functions within oxygen generating organelles. In *Gonyaulax* both oxygen evolution and carbon fixation are bone fide circadian rhythms.

Measuring Rubisco protein levels, as well as the O_2 evolution and CO_2 fixation rates over a 48 hours period indicated that circadian rhythm in carbon fixation is not due to changes in Rubisco levels. However immunocytochemical analyses of cells showed that changes in suborganellar localization of Rubisco within each plastid could account for its rhythmic activity. These observations suggested that the plastids of day-phase cells contain regions with different protein complements compared to night-phase cells. This was the first time that the circadian activity of an enzyme had been explained by its distribution in an organelle.

Since dinoflagellates as a class are responsible for a considerable fraction of the oceans primary production, it is important to ask how the photosynthetic organelle in these organisms is generated and maintained. The precursor proteins of dinoflagellate plastids show a bipartite transit peptide with two distinct domains: an N-terminal hydrophobic sequence, which has similarities to signal sequences of ER-targeting proteins, followed by a second region with characteristics of transit peptides of higher plants. Protein targeting into dinoflagellates plastids thus occurs via the secretory pathway. Interestingly, I showed that the mechanistic requirements of protein targeting to these triple membrane-bound plastids appeared to results from their ultrastructure not their phylogeny, as the

triple membrane bound plastids of the phylogenetically distinct *Euglena* use an identical mechanism.

Lastly I demonstrated a Brefeldin-A (BFA) sensitive step in the carbon fixation rhythm of Gonyaulax. BFA blocks the protein transport from the Golgi and thus, in the case of dinoflagellates, protein import to the plastids. Immunocytochemical analyses at electron microscope level was combined by measuring the rate of CO_2 fixation of drug-treated cells and compared with normal cells. Accordingly we were able to show that blocking the import of newly synthesized Rubisco to the plastids disrupts Rubisco sequestration and consequently the ability to fix CO_2. These experiments not only represent the first report of BFA action in dinoflagellates but also underscore the importance of enzyme location in regulating circadian rhythms.

Keywords: Dinoflagellates, Photosynthesis, Circadian rhythms, Protein import, Secondary plastids, Pyrenoids , Rubisco form II, PCP, Nuclear-encoded proteins.

Table de matière

La liste des tableaux

La liste des figures

CHAPTER 1

CHAPTER 2

CHAPTER 3

CHAPTER 4

La liste des abréviations

ARF: ADP-ribosylation factor

ATPase: adenosine triphosphatase

BFA: Brefeldin A

CAO: chlorophyll a oxygenase

CCG: clock controlled gene

CCM: carbon-concentrating mecanisme

cDNA: complementary DNA

CER: chloroplast endoplasmic reticulum

CHAPS: cholamidopropyl-dimethylammonio propanesulfonate

CT: circadian time

DVM: diel vertical migration

DTT: dithiothreitol

EDTA: ethylene diamine tetra acetic

ELISA: enzyme linked immunosorbent assay

ER: endoplasmic reticulum

FITC: fluorescein isothiocyanate

GAPDH: glyceraldehyde-3-phosphate dehydrogenase

GDP: guanosine diphosphate

GEF: guanine nucleotide exchange factors

GFP: green fluorescent protein

GTP: guanosine triphosphate

GTPase: guanosine triphosphatase

h: hour

IEF: isoelectric focusing

LBP: Luciferin binding protein

LCF: luciferase

LD: Light:dark

LHCP: light-harvesting chlorophyll a/b binding protein

mM: millimolar

mL: millilitre

µm: microgram

mg: milligram

mRNA: messanger RNA

NADP: nicotinamide adenine dinucleotide phosphate

nm: nano meter

OD: optical density

PCP: peridinin-chlorophyll *a*-binding protein

PRC: phase respond curve

PlasmoAP: *Plasmodium falciparum* apicoplast-targeted proteins

PS: photosystem

RLS: rate limiting step

RNAi: RNA interference

Rubisco: Ribulose bisphosphate carboxylase/oxygenase

SDS: Sodium dodecylsulfate

SDS-PAGE: SDS polyacrylamide gel electrophoresis

SNARE: soluble NSF attachment protein receptors

SOD: Superoxide dismutase

SRP: signal recognition particle

TEM: transmission electron microscope

Tat: twin-arginine translocation

Tic: translocons for the inner chloroplast membranes

Toc: translocons for the outer chloroplast membrane

tSNARE: target soluble NSF attachment protein receptors

vO_2/vCO_2: ratio of the reaction rate (v) with O_2 as a substrate and with CO_2 as a substrate

vSNARE: vesicle soluble NSF attachment protein receptor

UTR: untranslated region

UV: ultra violet

La dédicace

I dedicate this thesis to my *mother & father,*

Kianoush

And to the memory of:

maman khorshid,

mama ka & baba ka

Les remerciements

First of all I have to thank my supervisor, *David Morse*, for his tolerance, patience, scientific and financial support during all these years. Thank you for accepting me in your lab and putting your trust in me. I can definitely say you have been one of the best teachers and mentors I have ever had and definitely you are one of the major influences in shaping my character. Thank you for being so fun to work with and for everything you have taught me.

I want to thank *Louise Pelletier* who is the person who had helped me constantly with microscopy and also is one of my best friends whom I could always depend on. *Merci beaucoup pour tous. Je ne vais jamais oublier tes gentillesses.*

Next, I have to thank my dear lab-mates, *Yunling* and *Thierry*. Dear *Yunling*, I have learned so many things from you not only scientific but also how to keep a smile when almost nothing goes right!!! You have thought me to be patient and never to let go when I believe in something. Dear *Thierry*, my graduate study memories would never be complete without you. Thank you for all the great times and laughs we had share in the lab.

I have to express my gratitude to *Dr. M. Cappodocia* and *Dr. G. Laublin* for their kindness, assistance and continuous support.

A big thank to all the students, postdoctorate fellows and the staff of IRBV for making a scientific as well as enjoyable environment to work in. *Merci et bonne chance a tous*.

Special thanks to my friend *Nadia Rabah* for her help and friendship.

My gratitude towards my dear brother *Kiarash* for his special and unique point of view about life.

I have to thank my mother and father, for their endless support and love towards me even through our physically far distance. I can never put into words my gratitude toward you two. Thank you for everything you have taught and done for me.

And mostly I have to thank my beloved husband, *Kianoush*, who had helped and supported me unconditionally during my studies. *Kianoush*, I could have never come so far without you (*tu khoobi va in hameyé étéraf-hast*).

Avant-propos

In this Ph.D. thesis, two major questions regarding the cell biology of the dinoflagellates were answered. One is the correlation between the form II Rubisco and carbon fixation rhythm and the other is the protein import pathway into the plastids of dinoflagellates. As the introduction to the thesis a literature review of both topics seemed appropriate. The first part of the introduction is a summary of our understandings of the circadian regulation underlying the circadian rhythms of *Gonyaulax*. In the second part of the introduction a complete literature review on protein targeting to the chloroplasts of photosynthetic eukaryotes is provided.

CHAPTER 1- LITTERATURE REVIEW

1.1. Biochemistry and circadian regulation of output from the *Gonyaulax* clock: Are there many clocks or simply many hands?

This part of the thesis is a chapter from a book titled *Circadian Clocks in Eukaryotic Microbes.* Ed. Kippert, Fred, Publisher: Landes Bioscience (*In Press*). ISBN: 0306482320. The chapter will be published with the title: *Biochemistry and circadian regulation of output from the Gonyaulax clock: Are there many clocks or simply many hands?*

By: Nassoury, N., J. W. Hastings, D. Morse.

In this section we tried to collect the available data on the biochemistry and the circadian regulation of *Gonyaulax* circadian rhythms.

The manuscript was reviewed and corrected by my supervisor (David Morse) and Dr. Woodland Hastings after I had written the first draft.

The unicellular protist *Gonyaulax polyedra* (now *Lingulodinium polyedrum*) is a member of the dinoflagellates (Spector 1984), a group of organisms most closely related to a group of cellular parasites known as Apicomplexans. The dinoflagellates have a variety of life-styles, including free-living, parasitic and symbiotic; while many are autotrophic, some species are heterotrophs. The majority of the autotrophs have plastids surrounded by three membranes that contain the unusual carotenoid peridinin, whose presence confers the characteristic reddish color to the algae that gave rise to their original botanical classification as the Pyrrophyta (Greek *pyrrhos*, flame-colored).

The dinoflagellates, like their apicomplexan cousins, have a series of flattened sacs termed alveoli around the cell just underneath the plasma membrane. In the armored dinoflagellates, like *Gonyaulax* (Fig. 1.1.1), the alveoli are filled with cellulosic plates, whose patterns are used for taxonomic purposes. Their outer armor has horizontal and vertical grooves, in which lie their two flagella. This orientation gives rise to a characteristic spiraling swimming movement, and their classification as dinoflagellates (Greek *dinos*, whirling). The dinoflagellates are perhaps best known for their unusual nuclear features such as permanently condensed chromosomes, absence of histones, and the fact that the nuclear membrane remains intact through mitosis. The dinoflagellate chloroplast genome is similarly unusual, with many species encoding their plastid proteins on a series of single gene minicircles (Zhang, Green et al. 1999).

Dinoflagellates have contributed considerably to an understanding of how the circadian clock controls circadian rhythms as well as to the basic principles of phase resetting common to circadian oscillators. In this chapter, we discuss the biology and biochemistry of several circadian rhythms in these algae and the molecular mechanisms whereby they are controlled by the clock.

1.1.1. Desynchronization suggests more than one oscillator

It has long been appreciated that in a given organism many different processes may exhibit circadian rhythmicity. Some authors have tabulated such rhythms (Scheving and Halberg 1980), but such lists are seemingly endless, documented to number in the hundreds for the human, so the possibility that there would be different and separate

mechanisms for regulating each seems remote. Moreover, the concept of a single "master oscillator" controlling the timing of the many different functions in an organism has always seemed attractive. In this perspective, the clock mechanism is distinct from the measured rhythms, or "hands" of the clock, and ultimately the hands could be removed without affecting operation of the underlying oscillator.

Indeed, early studies with *Gonyaulax* paved the way to this paradigm. For example, the single clock model is supported by the observation that total light emitted after stimulation to exhaustion is rhythmic and has the same period and unusual temperature coefficient (less than 1.0) as the rhythm of spontaneous luminescence (Hastings and Sweeney 1957). In addition, the biochemical components of the luminescence system are evidently not themselves part of a putative feedback loop generating the rhythm because the phase of the rhythm remained the same after the luminescent system was depleted by exhaustive stimulation (Hastings and Sweeney 1958). In another test, after photosynthetic electron transport was specifically inhibited for some hours by DCMU, the phase of the photosynthesis rhythm, which resumed after removal of the drug, was the same as in untreated cells (Hastings, Astrachan et al. 1961).

In a different approach, the relative phase angles of rhythms for four different processes were evaluated after 17 days in constant conditions (McMurry and Hastings 1972). No differences were detected, indicating that under constant conditions the periods were all the same. Two other canonical features of circadian rhythms, namely the PRC and the temperature coefficient of the period were also the same for different rhythms.

While these results were confirmed in other experiments, challenges to the paradigm emerged in the early 1990s. First, different free running periods were reported for the glow and flashing rhythms of bioluminescence (von der Heyde, Wilkens et al. 1992), and for the flashing and aggregation rhythms (Roenneberg and Morse 1993) (Fig. 1.1.2A, B). However, the conditions responsible for causing the dissociation of the different rhythms were not well established. One possibility was that the color of the light to which the culture is exposed was responsible; another relates to the method of measurement, which requires a minute of darkness every half hour. Such dark pulses do have a significant effect on the period with a white background light (Broda, Gooch et al. 1986), and might

differ for the two rhythms, which have been found to differ in sensitivity to dark pulses given in a constant dim red background light (Morse, Hastings et al. 1994).

A noteworthy feature of the experiment shown in Figure 1.1.2B is that even when the two putative oscillators are running independently they still appear to interact in a kind of transient coupling, as indicated by the temporary compromises in the periods of both rhythms (Fig. 1.1.2C). Rhythms of sleep/wake and body temperature in humans are also known to similarly dissociate and interact. This has been referred to as relative coordination (Wever 1979), and different oscillators (X and Y) have been postulated to control the two rhythms (Kronauer, Czeisler et al. 1982; Kronauer, Jewett et al. 1991).

A second type of challenge has come from studies using brief applications of nitrate, an important nutrient, to generate a phase response curve. As discussed below, *Gonyaulax* has a nightly maximum in its nitrate reduction rhythm. The addition of nitrate to nitrate-starved cells causes phase delays, and these are of different magnitudes for the two rhythms, and the two exhibit markedly different free running periods thereafter (Roenneberg and Rehman 1996). The fact that the action of nitrate can be blocked by MSX, an inhibitor of glutamine synthase, which is involved in nitrate metabolism suggests that the nitrate metabolism rhythm may indeed impact on the clock mechanism driving the rhythm.

Some evidence suggests that even more than two oscillators might be present. When the global patterns of circadian controlled protein synthesis in *Gonyaulax* are examined, it appears that they can be placed into three different groups (Fig. 1.1.3A). These correspond to the start, middle, and end of night phase (Markovic, Roenneberg et al. 1996), suggesting that three oscillators might be involved in the different rhythms, which also appear in three main groups (Fig. 1.1.3B). Some of the proteins associated with each of these three groups have now been identified and shown to be associated with specific rhythms. For example, synthesis of the luciferin binding protein falls into the early night group, at a time appropriate for initiation of the bioluminescent flashing rhythm (Morse, Fritz et al. 1990). The synthesis of the enzyme Rubisco, which catalyses a key step in carbon fixation, begins at mid-night phase, a time when *in vivo* carbon fixation rates are observed to rise (Nassoury, Fritz et al. 2001), and the onset of PCP synthesis occurs at later night phase, a time when oxygen evolution rates begin to increase. This correlation

between the temporal regulation of protein synthesis and the physiological rhythms in which the protein participates suggests that three different oscillators might regulate protein synthesis in *Gonyaulax*.

While none have yet been identified in *Gonyaulax*, clock genes and their protein components have now been identified and characterized in several other systems (Dunlap 1999; Harmer, Panda et al. 2001). The identity of the components vary, but all systems include a gene whose product feeds back to repress its own transcription. How the clock mechanism regulates its hands (i.e. the rhythms) with their different phases, is a key open question in circadian biology. In many cases this is presumed to involve clock controlled genes (CCGs), so perhaps clock gene products functioning as transcription factors might regulate CCGs directly. Interestingly, it has recently been reported that two different clock controlled genes in *Arabidopsis* are transcribed with different circadian periods in constant conditions (Michael, Salome et al. 2003). *Arabidopsis*, a model plant system where the molecular mechanisms of the clock are slowly falling into place, may thus help to understand how multiple clocks might function in regulating the different *Gonyaulax* rhythms.

1.1.2. The Several Rhythms of Gonyaulax

Among the many different rhythmic processes reported in *Gonyaulax* are three aspects of *in vivo* bioluminescence (total stimulatable emission, spontaneous flashing frequency and spontaneous glow (Hastings and Sweeney 1958; Hastings 1960)), photosynthesis (Hastings, Astrachan et al. 1961), cell aggregation (motility) (Roenneberg and Hastings 1992) and the timing of cell division (Sweeney and Hastings 1958; Homma and Hastings 1989) (Fig. 1.1.3B). In addition, several rhythms (e.g., bioluminescence, photosynthesis and cell division) have some defined biochemical component changes in which might constitute the point of regulation. A number of other biochemical components have been shown to exhibit rhythms, such as nitrate reductase (Ramalho, Hastings et al. 1995), superoxide dismutase (Colepicolo, Camarero et al. 1992) and melatonin (Pöggler, Balzer et al. 1991) without clear knowledge as to what physiological rhythms, if any, might be associated with the particular changes.

Measurements have been automated for different rhythms, including bioluminescence, aggregation and photosynthesis (Taylor, Wilson et al. 1982; Broda, Gooch et al. 1986) and some (photosynthesis and bioluminescence) have been shown to occur in single cells (Sweeney 1960; Krasnow, Dunlap et al. 1981). Single cells are models of minimal complexity where some of the complications found in multicellular organisms are absent (Roenneberg and Mittag 1996; Hastings 2001; Roenneberg and Merrow 2001), and this brings into sharp focus the cellular basis of circadian behavior.

1.1.3. Bioluminescence

Bioluminescence, the production of light from chemical energy in a living organism, is a beautiful and dazzling phenomenon. At least 30 different systems are known, widely distributed among different groups of organisms ranging phylogenetically from bacteria to fish, with most having no similarity in reaction components (Wilson and Hastings 1998). However, all involve the oxidation of a substrate (termed a luciferin) by molecular oxygen catalyzed by a luciferase enzyme specific to each system.

In the *Gonyaulax* system, the luciferin is a linear tetrapyrrole structurally related to chlorophyll (Nakamura, Kishi et al. 1989). It is highly susceptible to non-luminescent autoxidation, and is sequestered in the cell by a luciferin binding protein (LBP). The binding of luciferin is strong to LBP at a basic pH and to luciferase (LCF) at acidic pH (Morse, Pappenheimer et al. 1989). This and other considerations suggest that flashing is regulated by changes in pH.

The cellular organization of the two proteins supports this idea, as they are found together in discrete light emitting organelles termed scintillons (Johnson, Inoue et al. 1985; Desjardins and Morse 1993), which are present in the cell at night but absent during the day (Fritz, Morse et al. 1990) (Fig. 1.1.4A, B). Isolated and purified scintillons contain only LCF, luciferin and LBP, and can be stimulated to emit a flash by a drop in pH (Fogel and Hastings 1972). In the cell, scintillons are cytoplasmic protrusions into the acidic vacuole, almost completely surrounded by the vacuolar membrane (Nicolas, Nicolas et al. 1987), which conducts an action potential that triggers bioluminescence (Eckert 1965; Eckert and Sibaoka 1968). The mechanism is proposed to involve an opening of proton channels thereby decreasing the pH of the scintillon.

Bioluminescence, being easily measured, is the most extensively studied of the *Gonyaulax* rhythms (Krasnow, Dunlap et al. 1980; Hastings 2001). Light emission occurs in two different modes (Fig. 1.1.4C). Flashing, the display that is visible to the naked eye consists of brief (0.1 sec) intense (peak intensity, 10^9 quanta/sec/cell) bursts of light. These flashes appear in strip chart recording of bioluminescence as vertical lines (amplitudes are truncated by the slowness of the pen). Both spontaneous flashing and that in response to stimulation are greatest in the middle of the night phase, and the latter is believed to decrease predation by startling or diverting predators (Esaias and Curl 1972; Abrahams and Townsend 1993). Each cell typically produces spontaneously only a single flash (~10^8 quanta) per night (Krasnow, Dunlap et al. 1980).

The second mode is called glow; it consists of a low intensity emission that gradually rises to a peak (~10^4 quanta sec^{-1} $cell^{-1}$) and then declines to zero over a period of several hours at the end of the night phase. The glow cannot be detected by the eye (it is masked by flashes) but is visible as a steady change in the baseline light emission on the chart recorder trace. It is believed to result from the daily breakdown of scintillons and not to have ecological significance. The total amount of light produced each cycle from the glow is about 10^7 quanta $cell^{-1}$.

Several different kinds of measurements of luminescence have been used to follow rhythmicity. It was first measured by total stimulatable light (Sweeney and Hastings 1957). Many aliquots were dispensed and measured individually at intervals (1 to 4 hours) thereafter. Samples were stimulated mechanically for a minute by stirring or bubbling air to exhaustion, by injecting acetic acid, and the total light emitted determined, after which the sample was discarded. Total light is greatest in the middle of the night phase, and corresponds to about 10^8 quanta per cell (Seliger, Biggley et al. 1969). This may reflect the amount of luciferin bound to LBP, which has been estimated to be 2 x 10^8 molecules in night phase cells (Morse, Pappenheimer et al. 1989). The amount of luciferin (Bode, DeSa et al. 1963), the amount of LBP (Morse, Milos et al. 1989) and the number of scintillons (Fritz, Morse et al. 1990) are all rhythmic.

In measuring stimulatable light emission it was noted that light emission was exhausted more rapidly from night-phase cells than from day-phase cells. This suggests that the cells are more sensitive to stimulation during the night, which thus constitutes a rhythm

in its own right that must also be clock controlled with a separate signal transduction pathway.

Both flashes and glow occur spontaneously. The origin of spontaneous flashing is not known; it does not increase with increased surface area in the vial, where cells might collide, nor does it increase with culture density, which might increase the number of cell-to-cell collisions (Krasnow, Dunlap et al. 1980). Also, it is not less in cultures maintained on a vibration-free table. The flashing frequency (number of flashes per unit time) is greatest in the middle of the night phase. Although the traces of flashes from a night-phase culture appear very numerous, by calculation each cell emits only one flash over the course of the night. Since the flashes are distributed over a wide envelope of time, this means that the circadian time at which individual flashes occur in the different cells is very different (Krasnow, Dunlap et al. 1981).

For the glow, the timing appears to be quite precise, to within a few minutes per day (Njus, Gooch et al. 1981). Its acrophase, however, is very different from that of flashing, falling at the very end of the night phase. Since this is very close to the time when the maximum number of cell divisions occurs (see below), it was thought at first that the glow might represent a "leak" in the biochemical regulation at that time. However, later experiments definitively disproved this possibility. Using cultures of newly divided (and thus synchronized, but slow growing) cells, there were no divisions 24 hrs later but the glow peak at that time was undiminished (Homma and Hastings 1988). This clearly showed that the two phenomena are unlinked. It is postulated that the glow derives from a breakdown of the scintillons, whereby the biochemical components are released into the acidic vacuole.

Flashing and total light both involve LCF and their rhythms are phased similarly, but their signal transduction pathways from the clock may be very different. The rhythm of total stimulatable light emitted is much more directly linked to the bioluminescence biochemistry, as it correlates with the number of scintillons (Fig. 1.1.4D, E), which varies ten-fold each cycle (Fritz, Morse et al. 1990). Since scintillons contain LBP and LCF, it is not surprising that the cellular levels of each protein also change ten-fold between day and night (Dunlap and Hastings 1981; Johnson, Roeber et al. 1984; Morse, Milos et al. 1989).

This daily rhythm of LBP has been extensively studied, and LBP synthesis *in vivo* increases over 50 fold for several hours at the start of the night phase (Fig. 1.1.4D), resulting in rising LBP levels (Fig. 1.1.4E) (Morse, Milos et al. 1989). LCF abundance also exhibits a robust rhythm, and the control of both is clearly at a translational level, as the amount of mRNA is constant over a 24h period (Morse, Milos et al. 1989; Mittag, Li et al. 1998). However, their lifetimes 12 hours or longer (Rossini, Taylor et al. 2003), and compartmental or structural changes over time could alter the ability of the message to be translated. The *in vitro* synthesis rates in a heterologous (rabbit reticulocyte) system are the same with *lbp* mRNAs isolated at different time points, indicating that a cytoplasmic activator or repressor is involved in the translation of *lbp* mRNA.

To investigate this, the complete *lbp* cDNA, including the 5′ and 3′ UTRs, was cloned and sequenced (Lee, Mittag et al. 1993). Mobility shift assays were used to look for protein factor(s) binding to the untranslated regions (UTRs) of the mRNA. No proteins were found to bind the 5' UTR, but a protein was detected in *Gonyaulax* extracts that binds specifically to a 22 nucleotide region of the *lbp*3′ UTR containing seven U(U)G repeats (Fig. 1.1.5). The binding activity of the ~45 kDa dimeric protein cycles on a daily basis and is greatest during the day phase (Mittag, Lee et al. 1994), suggesting that it may function as a clock-controlled repressor preventing the translation of *lbp* mRNA during the day. This might be expected to act at the level of initiation, and thus involve the 5' region of the message. Indeed, differential translational initiation of *lbp* mRNA appears to occur due to an open reading frame in the 5' UTR (Mittag, Eckerskorn et al. 1997). Although the distinctive UG repeat has not been found in genes coding for any other *Gonyaulax* clock-controlled proteins sequenced to date, including LCF, a protein from *Chlamydomonas* that binds to this sequence has been isolated and characterized (Mittag 1996; Zhao, Schneid et al. 2004), suggesting that it has a more universal occurrence.

If the bioluminescent glow derives from the degradation of scintillons, its rhythm must also involve signal from the clock mechanism different from that for flashing. Scintillon breakdown has not yet been visualized at the ultrastructural level, although the formation of scintillons can be observed as small protein aggregates that originate in the Golgi area as a dense material and migrate towards the cell periphery to form an association with the vacuolar membrane (Nicolas, Morse et al. 1991).

1.1.4. Rhythms in Photosynthesis and Chloroplast Ultrastructure

Photosynthesis is arguably the most important biological process on earth. The liberation of oxygen, which is highly reactive, and the accumulation of it and organic compounds resulting from reduction of carbon dioxide, were both key in evolution and the development of aerobic metabolism. Its optimization in all respects, including temporal, can be viewed as a feature selected for in evolution.

The chloroplasts in *Gonyaulax* experience daily changes in shape, position in the cell, and in biochemistry. Like most dinoflagellate plastids, they are surrounded by three membranes instead of the usual two or four (Gibbs 1981), and containing the unusual carotenoid peridinin (Raven 1970; Jeffrey, Seilicki et al. 1975). They are more or less oriented radially and are up to 50% longer in day than in night phase cells (Rensing, Taylor et al. 1980). Night phase plastids are more central and form pyrenoids, characterized by the presence of widely separated thylakoid stacks (Schmitter 1971; Herman and Sweeney 1975; Rensing, Taylor et al. 1980).

Both oxygen evolution(Sweeney 1960) and carbon fixation (Hastings, Astrachan et al. 1961) are rhythmic in *Gonyaulax* (Fig. 1.1.6 A, B). It is clear that the release of O_2 following removal of electrons from water requires absorption of light energy by photosystem II (PSII). The carotenoid peridinin, used to capture solar energy in the blue-green range of the spectrum, is found mostly bound to a unique soluble light-harvesting peridinin-chlorophyll *a*-protein (PCP) which has no similarity to other light harvesting proteins (Norris and Miller 1994; Hofmann, Wrench et al. 1996; Le, Markovic et al. 1997). The soluble PCP is found inside the thylakoids of chloroplasts (Fig. 1.1.6C), where it feeds energy primarily into PSII (Govindjee, Wong et al. 1979). PCP was originally thought to be involved in the O_2 evolution rhythm because alterations of electron flux through PSII correlate with the rhythm, but PCP levels do not change appreciably over the daily cycle(Le, Jovine et al. 2001) suggesting the rhythm be caused by another factor, such as changes in the molecular organization of PSII complexes (Knoetzel and Rensing 1990).

It is interesting, in light of the above, that the synthesis of PCP *in vivo* is circadian regulated, with its acrophase the same as that of the rhythm of oxygen evolution (Fig.

1.1.6A) (Markovic, Roenneberg et al. 1996; Le, Jovine et al. 2001). This control of protein synthesis rate also occurs at the translational level, as PCP mRNA levels do not vary over the cycle (Le, Jovine et al. 2001). It is possible that a positive cis-acting translation factor functions in mediating clock control of PCP synthesis, as no protein can be produced from PCP mRNA in heterologous systems *in vitro*. Translational control is a recurring theme in *Gonyaulax* (Milos, Morse et al. 1990).

Increased O_2 evolution in day phase cells is accompanied by an increase in reactive oxygen species such as superoxide anion $O_2^{\cdot-}$ derived from the single electron reduction of oxygen by PSII. Superoxide dismutase (SOD) protects against $O_2^{\cdot-}$ so it is thus not surprising that the amount and activity of a plastid SOD isoform changes over the circadian cycle by almost four-fold in *Gonyaulax*, also regulated translationally (Okamoto, Robertson et al. 2001).

Progress has been made in understanding the mechanism of circadian CO_2 fixation. The rate-limiting step is catalyzed by the enzyme ribulose-1, 5-bisphosphate carboxylase/oxygenase (Rubisco) in all organisms (Hartman and Harpel 1994), so it is a likely candidate for clock control. Rubisco can bind both O_2 and CO_2 with O_2 acting as a competitive inhibitor of CO_2, and resulting in photorespiration, whereby the algae oxidize sugars instead of fixing carbon. This phenomenon is prominent in dinoflagellates containing type II Rubisco, which is much more oxygen sensitive than type I (Morse, Salois et al. 1995; Rowan, Whitney et al. 1996; Whitney and Andrews 1998), and prior to its discovery in dinoflagellates, had been found only in anaerobic bacteria. Cyanobacteria engineered to express only a form II Rubisco grow poorly (Pierce, Carlson et al. 1989), and it is still not clear why this relatively inefficient form of the enzyme has been evolutionarily conserved by dinoflagellates.

The circadian control over CO_2 fixation is not due to changes in the amount of the Rubisco enzyme (Bush and Sweeney 1972; Nassoury, Fritz et al. 2001). However, there are changes in the sub-organellar distribution of Rubisco correlated with the rhythm. When CO_2 fixation rates are low, Rubisco is distributed uniformly over the chloroplast stroma; when high, it is found only in pyrenoids (Fig. 1.1.6D, E) (Nassoury, Fritz et al. 2001). The increased spacing between thylakoid membranes also reduces the relative amount of PCP in the pyrenoid making it a region specialized for CO_2 fixation not O_2

evolution. A lower rate of oxygen evolution in the pyrenoid should allow CO_2 to compete more efficiently for the active site of Rubisco.

It is not known how Rubisco moves from the peripheral regions of the plastid to the regions of the pyrenoid, or what maintains this sequestration of the enzyme. However, it is interesting that the circadian rhythm of bioluminescence in the dinoflagellate *Pyrocystis lunula* is associated with the movement of the luminous organelles from one cellular location to another (Widder and Case 1982). This movement appears to require the actin cytoskeleton, as does movement of the chloroplasts (McDougall 2002).

It is striking that CO_2 fixation and O_2 evolution rhythms have different acrophases in cells kept in constant light, with maximum carbon fixation rates preceding maximum oxygen evolution by almost 6 hours (Fig. 1.1.6A, B). This suggests that in the normal light-dark cycles, carbon fixation may begin in the dark before oxygen can be generated at all. It also suggests that the two rhythms may be regulated by different clock mechanisms (Nassoury, Fritz et al. 2001). It is thus interesting to note that the changes in Rubisco synthesis rates *in vivo* track the CO_2 fixation rhythm, while PCP synthesis parallels the O_2 evolution rhythm (Fig. 1.1.6A, B). As was found for PCP, Rubisco synthesis is also under translational control in *Gonyaulax* (Hollnagel, Pinto et al. 2002).

1.1.5. Swimming Behavior and Nitrate Reduction

Motility is virtually always rhythmic in motile organisms having circadian clocks. In *Gonyaulax* this is exhibited in its swimming behavior and is complex. As mentioned above, the period of this rhythm may differ under certain conditions by several hours from that of the bioluminescence flashing rhythm (Roenneberg and Morse 1993), implicating a different cellular clock as its driving mechanism.

In culture flasks or dishes, the cells form patterns at and below the surface during the day phase (Fig. 1.1.7A) and then sink down to form a lawn at the bottom of the flasks at night (Roenneberg, Colfax et al. 1989). The patterns formed during the day depend on several factors, including the shape of the container and cell density as well as the direction and intensity of the light source (Roenneberg and Hastings 1992).

This rhythm is related to diel vertical migration (DVM) in the water column, where cells rise toward the surface near the end of the night and sink down 10 meters or more several

hours before dusk (Fig. 1.1.7B) (Eppley, Holm-Hansen et al. 1968; Gliwicz 1986). DVM may be physiologically important in the ocean since nitrate is generally depleted near the surface, where temperature and light intensity are higher (Heaney and Eppley 1981; Roenneberg and Foster 1997). DVM thus allows for nitrate uptake during the night and photosynthesis during the day.

In the laboratory, regulation of the DVM has a circadian component but is also dependent on both phototaxis and gravitaxis. During subjective day, *Gonyaulax* exhibits positive phototaxis to medium intensity light and negative phototaxis to high intensity (Eppley, Holm-Hansen et al. 1968; Roenneberg and Hastings 1992), while a uniformly negative phototaxis occurs during night phase. This presumably allows the algae in nature to find a preferred level of daytime illumination by regulating their position in the water column (Heaney and Eppley 1981). However, *Gonyaulax* also have a negative gravitaxis during the day (i.e., they move toward the surface) that is absent during the night. Changes in the buoyant density of cells could also be involved in the movement of the cells over such large distances.

Both experimental and theoretical studies suggest that nitrate also plays a role in regulating the DVM (Cullen and Horrigan 1981; Heaney and Eppley 1981; Yamazaki and Kamykowski 2000). In nitrate-depleted media, cells descend earlier during the day than do nitrogen sufficient cells (Heaney and Eppley 1981), a result that may be due to its action in shortening of the circadian period (Sweeney and Folli 1984). In fact, application of nitrate to nitrate-starved cells at the time of the night-to-day transition provokes a phase delay in their ascent (Roenneberg and Rehman 1996). These observations suggest that algae encountering a high nitrate concentration late at night would delay their vertical rise in the water column. This delay could allow the algae to balance their need for reduced nitrogen with their need for photosynthate. Experimentally, cells starved for nitrate also tend to descend faster in the water column, thereby extending the duration of their exposure to higher nitrate levels.

NR activity in *Gonyaulax* is circadian, with peaks of both activity and protein at midday (Ramalho, Hastings et al. 1995; Fritz, Stringher et al. 1996). Furthermore, immunological studies show that the *Gonyaulax* enzyme is localized in the chloroplasts (Fritz, Stringher et al. 1996) where photosynthesis takes place. However, as nitrate concentrations are

often low at or near the surface, *Gonyaulax* must also be able to use stored photosynthate as an energy source. In support of this, several studies suggest that nitrate assimilation can occur in darkness (Harrison 1976; Heaney and Eppley 1981; Paasche, Bryceson et al. 1984). *Gonyaulax* thus has a specialized circadian biochemistry that favors nitrate metabolism during the day phase, yet a circadian behavior that allows the cells to encounter nitrate at higher concentrations during the night.

1.1.6. Cell division

G. polyedra is reported to have roughly 200 pg of DNA per nucleus (Holm-Hansen 1969), which is 40 times that of the human nucleus. The nuclear envelope does not break down during mitosis, and the spindle traverses the nucleus in a membrane-bound conduit (Triemer and Fritz 1984; Perret, Davoust et al. 1993). The attachment between chromosomes and the spindle is thus facilitated by or traverses the nuclear envelope. Nonetheless, *Gonyaulax* appears to have a typical eukaryotic cell cycle with G1, S, G2 and M phases (Homma and Hastings 1989; Homma and Hastings 1989).

Cell division in *Gonyaulax* exhibits a circadian rhythm with an acrophase about an hour after light onset in a 12:12 light-dark cycle. Mother and daughter cells remain attached for about an hour after mitosis (Fig. 1.1.8 inset, top), allowing a rhythm to be measured in the number of "pairs" (Fig. 1.1.8, left ordinate). As a consequence of the rhythm, the cell number exhibits a staircase-like pattern with time (Fig. 1.1.8, right ordinate). This rhythm is entrainable and can be phase shifted by light; it persists in constant light with a temperature-overcompensated period similar to other *Gonyaulax* rhythms (Sweeney and Hastings 1958). In the one study reported it failed to dissociate from the other rhythms (McMurry and Hastings 1972).

Since the doubling time is 2 to 3 days, cell division does not occur for every cell every dawn. Mitosis is thus said to be "gated" by the circadian clock. It is as if the clock opens a window of opportunity for mitosis at dawn, during which those cells that are of a sufficient size and DNA content can divide. It is likely that clock control is exerted at the G1/S transition rather than at the G2/M transition (Homma and Hastings 1989; Homma and Hastings 1989). In *Gonyaulax*, a roughly 4 hour S phase starts roughly 12 hours before M phase (Homma and Hastings 1989), suggesting that the length of G2 will be

constant. This has been confirmed in *Amphidinium*, where adverse growth conditions lengthen only the amount of time spent in G1(Olson and Chisholm 1986).
There may be a strong evolutionary force for phasing DNA replication to occur during the dark, where damage due to ultraviolet radiation may be avoided. This hypothesis, termed "escape from light" (Pittendrigh 1993), receives support from the fact that DNA replication and cell division take place at night in many microorganisms with a near 24-h cell division cycle (Edmunds 1984). It has also been shown that in *Chlamydomonas*, which is known to have a clock-controlled cell division cycle, the light sensitivity is not only rhythmic but also in phase with the times in which S/G2 is expected to occur (Nikaido and Johnson 2000). However, in some dinoflagellates, the acrophase of the cell division rhythm differs (Sweeney and Hastings 1961); for *Prorocentrum micans* it is in the middle of the day phase, so the explanation of light avoidance is not applicable in all cases.

1.1.7. Circadian regulation of transcription and translation

The molecular nature of the putative core oscillator may be elucidated by knowledge of how it controls an "output" system, which may involve the regulation of gene expression at transcriptional, translational or post-translational levels (Loros and Dunlap 1991; Dunlap 1993; Friesen, Block et al. 1993; Takahashi, Kornhauser et al. 1993). For many overt rhythms it is difficult to specify the biochemical identity of clock controlled component(s), but in *Gonyaulax,* the synthesis rates of enzymes that catalyze the rate limiting steps of various reactions appear to be direct targets of the circadian clock. As described above, this occurs for enzymes in photosynthesis and bioluminescence rhythms, but what about the patterns of synthesis for proteins more generally?
In fact, it appears that circadian regulation of a large number of proteins in *Gonyaulax* occurs at the translational level. Pulse labeling of *Gonyaulax* proteins at times 12 hours apart, followed by 2D gel analysis, showed that many are preferentially synthesized at one phase or the other, and regulated translationally (Milos, Morse et al. 1990). Determined at more frequent time points (Markovic, Roenneberg et al. 1996), ten of these were found to fall into three time frames, with about tenfold differences from peak to trough; three of these are shown in Fig. 1.1.3. But while their synthesis rates are strongly

circadian controlled, the cellular concentrations of some of the proteins do not exhibit pronounced rhythms, such as glyceraldehyde-3-phosphate dehydrogenase (Fig. 1.1.9A). These observations are explicable if the protein has a long turnover time, as in this case the daily pulse of synthesis would add to the total cellular content of the protein by only a few percent (Fig. 1.1.9B) (Fagan, Morse et al. 1999).

Transcriptional control is a predominant theme for circadian regulation in both models and experimental results (Dunlap 1999; Harmer, Panda et al. 2001). The advent of the microarray technique provided the opportunity to search for such possibilities on a global scale in dinoflagellates. This was carried out with a different dinoflagellate, *Pyrocystis lunula*, whose luminescence is also circadian controlled (Colepicolo, Roenneberg et al. 1993). About 3,500 cDNAs were prepared and used to compare the abundance of transcripts at circadian times separated by 12 hours (Okamoto and Hastings 2003). Using ratios of ≥ 2 or ≤ 0.5 as a cutoff, about 3% of the genes screened were identified as circadian-controlled, and appeared to fall in a distinct class, rather than in the tail of a normal distribution (Fig. 1.1.10). More than 50% of these could be identified with diverse known genes. Light exposures at times expected to induce phase shifts in the rhythm revealed 30 differentially expressed genes, including some potentially participating in photic entrainment and others in pathways connecting a central oscillator to output rhythms. Five genes, which may represent core clock genes, appeared in both screens but there were no similarities with clock genes from other organisms.

Circadian control may also occur at the post-translational level (Edery, Zwiebel et al. 1994). Translocation and compartmentalization may be involved (Fritz, Milos et al. 1991; Techel, Chuang et al. 1996). In *P. lunula*, it has been shown that the luciferase is not synthesized and destroyed each day (Knaust, Urbig et al. 1998), and its message is not circadian (Okamoto and Hastings 2003). Instead, it is inactivated in day phase by translocatation to a different cellular compartment where it is no longer coupled to the flash generation mechanism (Widder and Case 1982; Widder and Case 1982; McDougall 2002). The circadian control must therefore be mediated via protein(s) different from those involved in the *Gonyaulax* regulation, which underscores the diversity of mechanisms, even within a narrow phylogenetic group.

1.1.8. Conclusion

It is difficult to escape the conclusion that a model with a single master biochemical oscillator is inadequate to explain many aspects and features of the many different rhythms in *Gonyaulax*. At the same time, it is not reasonable to suggest that each different rhythm has a separate driving oscillator. Indeed, different rhythms evidently interact in a kind of coupling, as illustrated in Figure 1.1.2.C for the flashing and aggregation rhythms, where a compromise phase is adopted transiently before each rhythm continues with a separate period. One of the key questions concerns how a cellular oscillatory mechanism can give rise to two (or more?) different periods for different clock-controlled processes, analogous perhaps to a clutch mechanism with different slippage for different processes. Continuing with the analogy, signal transduction pathways for different processes may be viewed as clutches. The several rhythms in *Gonyaulax*, especially those of bioluminescence and carbon fixation, provide systems where answers to these questions may be forthcoming in future investigations.

Figure 1.1.1. The unicellular protist *Gonyaulax*

(A) Scanning electron micrograph of a *Gonyaulax* cell (Photo courtesy of N. Nassoury). (B) Transmission electron micrograph (TEM) of day phase *Gonyaulax*. (C) TEM of night phase *Gonyaulax*. Scale bars one micron. TEMs reprinted from Fritz L, Morse D, Hastings JW. The circadian bioluminescence rhythm of *Gonyaulax* is related to daily variations in the number of light-emitting organelles. J Cell Sci 1990;95:321-8.

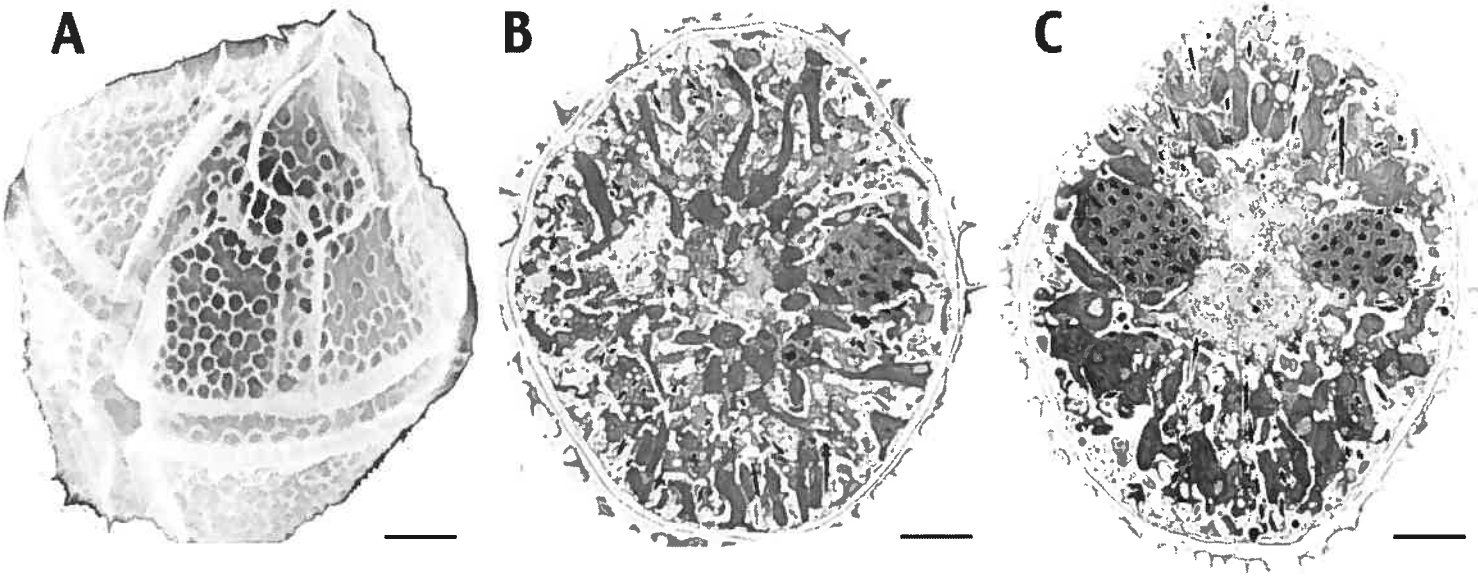
A
B
C

Figure 1.1.2. Evidence for several clocks

(A) The acrophases for flashing (squares) and glow (circles) rhythms in a culture maintained in constant dim light for two weeks. The free-running period of the glow rhythm is shorter than that of the flashing rhythm in this experiment. Data redrawn from (von der Heyde, Wilkens et al. 1992). (B) Acrophases of bioluminescent flashing (squares) and cell aggregation (circles) rhythms in a culture kept in constant dim red light. The period of the flashing rhythm is somewhat greater than 24 hours and that for the aggregation rhythm much shorter than 24 hours. (C) Period changes indicative of relative coordination during the course of the experiment shown in (B), analyzed by calculating the spectral analysis for 4-day windows across the time series of the unsmoothed data. Data for B and C redrawn from (Roenneberg and Morse 1993).

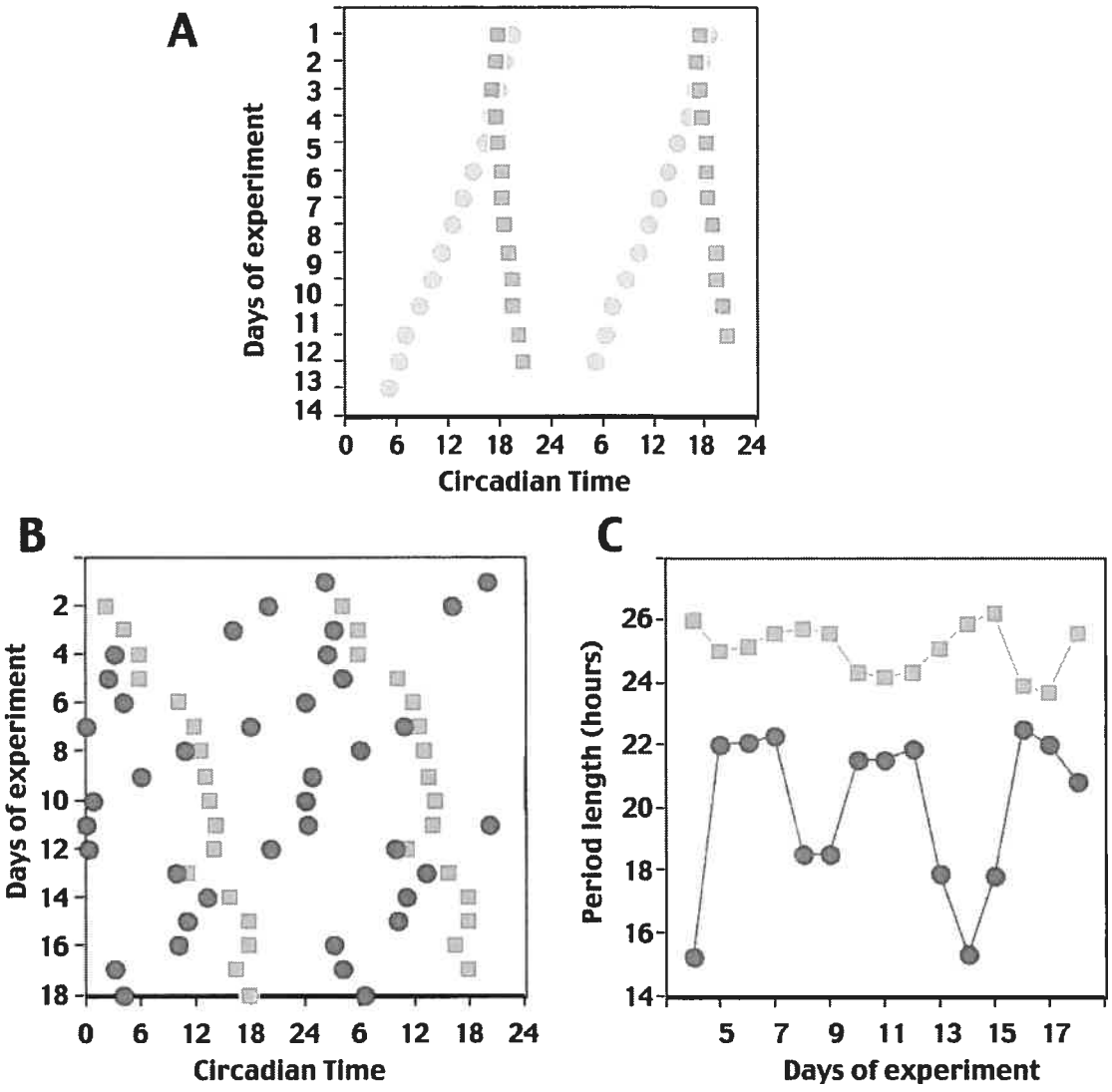
A
Days of experiment
1
2
3
4
5
6
7
8
9
10
11
12
13
14
0 6 12 18 24 6 12 18 24
Circadian Time
B
Days of experiment
2
4
6
8
10
12
14
16
18
0 6 12 18 24 6 12 18 24
Circadian Time
C
Period length (hours)
26
24
22
20
18
16
14
5 7 9 11 13 15 17
Days of experiment

Figure 1.1.3. Three different phases of physiological rhythms and circadian protein synthesis.

(A) *In vivo* labeling of proteins and 2D PAGE analysis shows there are three principal phases of protein synthesis: those involved in bioluminescence (such as LBP), those involved in photosynthetic CO_2 fixation (such as ribulose 1,5-biphosphate carboxylase) and those involved in photosynthetic O_2 evolution (such as peridinin-chlorophyll-a-binding protein). Data redrawn from (Markovic, Roenneberg et al. 1996). (B) The three main acrophases of physiological rhythms are those peaking near the dark to light transition (CO_2 fixation, luminescent glow and cell division), those peaking during mid-day (photosynthetic O_2 evolution) and those peaking during mid-night (bioluminescence).

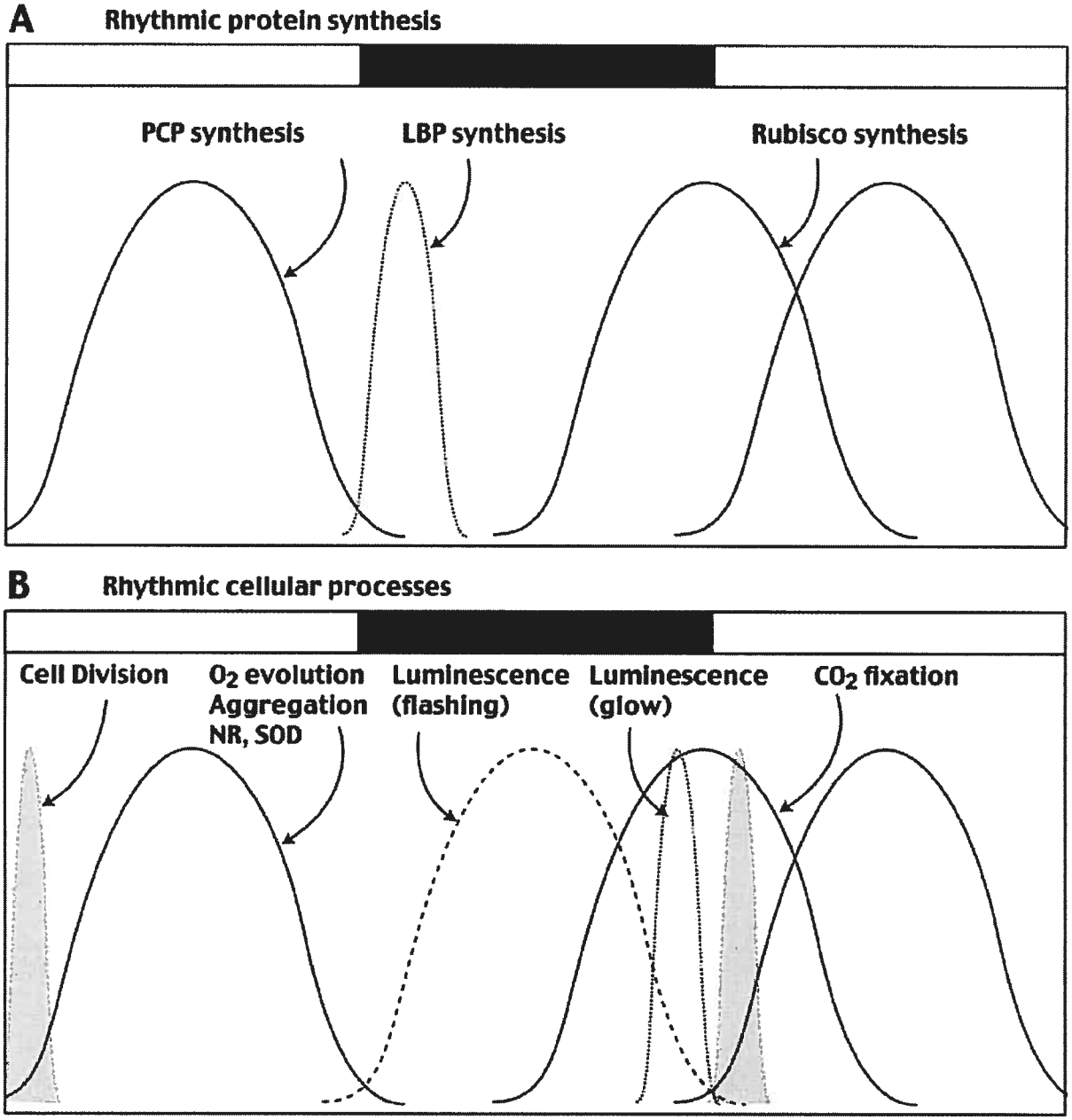
A
Rhythmic protein synthesis
PCP synthesis
LBP synthesis
Rubisco synthesis
B
Rhythmic cellular processes
Cell Division
O_2 evolution
Aggregation
NR, SOD
Luminescence
(flashing)
Luminescence
(glow)
CO_2 fixation

Figure 1.1.4. Bioluminescence

(A) and (B) Fluorescence micrographs of single night and day phase cells, respectively, showing that the scintillons (the bioluminescence organelles) are much more abundant at night. Data redrawn from (Morse, Fritz et al. 1990). (C) Chart recording of spontaneous luminescence from a culture in DD. The vertical lines result from brief and bright flashes, while the glow is seen as changes in baseline light emission. Night and day phases based on prior light dark cycle indicated above by dark (night) and light bars. (D) Circadian changes in bioluminescence capacity and rate of synthesis of LBP and (E) cellular levels of LBP and number of scintillons. Cultures maintained in LL, with night and day phases indicated above D. Data redrawn from (Morse, Milos et al. 1989; Fritz, Morse et al. 1990).

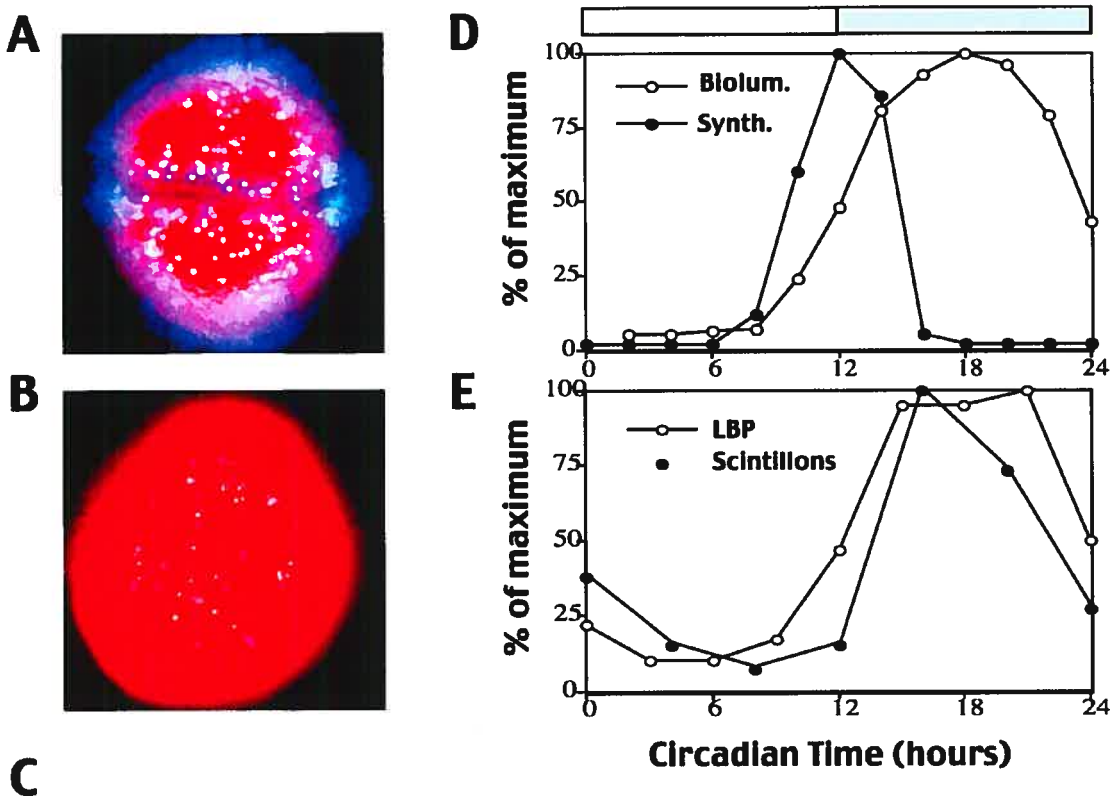
A
B
C
D
E
Bioium.
Synth.
% of maximum
100
75
50
25
0
0
6
12
18
24
LBP
Scintillions
% of maximum
Circadian Time (hours)

Figure 1.1.5. *Gonyaulax* proteins bind the 3'UTR of LBP RNA

A schematic view of LBP mRNA shows a 22-nucleotide region rich in UG in the 3'UTR. The electrophoretic mobility of this UG-rich region (inset, lane 1) can be reduced by binding to proteins extracted from *Gonyaulax* (inset, lane 2). Data reprinted from Mittag M, Lee D-H, Hastings JW. Circadian expression of the luciferin-binding protein correlates with the binding of a protein to the 3' untranslated region of its mRNA. Proc. Natl. Acad. Sci. USA 1994;91:5257-5261.

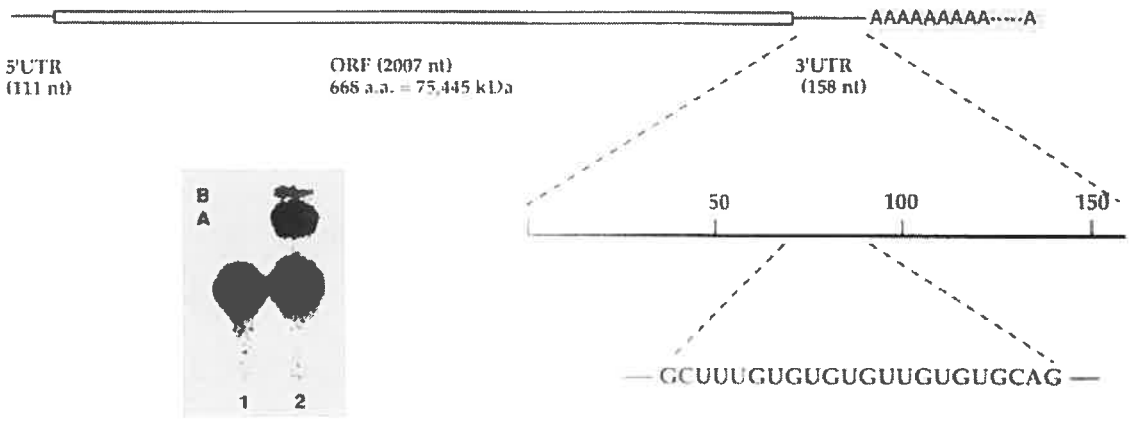
AAAAAAAAA·····A
5'UTR
(111 nt)
ORF (2007 nt)
668 a.a. = 75,445 kDa
3'UTR
(158 nt)
50
100
150
— GCUUUGUGUGUGUUGUGUGCAG —
B
A
1
2

Figure 1.1.6. Photosynthesis

(A) Circadian changes in rates of oxygen evolution and *in vivo* synthesis rates for the light harvesting protein PCP in cultures maintained in constant light and temperature (B) Circadian changes in rates of carbon fixation and the synthesis of Rubisco, showing that the acrophase of the rhythm occurs about six hours earlier than for oxygen evolution. (C) A schema of a thylakoid membrane inside the chloroplast, showing Rubisco located in the stroma and PCP inside the thylakoid lumen. (D) An immunofluorescence labeling study of cells that fix carbon well stained with either anti-Rubisco (left) or anti-PCP (right). The bulk of the PCP is near the cell periphery while the bulk of the Rubisco is nearer the cell center. (E) An immunofluorescence labeling study of cells that fix carbon poorly stained with either anti-Rubisco (left) or anti-PCP (right). Both proteins are distributed evenly throughout the plastids. Data redrawn from (Markovic, Roenneberg et al. 1996; Nassoury, Fritz et al. 2001). (Photos in D, E courtesy L. Fritz)

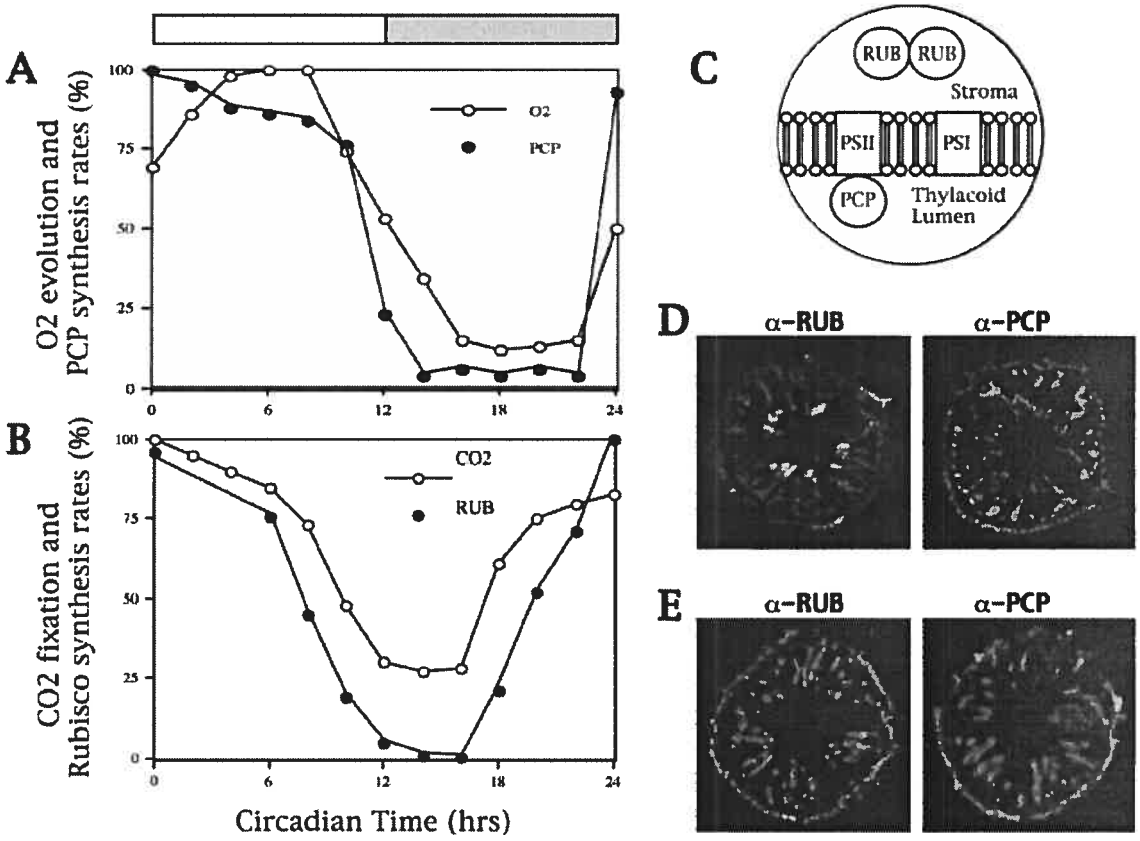
A
O2 evolution and PCP synthesis rates (%)
O2
PCP
B
CO2 fixation and Rubisco synthesis rates (%)
CO2
RUB
Circadian Time (hrs)
C
RUB
RUB
Stroma
PSII
PSI
PCP
Thylacoid Lumen
D
α-RUB
α-PCP
E
α-RUB
α-PCP

Figure 1.1.7. Cell motility

(A) Cells growing in a Petri plate photographed during the day phase showing a characteristic ribbon pattern of swimming cells. (Photo courtesy T. Roenneberg) (B) The distribution of *Gonyaulax* cells over the day (LD 12:12; dark bars night) in a 2 meter-deep laboratory vessel (vertical scale). In the ocean, these vertical movements may take place over a 10 m range. Data is redrawn from (Heaney and Eppley 1981).

A

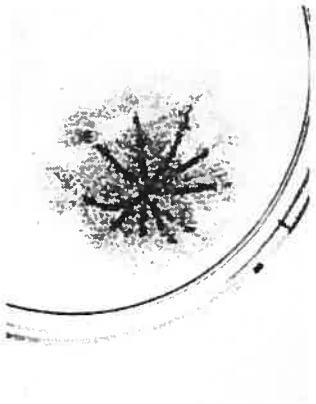

B

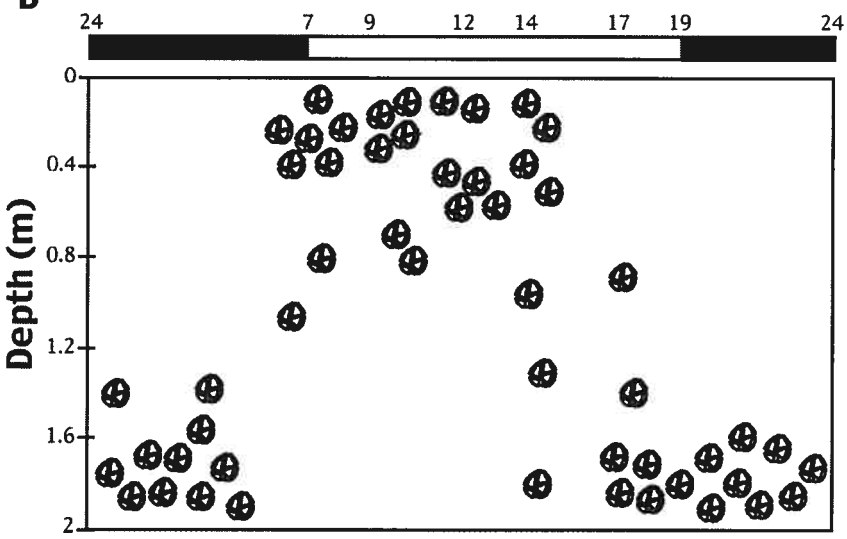

Figure 1.1.8. Cell Division

The number of cells undergoing division, as measured by paired cells (left ordinate, solid circles), exhibits a rhythm gated by the circadian clock to occur at roughly an hour after subjective dawn in *Gonyaulax*. The number of cells in the population (right ordinate, open circles) increased only by about 30% at each step, as individual cells take up to three days to double their mass. Data redrawn and extrapolated from (Sweeney and Hastings 1958). An inset at the top of the graph shows at the same magnification the large pre-mitotic cells (lower left), the paired cells characteristic of cell division (top), and the smaller post-mitotic daughter cells (lower right).

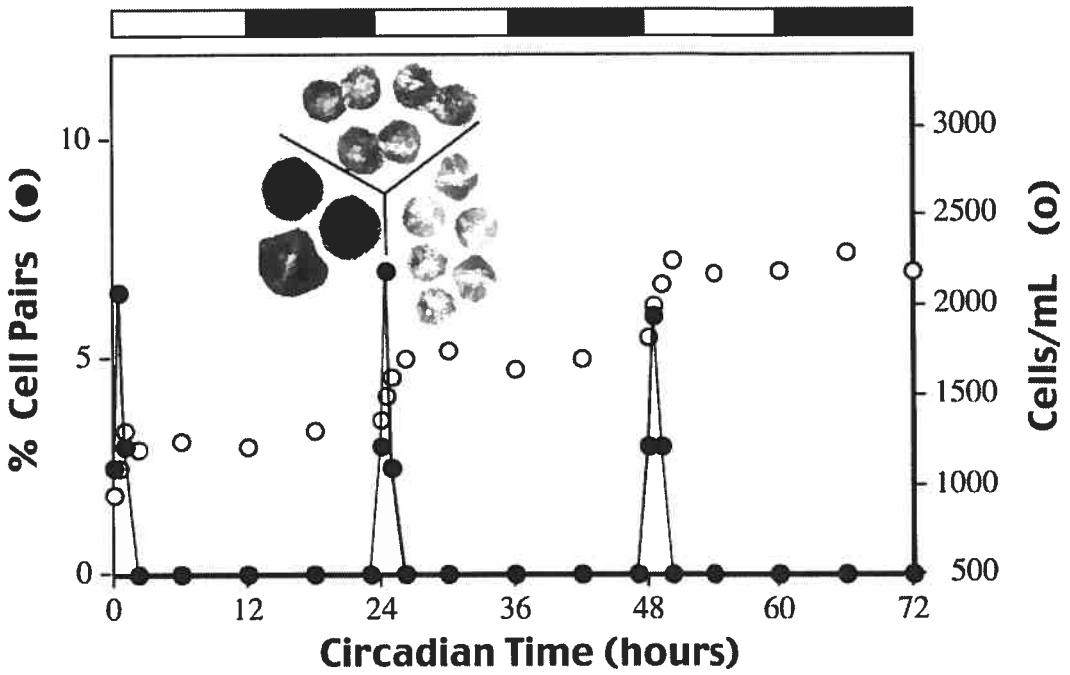
% Cell Pairs (●)
Cells/mL (o)
Circadian Time (hours)
0
5
10
500
1000
1500
2000
2500
3000
0
12
24
36
48
60
72

Figure 1.1.9. Synthesis and abundance of GAPDH

(A) The circadian rhythm in GAPDH synthesis is high amplitude, being virtually undetectable during midday. However, the amplitude of either the protein amount or the enzyme activity is much reduced due to the relatively long half-life of the protein in the cell. Data reprinted from Fagan T, Morse D, Hastings J.W Circadian synthesis of a nuclear encoded chloroplast Glyceraldehyde-3-phosphate dehydrogenase in the dinoflagellate *Gonyaulax polyedra* is translationally controlled. Biochemistry 1999;38:7689-7695. (B) Rhythmically synthesized proteins with low degradation rates ($t_{1/2}$ long) have smaller amplitude rhythms than do proteins with fast degradation rates ($t_{1/2}$ short) when total protein is measured.

A

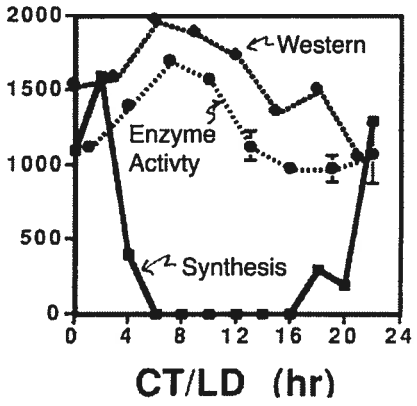
2000
1500
1000
500
0
0
4
8
12
16
20
24
Western
Enzyme
Activty
Synthesis
CT/LD (hr)

B

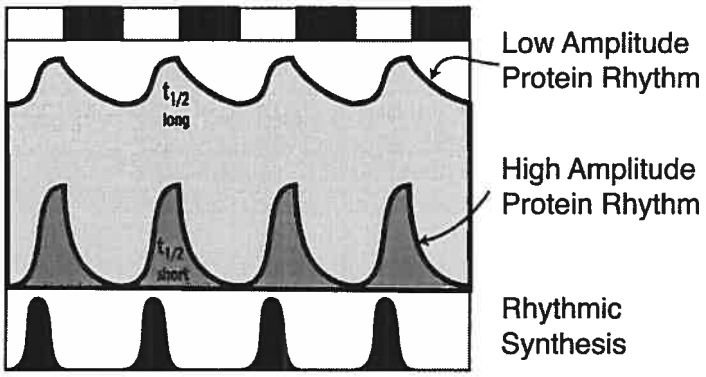
$t_{1/2}$ long
$t_{1/2}$ short
Low Amplitude
Protein Rhythm
High Amplitude
Protein Rhythm
Rhythmic
Synthesis

Figure 1.1.10. Clock control of transcription in dinoflagellates

Relative expression levels of dinoflagellate (*P. lunula*) genes at circadian times 12 hours apart. Distributions of genes (ordinates, number of genes in bins of 0.1 ratio units) as a function of the fluorescence ratios for CT 2/14 (top) and CT8/20 (bottom). Genes with a ratio close to 1 are the most frequent. Data reprinted from Okamoto OK, Hastings JW. Novel dinoflagellate circadian-clock genes identified through microarray analysis of a phase shifted clock. J. Phycology 2003;39:1-9.

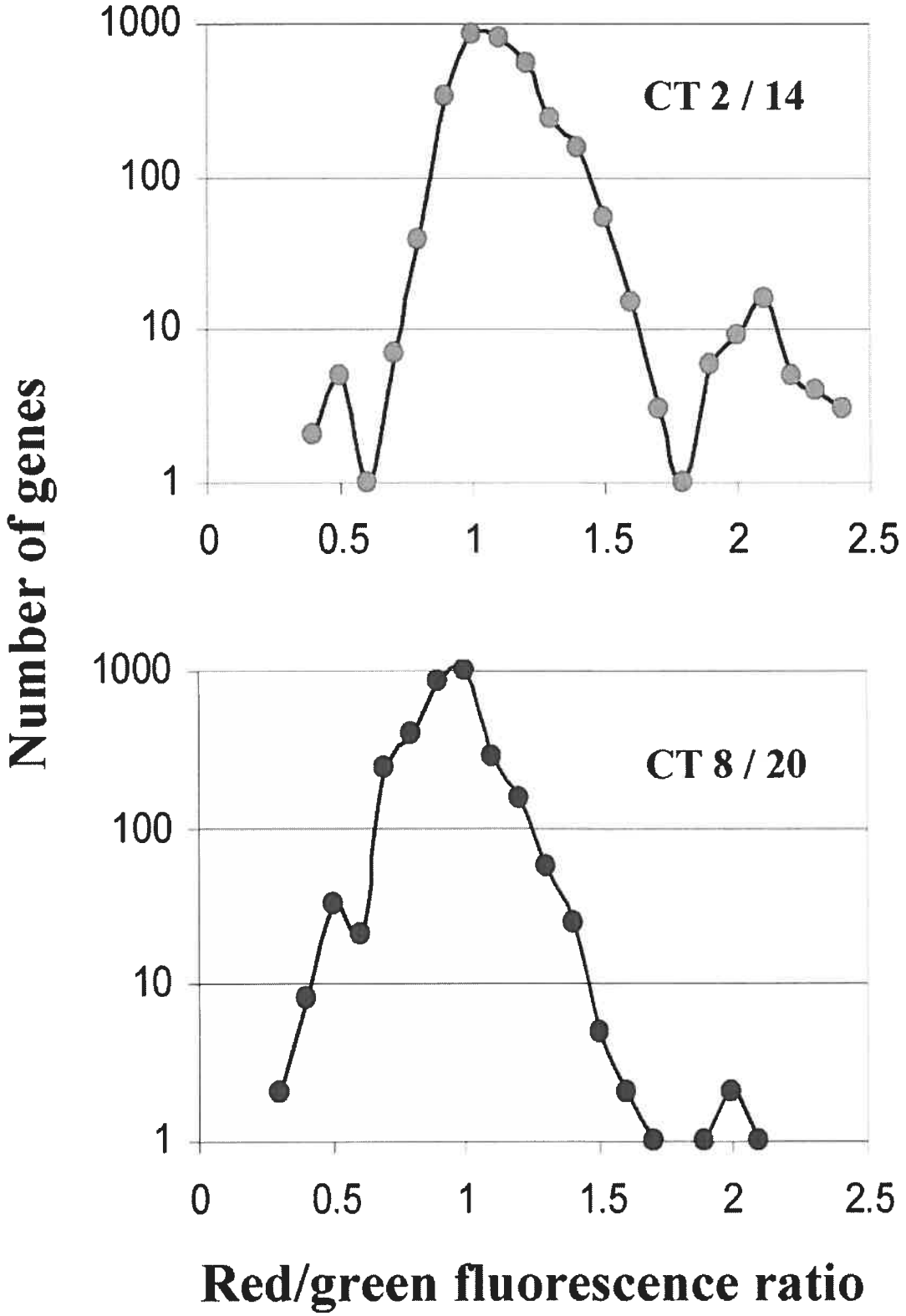
CT 2 / 14
CT 8 / 20
1000
100
10
1
0
0.5
1
1.5
2
2.5
Number of genes
Red/green fluorescence ratio

1.2. Protein targeting to the chloroplasts of photosynthetic eukaryotes: getting there is half the fun

Nassoury, N. and D. Morse (2004) Protein targeting to the chloroplasts of photosynthetic eukaryotes: getting there is half the fun). Biochimica et Biophysica Acta Molecular Cell Research (in press)

This review article attempts to put all the available pieces of the "protein targeting to the chloroplasts" puzzle in place. I thought it will be useful to have a review not only summarizing the new data available but also to look at protein targeting through an evolutionary point of view. The manuscript was reviewed and corrected by my supervisor (David Morse).

The plastids of many algae are surrounded by three or four membranes, thought to be a consequence of their evolutionary origin through secondary endosymbiosis between photosynthetic and non-photosynthetic eukaryotes. Each membrane constitutes a barrier to the passage of proteins, so protein targeting in these complex plastids has an extra level of difficulty when compared to higher plants. In the latter, protein translocation across the two membranes uses multi-protein complexes that together import proteins possessing an N-terminal leader sequence rich in serine and threonine (S/T). In contrast, while targeting to most complex plastids also involves an S/T-rich region, this region is preceded by an N-terminal hydrophobic signal peptide. This arrangement of peptide sequences suggests that proteins directed to complex plastids pass through the ER, as do other proteins with hydrophobic signal peptides. However, this simplistic view is not always easy to reconcile with what is known about the different secondary plastids. In the first group, with plastids bounded by three membranes, plastid-directed proteins do indeed arrive in Golgi-derived vesicles, but a second hydrophobic region follows the S/T-rich region in all leaders. In the second group, where four membranes completely surround the plastids, it is still not known how the proteins arrive at the plastids, and in addition one member of this group uses a targeting signal rich in asparagine and lysine in place of the S/T-rich region. In the third group, the fourth bounding membrane is contiguous with the ER, but it is not clear what distinguishes plastid membranes from others in the endomembrane system. Knowing what to expect is important, as genomic sequencing programs may soon be turning up some of the missing pieces in these translocation puzzles.

The evolution of the molecular machinery for oxygenic photosynthesis in cyanobacteria-like cells more than 3.5 billion years ago (Schopf 1993) changed the form of life forever on this planet. Furthermore, these cells were so valuable as energy producing machines that some eukaryotes enslaved them to form an endosymbiont. During time, the endosymbiont lost its autonomy and gradually transformed into an organelle. The host cell as well lost autonomy, since the partnership between the two formerly separate entities was beneficial for both. This symbiogenesis represents the merger of two cells to form a novel chimeric organism (Cavalier-Smith 2000), on which natural selection would act to prevent the scattering of this amalgamation (McFadden 1999). An additional mechanism to ensure the permanence of the arrangement is the transfer of genes from one

partner to the other. However, gene transfer gives rise to a variety of new problems related to the evolution of a transport system for the proteins encoded by the transferred genes. The fundamental difference between an organelle and an intracellular symbiont is thus the existence of a specific mechanism that makes possible protein import to the organelle (Cavalier-Smith and Lee 1985). All these complications appear to have made symbiogenesis an infrequent evolutionary event in the several billion year history of cells (Cavalier-Smith 2000), yet one nonetheless essential for the formation of mitochondria and different types of plastids in photosynthetic eukaryotes.

1.2.1. Symbiogenesis has happened infrequently

It is now generally accepted that mitochondria are derived from a single endosymbiotic event between a host cell and an α-proteobacteria very early in the evolution of eukaryotes. This is the only symbiogenic event that is broadly agreed to be of monophyletic origin (Lang, Gray et al. 1999). The origin of chloroplasts is another indisputably symbiogenic event, but there are still unsettled issues about the number of times that this event has taken place. For example, plastids of chlorophytes (green algae, similar to plastids of land plants), rhodophytes (red algae) and the glaucophytes are generally termed "primary plastids", meaning that they have evolved directly from a symbiotic event between a photosynthetic prokaryote (cyanobacteria) and a eukaryote (Fig. 1.2.1). All primary plastids are surrounded by two membranes that correspond to the plasma membranes of the original eukaryotic and prokaryotic partners. Eventually, the prokaryote genes were transferred to the eukaryote genome and mechanisms to translocate proteins from the transferred genes back to the prokaryote were developed (Martin and Herrmann 1998; Dyall, Brown et al. 2004).

But how many times had the transformation of endosymbionts to primary plastids actually taken place? The proponents of a monophyletic origin for the primary endosymbiosis have a strong case, based on plastid gene phylogenies, plastid gene order (Delwiche and Palmer 1997) and the similarity in gene content among plastid genomes (Martin, Stoebe et al. 1998; Cavalier-Smith 2000; Palmer 2003). To a first approximation, the phylogenetic relationships inferred between the chlorophytes, rhodophytes and glaucophytes are the same whether nuclear genes or plastid genes are

used (Fig. 1.2.1). However, proponents of a separate origin for the host cells of red and green algae believe that the details of the reconstructions show inconsistencies between nuclear and plastid gene phylogenies, and that this is sufficient to cast doubt on the monophyletic origin idea (Stiller and Hall 1998). With respect to the identities of genes retained, Stiller and colleagues have also shown that different plastid genomes have no more similarity to each other than they do to mitochondrial genomes once genes related to organelle-specific function are factored out. They suggest that the similarities in plastid genome contents can be explained by convergent evolution as a result of control on the gene loss rather than a shared evolutionary history (Stiller, Reel et al. 2003).

Curiously enough, the first gene phylogenies tended to support a polyphyletic origin of the primary plastids, for example in the separate branches of red and green algae when Rubisco phylogeny is examined (Martin, Somerville et al. 1992; Morden, Delwiche et al. 1992). Later interpretations of these data invoked lateral gene transfer to account for the two different branches, thus allowing these data to peacefully coexist with the growing consensus for a monophyletic plastid origin (Delwiche and Palmer 1996) and with the puzzling presence of a form II Rubisco in the dinoflagellates (Morse, Salois et al. 1995). However, a similar divergence is seen with chlorophyll a oxygenase (CAO) gene phylogenies. This component of the biosynthetic pathway for chlorophyll *b* synthesis is expressed in prochlorophytes and green algae but is not found in cyanobacteria, rhodophytes or glaucophytes (Tomitani, Okada et al. 1999). To reconcile this with a monophyletic origin, either the gene was developed independently in chlorophytes or lost in cyanobacteria and two of the three primary plastid classes (Stiller, Reel et al. 2003). Given that to date, plastids do not ally themselves with any particular group of cyanobacteria, there is still not sufficient data to exclude multiple endosymbiosis possibly from different groups of cyanobacteria (Delwiche and Palmer 1997; Palmer 2003; Stiller, Reel et al. 2003).

As if the problems with primary plastids were not enough, there are also seven groups of "secondary plastids" (Fig. 1.2.1). These plastids all share a distinguishing feature of being surrounded by more than two membranes. Two groups harbor plastids surrounded by three membranes (Euglenoids and dinoflagellates), while the other five contain four membrane-bound plastids (Apicomplexa, Cryptophytes, Haptophytes, Heterokonts, and

Chlorarachniophytes). These plastids, also known as complex or second-hand plastids, are thought to be the consequence of a secondary endosymbiosis between a photosynthetic and a non-photosynthetic eukaryote (Gibbs 1978), and are principally responsible for the diversity of different algal groups. As with the primary plastids, the partnership has become irreversible due to the transfer of plastid genes to the new host nucleus. This adds a new layer of complexity to the return of nuclear-encoded genes, as will be discussed below. In addition, it might be expected that the different numbers of membranes around the plastid should hold important information about the evolutionary history of the organelle, but this is not the case at least for the triple membrane bound plastids of Euglena (where the plastid is derived from a green alga) and the dinoflagellates (where most of the plastids have a red algal origin).

Once again, the number of times that secondary symbiogenesis has happened is a key question. One viewpoint holds that each of these seven groups have obtained their plastids independently through a separate secondary endosymbiotic event (Delwiche and Palmer 1997; Palmer 2003). An alternative view, based on complexity of symbiogenesis, is that only two major independent secondary symbiosis events have occurred, the engulfment of either a green alga or a red alga by another eukaryote (Cavalier-Smith 1982; Cavalier-Smith 2000). Here, the chlorarachinophyte plastids, like those of the euglenophytes, are thought to have derived from a green algal precursor (Ishida, Cao et al. 1997), despite the nuclear phylogeny that places the heterokonts (with their red-algal derived plastids) between them (Baldauf, Roger et al. 2000). Furthermore, the secondary plastids of chromalveolates (Cavalier-Smith 1999), a group comprised of haptophytes, dinoflagellates, apicomplexa, cryptophytes and heterokonts, are thought to trace back to a single common secondary symbiosis of a red alga (Baldauf, Roger et al. 2000; Van de Peer, Baldauf et al. 2000; Fast, Kissinger et al. 2001; Yoon, Hackett et al. 2002; Harper and Keeling 2003) despite the nuclear gene phylogeny that places the euglenozoa and the chloroarachniophyta among them (Baldauf, Roger et al. 2000). Thus, despite the importance of plastid origins in the analysis of protein targeting mechanisms, it is clear more work is required to resolve the differences between host cell and organelle phylogenies.

Lastly, it must be noted that there are also some cases of tertiary endosymbiosis, where secondary plastids have been replaced with secondary plastids from a different host (Saldarriaga, Taylor et al. 2001). This further complicates both evolutionary relationships and protein targeting mechanisms, but discussion of these is beyond the scope of this review.

1.2.2. Plastid membranes are biological barriers

We have mentioned plastids that are surrounded by two, three and sometimes even four membranes, but where do these membranes come from? It is generally accepted that new membranes are always formed by division or fusion of preexisting membranes, and they have only been "made from scratch" a few times in evolution (Blobel 1980; Cavalier-Smith 2000). Therefore, each membrane around a plastid must have its own evolutionary history. Cyanobacteria, of course, are Gram-negative, with an outer periplastic membrane in addition to the normal plasma membrane. The engulfment of these bacteria might be expected to produce an organelle with three bounding membranes. The outermost membrane would then correspond to the phagotrophic vacuole of the host (Cavalier-Smith 1982) and the innermost membrane to the cyanobacterial plasma membrane. Which of the three membranes was lost to produce two membrane-bound plastids? The inner membrane still seems similar to that of the cyanobacterial plasma membrane, so either the cyanobacteria escaped from the phagotrophic membrane and began dividing in the cytoplasm (Cavalier-Smith 1982) or the original outer membrane of the cyanobacteria was lost during an organelle division (Killian and Kroth 2003). Unfortunately, biochemical analyses of the outer membrane have failed to resolve this issue. On the one hand, the current outer membrane has high amounts of carotenoids and galactolipids (Joyard, Teyssier et al. 1998) similar to those found in cyanobacterial outer membrane. These galactolipids in particular are reported to be involved in interactions between the transit peptide and the outer plastid membrane (Bruce 1998). On the other hand, the outer membrane also has high levels of phosphatidylcholine (Joyard, Teyssier et al. 1998). This "eukaryotic" type lipid is transferred from the ER by lipid transfer proteins and are thought to have substituted the original bacterial liposaccharides (Cavalier-Smith 1993). The outermost membrane may thus be chimeric in nature (Cavalier-Smith 1987). As

recently noted, however, regardless of which membrane was lost, that remaining functions as an acceptor for proteins and lipids from the two sides it has been separating (Killian and Kroth 2003). The magic disappearing act of the third membrane is thus really nothing more than sleight of hand.

For plastids that are surrounded by four membranes, the engulfment of a eukaryote harboring a two membrane bound plastid can neatly account for the topology. In this case, the outermost membrane would correspond to the plasma membrane of the new host, while the membrane adjacent to it would represent the plasma membrane of the endosymbiont. In the case of the triple membrane bound plastids, one of the four membranes around these plastids has presumably been lost, perhaps in a manner analogous to the loss of the third membrane from the primary plastids. Again, the exact nature of the lost membrane is less important than its capacity to transport proteins. We will discuss below the evidence that the outer membrane in these plastids functions as part of the endomembrane system of the host.

1.2.3. Prokaryotes and organelles share two main types of protein translocation machinery

Independent of the evolutionary origin of the membranes, each constitutes a barrier to the movement of proteins. This would have become a severe problem following transfer of genes from the plastid to the host cell nucleus, as nuclear-encoded proteins synthesized in the cytoplasm would then have to pass these barriers to re-enter the plastids. In this context, membrane barriers are a strong driving force for the evolution of protein import pathways and indeed, the development of a protein import machinery is proposed to be the key step for transforming the free living cyanobacteria to an organelle dependent on the host (Cavalier-Smith and Lee 1985). The idea of a membrane as a barrier to movement of proteins is closely associated with the idea of compartments, as different compartments maintain their identity through their specific and conserved complement of proteins. The mechanisms that orchestrate protein movement through membrane barriers are thus of vital importance to the cell.

As will be discussed below, several evolutionarily unrelated mechanisms catalyze protein translocation across membranes, and this presumably reflects the importance of this

process. However, the underlying logic of all protein translocation mechanisms is similar. For example, all mechanisms must have a method for identifying the protein to be translocated amongst the myriad of other proteins whose destiny is to remain where they are synthesized. Typically, this involves a peptide signal in the protein to be translocated, usually at its N-terminal end, and a receptor in the target membrane that recognizes and binds the signal. A useful analogy is to imagine the peptide signal as a key, designed to fit a particular protein receptor lock. The next element is the translocator itself, a normally impermeable channel extending through the membrane bilayer. To pursue the analogy, the channel is the door through which the proteins will pass. The receptor and channel can be, but are not necessarily, distinct molecules. Lastly, all translocation systems use energy to either push or pull the protein through the channel, and all have a means of ensuring the translocation occurs unidirectionally. This latter is usually ensured by the asymmetry of the energy generating machinery.

Prokaryotes possess two main types of protein translocation systems, required for exporting proteins to the periplasmic space (Table I). The most basic and most highly conserved protein translocation machinery is the Sec61/SecY complex (Sec61 in eukaryotes and secY in eubacteria and archea) (Rapoport, Jungnickel et al. 1996). The transmembrane component of this complex is a heterotrimeric protein that serves as a channel. It is formed from Sec61α (the homologous SecY in prokaryotes), Sec61γ (the homologous SecE in prokaryotes), and Sec61ß (the homologous Secß in archea or a non-homologous SecG in eubacteria).

The signal that identifies the protein to be translocated is a hydrophobic amino acid sequence at its N-terminal end, presented to the complex either as a nascent protein on a ribosome or in a complex with the soluble receptor protein SecA (Johnson and van Waes 1999). These two mechanisms are often termed signal recognition particle (SRP) dependent and SRP independent, respectively. SRP is a GTPase that, in its GTP bound form, can bind hydrophobic peptides on a protein as they emerge from a ribosome, and this binding often provokes translational arrest. Interaction of SRP with a membrane bound SRP receptor brings the SRP-ribosome complex into proximity of a translocator, and it is believed that interaction between the translocator, the SRP and its receptor trigger GTP hydrolysis on SRP (Song, Raden et al. 2000). SRP in its GDP-bound form

does not bind the hydrophobic peptides, which are then transferred to the translocator as synthesis restarts. The presence of ribosomes in the cytoplasm assures the directionality of translocation, and GTP hydrolysis during translation transport supplies the energy requirement for protein translocation.

In contrast to the SRP-dependent mechanism, an ATPase called SecA is also able to deliver cytoplasmic proteins to SecY. SecA binds to hydrophobic peptides and to a number of conserved residues on the cytoplasmic side of the channel complex that are proposed to act in signal recognition as well as in binding to SecA (Economou and Wickner 1994). The cytoplasmic location and ATPase activity of SecA ensures the unidirectionality of protein translocation through the SecY complex and fulfills the energy requirement for post-translational transport, respectively.

The SecY complex structure is known from X-ray diffraction of the archeal channel at 0.32 nm resolution (Van den Berg, Clemons et al. 2004). The channel is formed from α-helices and has an hourglass shape containing two aqueous funnels and a constriction in the middle lined by hydrophobic residues. The hydrophobic residues in the constriction are proposed to act as a gasket, able to keep water out when closed and to form a watertight seal around translocating proteins. The structure also suggests that the pore may open only when a signal is bound to the complex, an aspect important to the maintenance of membrane impermeability.

In spite of the common evolutionary history of the Sec61/SecY complex in prokaryotes and eukaryotes, this protein translocation machinery does not find widespread use in protein import into organelles. One possible reason for this is that the direction of protein translocation depends on the topology of the transmembrane components of the SecY complex, which in turn, depends on their site of synthesis. If SecY were encoded by the plastid, as is the case for non-green algae (Vogel, Fischer et al. 1996), the orientation of the protein would presumably be that designed for protein export from the plastid rather than protein entry. Alternatively, it may be that a mechanism different from that used for secreting proteins from the cell was required to distinguish plastid-targeted proteins. In any event, in all extant plastids the SecY complex is restricted to the thylakoid membranes and a different protein import mechanism has been developed for passing the bounding membranes of plastids.

In addition to the SecY complex, prokaryotes also possess a completely different protein export machinery, constructed from Tat gene products (for twin-arginine translocation) (Berks, Sargent et al. 2000). This name is derived from one of the two features that distinguish it from the SecY pathway: the signal identifying proteins translocated by the Tat pathway contains an obligatory pair of arginine residues immediately upstream of the hydrophobic region. The second distinguishing feature lies in the energy requirement for translocation: a pH across the membrane is required while ATP or soluble proteins are not. In prokaryotes, there are five genes implicated genetically, four in the TatABCD operon in *E.coli* and another version of the TatA gene, called TatE, found elsewhere in the genome.

The structure of this protein complex is still unknown, as is the mechanism employed for translocation. However, in higher plants, it is restricted to protein translocation across the thylakoid membranes (like the SecY complex, and probably for the same reasons). Interestingly, this pathway was actually first identified in higher plants as the maize mutant Hcf106, defective in a pathway that uses a ΔpH as the sole energy source for translocating proteins into the thylakoid (Voelker and Barkan 1995). This protein is homologous to TatA, TatB and TatE genes, and is predicted to have a single membrane-spanning region close to the N-terminal end. Another maize mutant, Tha4, was also found to inhibit the same pathway and is actually more closely related to TatA than is Hcf106 (Walker, Roy et al. 1999). This suggests that two versions of the protein must work together in both higher plants and prokaryotes. The bacterial TatC gene is an integral membrane protein, and is thus a more likely candidate for the channel. Again like SecY, the TatC gene has homologs in the nuclear genome of *Arabidopsis*, and in the chloroplast genome of the red alga *Porphyra* and the diatom *Odontella* (Bogsch, Sargent et al. 1998).

In addition to these well-studied pathways, other more poorly understood mechanisms are also present. For example, plastid thylakoid development can be inhibited by mutation in the Alb3 gene, which appears to encode a protein homologous to the YidC gene in bacteria and the Oxa1 gene in mitochondria (Kuhn, Stuart et al. 2003). Members of this family of proteins may act as integral membrane chaperones, which act to promote membrane insertion of proteins in a Sec-independent manner by recognizing and binding

hydrophobic regions on the protein. Thus, these proteins appear to act in membrane insertion rather than in translocation.

It is also important to note that most of the studies on prokaryotic protein translocation have used non-photosynthetic organisms. The distinction is not negligible, as cyanobacteria have highly differentiated thylakoid membranes that are distinct from the plasma membrane. Some studies indicate that different signal peptides may impart a specific destination to a protein (Mackle and Zilinskas 1994; Spence, Sarcina et al. 2003). However, partially formed photosystems have been found in the plasma membrane, suggestive of transfer either to or from the thylakoids (Zak, Norling et al. 2001). Perhaps protein targeting in cyanobacteria may use signals in the leader in some cases and signals in the mature protein in others as has been found for targeting to higher plant thylakoids (Schnell 1998).

1.2.4. The protein import machinery of primary plastids

The major components of the apparatus for importing proteins from the cytoplasm into the plastids of higher plants is now known in some detail and can serve as a basis for comparison with more complex plastid ultrastructures. The import machinery is found clustered in two protein complexes termed Toc and Tic (for translocons for the outer/inner chloroplast membranes) (Chen and Schnell 1999; Schnell and Hebert 2003). The Toc complex recognizes and binds plastid preproteins, and then translocates them across or inserts them in the outer membrane. Toc and Tic components connect at plastid envelope contact sites presumably by preprotein binding, and the protein is inserted into the Tic components of the inner membrane. Stromal chaperons then bind to the preprotein and pull it inside, acting to translocate the preprotein through the two membranes simultaneously.

The major Toc components identified to date are Toc159, Toc33/34, and Toc75 (Fig. 1.2.2) (Jarvis and Soll 2002). It is important to note that some of these components have homologues in cyanobacteria while other do not. Toc159 has GTP-binding motifs in a cytoplasmic domain which share homology with a distinct family of membrane GTPases (Hirsch, Muckel et al. 1994; Kessler, Blobel et al. 1994). This protein is presumed to be the main receptor for precursor proteins (Jarvis and Soll 2002) and does not seem to have

significant homology to any cyanobacterial protein (Reumann and Keegstra 1999). Instead, it shows partial similarity to the α-subunit of the host SRP (signal recognition particle) receptor and may thus be of host origin (Keegstra and Froehlich 1999). Functionally, this protein appears to act like a SRP as well: it is found in comparable amounts soluble in the cytoplasm and integrated in the membrane, and it is proposed that Toc159 serves as a preprotein receptor by cycling between cytoplasm and the outer plastid membrane (Hiltbrunner, Bauer et al. 2001).

Toc33/34 also has a GTP-binding motif similar to that found in Toc159 (Kessler, Blobel et al. 1994), and shares limited sequence identity to cyanobacterial proteins. However, this low similarity is intriguing as the cyanobacterial proteins in question are the only small G proteins in the bacteria and the homologous region corresponds to the GTP-binding domain of Toc34 (Reumann and Keegstra 1999). One proposed role for Toc34 is in recognition of preprotein sequences (Kessler, Blobel et al. 1994), as binding to Toc159 is enhanced by both GTP and preprotein binding (Becker, Jelic et al. 2004). Recently, it has been shown that the GTPase activity of Toc34 is necessary for docking of the receptor Toc159 at the Toc complex and that the interaction of Toc34 and Toc159 stimulates association with the translocon complex (Wallas, Smith et al. 2003).

Toc75 is reported to be the most abundant protein of the chloroplast outer membrane (Joyard, Billecocq et al. 1983; Summer and Cline 1999) and is completely different from Toc159 and Toc34. It shows homology to a protein found in the outer membrane of all Gram-negative bacteria including cyanobacteria (SynToc75) that is reported to form a voltage-gated channel with high affinity for peptides in reconstituted liposomes (Bolter, Soll et al. 1998). These Gram-negative bacteria homologues of Toc75 are involved in protein export and are reported to secrete virulence factors across the outer membrane (Reumann, Davila-Aponte et al. 1999). Interestingly, the Toc75 and its homologues in Gram-negative bacteria function in opposite directions compared to one another, with the nuclear-encoded Toc75 functioning in protein import and the synToc75 functioning in protein export. This apparent discrepancy may be related to the topology of the protein, as Toc75 is nuclear encoded in higher plants and may be inserted into the outer membrane in a direction opposite compared to that of synToc75. Alternatively, it may result from the unusual structure of the Toc75. Instead of the α-helical structure found for

channels such as the secY complex (Van den Berg, Clemons et al. 2004), both sequence (Schnell, Kessler et al. 1994) and functional analysis (Hinnah, Wagner et al. 2002) suggest that Toc75 is a ß-barrel. Indeed, it now appears that Toc75 belongs to a highly conserved Omp85 family of proteins also found in mitochondrial and bacterial outer membranes (Gentle, Gabriel et al. 2004). This structure is important as the larger and more rigid ß-barrel structure offers less opportunity for regulating channel size than do the smaller and more flexible α-helical structures, and suggests that proteins might pass more easily in both directions. The unidirectionality of protein translocation observed in plastid Toc75 might result from accessory proteins that bind only to one side of the channel or from an association with the inner membrane translocator.

The translocation across the inner membrane of higher plant plastids also uses a complex of several proteins, called the Tic complex, some of which are known to be of cyanobacterial origin. The major Tic proteins identified are Tic110, Tic 62, Tic55, Tic40, Tic32, Tic22 and Tic20 (Fig. 1.2.2) (Jarvis and Soll 2002). The first Tic component to be identified was Tic110, reported to be the most abundant translocation protein. The C-terminal of Tic110 can form a cation-selective high conductance ion channel and thus may be (or be a main part of) the import channel across the inner membrane (Heins, Mehrle et al. 2002). Furthermore, the bulk of this integral membrane protein has been shown to function as a docking site for stromal chaperons assisting the translocation of the precursor proteins (Kessler and Blobel 1996). Tic110 shares no sequence homology with any protein of known function and does not seem to have a cyanobacterial origin (Jarvis and Soll 2002).

Tic62 is an integral membrane protein that coimmunoprecipitates with Tic110 (and Tic55), suggesting that it forms part of the translocator (Kuchler, Decker et al. 2002). It is an integral membrane protein that interacts with ferredoxin-NADP oxidoreductase, suggesting it may be able to modulate protein import as a function of the organellar redox state. It is interesting that the N-terminal region of the protein has strong homology to putative proteins with unknown function in cyanobacteria, glaucophytes and crytomonads, although these proteins are most likely soluble and thus not functional homologs of Tic62. Perhaps this reflects conscription of a prokaryotic protein for a new function within the eukaryotic host.

Tic55 is another inner membrane component, and contains a Riesk-type iron-sulphur cluster and a mononuclear iron-binding site that are usually characteristic of redox proteins (Caliebe, Grimm et al. 1997). Tic55 appears to have homology with a hypothetical protein of unknown function in the cyanobacteria *Synechocystis,* hence suggesting it may have a symbiotic origin (Caliebe, Grimm et al. 1997; Reumann and Keegstra 1999).

The role of a recently discovered Tic32 is not yet clear, although it associates with other Tic components in immunoprepitation assays and with precursor proteins during translocation by cross-linking assays (Hormann, Kuchler et al. 2004). Tic32 appears essential for viability, as deletions of the gene in *Arabidopsis* are lethal during embryo development.

Tic22 is a peripheral inner plastid membrane protein and is thought to be the first protein that associates with precursor proteins as they emerge from the Toc complex and consequently directs them to the inner membrane translocon (Kouranov, Chen et al. 1998). Tic22 is also considered to be the functional connection of the inner and outer membrane translocon. There is a cyanobacterial homologue of Tic22 but it has no known function (Reumann and Keegstra 1999).

Another component of the Tic apparatus with a homologue of unknown function in the cyanobacteria *Synechocystis* is Tic20. Tic20 is an integral protein that appears to have a role in protein conductance (Kouranov, Chen et al. 1998). Tic20 was considered to be an ideal candidate for the inner membrane protein-translocating channel because of its structural similarities to prokaryotic amino acid transporters in *Bacillus subtilis* and *Methanococcus jannaschii* (Reumann and Keegstra 1999). This is supported by the observation that *Arabidopsis* plants expressing Tic20 in antisense show a 50% decrease in the levels of protein import efficiency (Chen, Smith et al. 2002). The exact role of Tic20 is uncertain, however, as Tic110 functions as an ion channel (Soll 2002). Tic110 protein levels do increase in antisense Tic20 plants, which might imply compensation for a defective inner membrane translocon (Chen, Smith et al. 2002). It is possible that Tic110 and Tic20 form distinct translocation channels, or alternatively, act together to form the ion channel (Soll 2002). Actually, both Tic22 and Tic20 can associate with Tic110 and the main Toc proteins and so help to construct the Toc-Tic supercomplex

(Kouranov, Chen et al. 1998). This is important as the Toc-Tic supercomplex is deemed accountable for the regions of the plastid envelope where the inner and outer membrane are in close contact together. In fact, immunolocalization studies have restricted protein intermediates to these regions (Schnell and Blobel 1993).

The chlorophytes have most of the protein translocators found in higher plants, with Tic 55 as the only exception. Similarly, with the exception of Toc159 and Tic55, homologs to higher plant protein translocators are also found in the genome of the red alga *Cyanidoschyzon* (Matsuzaki, Misumi et al. 2004). This strongly supports the monophyly of red and green algal plastids. So far, little is known about plastid protein translocators in the Glaucophytes.

1.2.5. Evolution of the plastid translocators

There are several different hypotheses for the evolutionary origin of the protein import apparatus. In one scenario, the synToc75 of *Synechocystis*, which initially secreted proteins across the outer membrane of cyanobacteria, was transferred to the nucleus of the host and formed the initial translocator channel capable of importing proteins after its insertion (in reverse) into the outer membrane of the plastid (Reumann, Davila-Aponte et al. 1999). This suggests that the ancestral transit peptide may have evolved from the bacterial secretion signals that were the original substrates of SynToc75 (Reumann, Davila-Aponte et al. 1999), and would explain why the stromal peptidase that cleaves the leader peptide of plastid precursor proteins has sequence similarity to *Synechocystis* peptidases (Reumann and Keegstra 1999). The inner membrane channel might then have been formed by modifying the amino acid-transporting Tic20 protein to increase the size of the proteins translocated and the efficiency of translocation (Reumann and Keegstra 1999). Additional contemporary components of the protein import machinery may eventually have been added to optimize efficacy, especially in the aftermath of extensive gene transfer to the nucleus. Presumably, these additional components were derived from the host, as components like Toc159 and Tic110 do not have bacterial counterparts. Another scenario, recently advanced by Kilian and Kroth (Killian and Kroth 2003), proposes that proteins produced from genes transferred to the nucleus might have used the secretory pathway in order to get to the phagotrophic vacuole in which the

endosymbiont originally found itself. This clearly puts the outer membrane as part of the hosts' secretory system (Killian and Kroth 2003), and suggests that early transferred genes had to acquire a signal peptide in order for the proteins they encoded to access the secretory pathway and thus pass the outermost membrane of the plastid. Passage through the inner membrane would then take place using non-specific ion channels (Reumann and Keegstra 1999) or by exploiting the ancestral Tic20 with its properties as amino acid transporters as described above. Interestingly, the secretory pathway proposal has the attractive feature of providing a plausible solution to the thorny issue of which came first, the translocator or the signal. A gene transferred from the endosymbiont to the nucleus might find itself able to enter the plastid by exploiting mechanisms already in use in the host cell if it fortuitously acquired a signal peptide. And why was the original endosymbiont not digested if it ended up in a phagocytic vacuole? Recent work has provided strong evidence that ER membrane recruitment is largely responsible for forming the phagocytic membrane in macrophages (Desjardins 2003). This suggests that original symbiont may not have entered a phagosome at all, and that a process inhibiting phagocyte fusion to an ER-derived membrane, rather than the more complicated task of getting the original prey out of a phagocytic vacuole, may have been involved in endosymbiosis.

However, the proposed entry of plastid-directed proteins into the secretory pathway solves one problem by introducing another: how would ER proteins be directed to the plastid. This is not a trivial issue and it arises again when protein import mechanisms into complex plastids are considered (see below). One view is that the ER and outer plastid membranes are contiguous allowing proteins to simply diffuse from one to the other. A second option requires vesicular transport. Here, vesicles full of plastid-directed proteins might be recognized and targeted specifically to the organelle, by development of a modified pair of SNARE proteins, for example (Cavalier-Smith 2003). Alternatively, vesicles containing many different nucleus-encoded plastid proteins might fuse with plastids and other various compartments (Killian and Kroth 2003). This form of transport would maintain plastid identity if the chloroplast proteins were specifically extracted from the mixture of proteins delivered to the intermembrane space. Kilian and Kroth propose that the N-terminal region of the protein, immediately following the signal

peptide, became modified to function as a transit peptide. In this scenario, the transferred proteins were escorted by a bipartite presequence containing a signal peptide as well as a transit peptide (similar to present-day secondary plastids), and the removal of the signal peptide exposed the transit peptide. The translocon in the inner membrane (Tic) would ensure the correct and efficient protein transport into the endosymbiont of any proteins with this transit peptide. In the next logical step in this scenario, when a protein translocator became established in the outer membrane (Toc), the secretory pathway was of no further use and the now unneeded signal sequence could be lost. One must keep in mind that this tedious gain of the signal peptide, development of a transit peptide and final loss of the signal peptide is proposed to have happened only to the genes transferred to the host at the very primary stages of endosymbiosis (Killian and Kroth 2003). This hypothesis nicely explains the presence of Toc159 in the outer membrane, as its similarity to host cell signal recognition particle receptor suggests it may have been introduced into the outer membrane to allow recognition of a hydrophobic signal peptide (Heins and Soll 1998). Presumably this role is accomplished by Toc34 in red alga where Toc159 is not found (Matsuzaki, Misumi et al. 2004).

1.2.6. Evolution of the targeting sequence

These proposed gymnastics of the signal and transit peptides at the N-terminal end of the proteins underscore the vital relationship between the sequence key and the receptor lock that allows a protein passage through the translocator channel door. Indeed, while the development of the protein import apparatus is crucial in transforming the free-living endosymbiont to an organelle, and presumably an inevitable consequence of gene transfer from the endosymbiont genome to the host nucleus, this must occur in concert with the mechanism for discriminating which proteins should be reintroduced into the plastid. How might a targeting sequence be added to the N-terminal end of the protein? Some clues are available from studies of mitochondrial genes. One possible mechanism is exemplified by the rps14 gene of maize, which when transferred from the mitochondrion to the nucleus landed in the intron of the mitochondrial directed sdh2 gene (Kubo, Harada et al. 1999). Alternative splicing thus allows the rps14 gene to freeload on the sdh2

targeting system. In another example, the rps10 gene was transferred into a duplicate gene for mitochondrial hsp22 (Adams, Daley et al. 2000). Thus over evolutionary time scales, transfer of a given gene to the nucleus might have occurred many times, until eventually the gene found itself adjacent to a sequence that could serve as a targeting signal. The idea of repeated gene transfers has received experimental support from measured gene transfer rates to the nucleus from mitochondria (Thorsness and Fox 1990) and chloroplasts (Huang, Ayliffe et al. 2003), and of course any new gene fusions will be maintained if they provide a selective advantage for the host. Alternatively, the targeting signal could have been stitched onto the transferred genes through exon shuffling. This later idea has experimental support for the generation of plastid-directed and mitochondrial-directed proteins (Wolter, Fritz et al. 1988; Long, de Souza et al. 1996). However it happens, the addition of targeting signals apparently happened early in evolution. The prototypical "transit peptide" found in chlorophytes and higher plants is a stretch of amino acids rich in hydroxylated amino acids such as serine and threonine and contains some basic but few acidic amino acids (Keegstra 1989). This same transit peptide is also used for translocation into rhodophyte (Apt, Hoffman et al. 1993) and glaucophyte (Jakowitsch, Neumann-Spallart et al. 1996) plastids, suggesting that the gene transfers and targeting signal acquisitions occurred prior to the divergence between the different primary plastid-containing lineages (compare Fig. 1.2.1 and 1.2.2). Furthermore, the same serine/threonine-rich sequence is also used for entry into the inner two membranes of dinoflagellate (Nassoury, Cappadocia et al. 2003) and diatom (Lang, Apt et al. 1998) plastids, suggesting that gene transfer to the nuclei of the secondary plastid-containing lineages may have occurred after the first transit sequence was already in place. However, apicoplast targeting sequences in *Plasmodium* (Foth, Ralph et al. 2003) and the transit peptides on proteins encoded by the cryptomonad nucleomorph (Douglas, Zauner et al. 2001) contain roughly much more lysine and asparagine as they do serine and threonine (Fig. 1.2.2). Whether these are derived modifications in these specific lineages or a reflection of different protein translocation systems is an open question at this point.

1.2.7. Protein import into the secondary plastids with three membranes

Interestingly enough, the leader sequence of proteins entering the triple membrane bound plastids of Euglenids and dinoflagellates is similar to that predicted by the secretory membrane hypothesis (Killian and Kroth 2003). The N-terminal domain is hydrophobic and is followed by a transit peptide domain rich in serine and threonine (Fig. 1.2.2). The only unusual feature of these leader sequences is the presence of a second hydrophobic region that follows the S/T-rich region.

Euglena plastids are undeniably the most extensively studied secondary plastids and in fact the passage of nuclear encoded plastid proteins through the secretory system were initially shown in *Euglena* by immunolocalization of the light-harvesting protein LHCPII at the EM level (Osafune, Yokota et al. 1990). Several years later, it was shown that the presequence of the LHCPII did indeed have a functional ER targeting domain (Kishore, Muchhal et al. 1993). Furthermore, pulse-chase experiments have shown that newly synthesized preLHCPII is found first in the ER then in the Golgi apparatus before arriving in the chloroplasts (Sulli and Schwartzbach 1996). All *Euglena*'s chloroplast protein presequences have an unusual second hydrophobic core located downstream of the transit peptide domain. This second hydrophobic region acts as a stop transfer sequence after the plastid proteins begin co-translational translocation to the ER, so that the C-terminal end of the protein is found in the cytoplasm. The first hydrophobic region is followed by a signal peptidase site, so that when synthesis is complete, the final product is a single pass membrane protein with the N-terminal transit peptide inside the ER lumen and the bulk of the protein in the cytoplasm (Sulli, Fang et al. 1999). These integral membrane proteins maintain their peculiar topology during vesicular transport to the plastid, so that following fusion with the outermost chloroplast membrane; the precursor is embedded in the outer membrane with a transit peptide dangling down into the intermembrane space. At this juncture the membrane-bound protein is presumably capable of moving laterally in the membrane until the transit peptide reaches import receptors located in the middle membrane. One likely scenario is that Toc complexes in the middle membrane, homologous to those in the outer membrane of primary plastids, would then bind and begin importing the protein. A potential contact between Toc and

Tic complexes, as found in higher plant plastids, could then result in import into the plastid stroma. The inner membrane translocators are presumed here to be homologues of the Tic complex. Independent of their identity, concerted translocation across the three membranes would couple ATP hydrolysis to translocation using Hsp70-like proteins in the stroma. This is important as energy will presumably be required to pull the hydrophobic anchor free of the outer membrane (Sulli, Fang et al. 1999).

Recently, a similar role as protein anchor has been demonstrated for the second hydrophobic core in the leader sequence of the dinoflagellate plastid-directed proteins (Nassoury, Cappadocia et al. 2003). The protease sensitivity of proteins synthesized by in vitro translation in the presence of microsomes shows that the bulk of the protein is also on the cytoplasmic side of the ER membranes, implying they will approach the plastid as Golgi-derived vesicles with only the transit peptide inside (Nassoury, Cappadocia et al. 2003). This is important because *Euglena* is phylogenetically unrelated to dinoflagellates. The similarities in protein translocation mechanisms thus indicate that they are a requirement of plastid ultrastructure, not phylogeny.

The crucial feature of this translocation mechanism is the second hydrophobic region in the leader sequence. As will be discussed below, four membrane bound plastids have targeting signals that differ by the absence of the second hydrophobic region. It seems reasonable that loss of one membrane from an initial four membrane bound plastid could be compensated for by accentuating any existing hydrophobic character in the targeting signal or even the mature protein sequence. One intriguing question is why the second hydrophobic region should be required at all. We have speculated that targeting to the plastid may not be specific (Nassoury, Cappadocia et al. 2003), perhaps as a result of the protein having its bulk in the cytoplasm. This topology suggests that the proteins may lack the usual cytoplasmic sorting signals expected to associate with adaptors or coat recruitment proteins which charge the vesicles with the appropriate cargo (Kirchhausen, Bonifacino et al. 1997). The hydrophobic membrane anchor would anchor the proteins to the plasma membrane if accidentally secreted and could permit their recovery.

1.2.8. Protein import into the secondary plastids with four membranes and CER

The second hydrophobic region is never found in leader sequences that target proteins to the stroma of four membrane-bound plastids. Instead, the targeting signals contain only the hydrophobic ER-signal sequence followed by the transit peptide (Fig. 1.2.2). Despite this general similarity, details of the targeting mechanism differ in the two main groups of four membrane-bound plastids. The first group of four membrane-bound plastids is found in most heterokonts and cryptophytes, and is characterized by having ribosomes attached to their outer membrane (often called chloroplast ER, or CER) (Gibbs 1979). The evolutionary origin of this membrane is moot since it is thought to be derived from the food vacuole surrounding the endosymbiont and its modification to an ER membrane remains mysterious (Kroth 2002). However, in several organisms the CER is reported to be continuous with the ER and the nuclear envelope (Gibbs 1979; Ishida, Cavalier-Smith et al. 2000). Are the ER and CER functionally distinct albeit their continuity? This seems likely in heterokonts, as GFP accumulates in the plastid when fused with a plastid preprotein signal peptide, whereas GFP accumulates in the ER when an ER-targeting signal peptide is used instead (Apt, Zaslavkaia et al. 2002). It has been suggested there is a subtle difference between the two signal peptides and their recognition sites (Schwartzbach, Osafune et al. 1998), even though diatom plastid presequences do enter canine microsomes *in vitro* (Bhaya and Grossman 1991). As a caveat, however, these observations do not exclude the possibility that some plastid-targeted proteins directed to the ER instead of the CER could then be transferred to the CER through the ER/CER lumenal connections (Ishida, Cavalier-Smith et al. 2000). A receptor/translocator could be used to sieve out proteins with a transit peptide from others in the general secretory pathway.

Regardless of the location of translation (i.e., ER or CER), the mechanism used to pass the three additional plastid membranes still remains unknown. Thus far, two models have been proposed. The first involves vesicular shuttling between the two middle membranes, and is supported by microscopic observation of vesicles in the space between them (Gibbs 1979). In this model, plastid-directed proteins with a signal peptide in their leader sequence exploit the secretory pathway of the host for targeting to the outer membrane. Once past this first barrier, proteins found themselves outside the host cell and at the exterior surface of a membrane topologically equivalent to the former plasma membrane

of the endosymbiont. This membrane was presumably capable of endocytosis when the eukaryote endosymbiont was free-living, and if proteins delivered from the host cell were taken up by a similar mechanism, they would find themselves in vesicles between the two middle membranes. Vesicle fusion would then place the proteins in front of the innermost plastid membrane, where transport into the stroma could be mediated by a Tic transport system (Kroth 2002; Killian and Kroth 2003). There is also some indirect support for the model, derived from the effects of Brefeldin A on plastid-directed protein transport in cryptomonads. Brefeldin A inhibits vesicular traffic in most eukaryotes (Helms and Rothman 1992), and in cryptomonads, causes swelling of the space underneath the outermost membrane of the plastid where the ribosomes are found attached (Wastl and Maier 2000). One interpretation of this result is that vesicular traffic inside the plastid is also sensitive to the drug allowing proteins to build up there. Interestingly, this model does not require Toc translocator components, in agreement with the lack of Toc homologs in the almost complete diatom nuclear genome sequence (McFadden and van Dooren 2004).

The second model for protein transport into the CER-containing plastids proposes the presence of a protein translocator, possibly a duplicate of the Toc complex, in both of the middle two membranes of the plastid (Cavalier-Smith 1999; van Dooren, Schwartzbach et al. 2001). In common with the previous model, the signal sequence would allow passage across the outermost membrane and the transit peptide would allow the protein to pass through a Tic complex of the inner-most membrane (van Dooren, Schwartzbach et al. 2001). However, the vesicular transport step, where proteins effectively vault over the middle two membranes, is replaced by true translocation through two successive Toc complexes, one on each of the membranes. Both of these two Toc complexes must be nuclear-encoded. While this is self-evident for most four membrane-bound plastids, it is not necessarily so for the cryptomonads and chlorarachniophytes that have a miniaturized nucleus termed a nucleomorph in between the middle two membranes (Gilson and McFadden 1997; Douglas, Zauner et al. 2001). The nucleomorph is thought to represent the remnants of the nucleus belonging to the host of the primary endosymbiont, as evidenced by phylogenetic analyses that place it among the algae with mainly primary plastids. However, the nucleomorph genome of the cryptomonad *Guillardia theta* does

not encode any Toc complex components (although it does encode a protein homologous to Tic22 and a chaperone-binding Tic complex-associated protein called IAP100) (Douglas, Zauner et al. 2001). The jury is still out on the chlorarachniophyte nucleomorph, as the full sequence is not yet available (Gilson and McFadden 2002). Interestingly enough, the cryptomonad nucleomorph genes encode either chloroplast-targeted proteins or are housekeeping genes required for expression of those plastid-directed genes (Douglas, Zauner et al. 2001). Obviously, these nucleomorph-encoded plastid-directed proteins must have a targeting mechanism in order to cross the two membranes surrounding their plastid. As one might guess, these proteins do have an N-terminal extension reminiscent of the transit sequence of higher plants (Douglas, Zauner et al. 2001), but differ in that these leaders contain almost twice as much asparagine and lysine as serine and threonine (Fig. 1.2.2). The preparation of import-competent chloroplasts from cryptomonads, surrounded by only two membranes, allowed a direct test of the similarity between the nucleomorph N-terminal extension and higher plant transit sequences. While nucleomorph-encoded proteins were efficiently imported, nuclear-encoded proteins truncated to remove the hydrophobic signal peptide were not (Wastl and Maier 2000). This result suggests there are two distinct import pathways for traversing the two inner membranes. Perhaps nuclear-encoded proteins employ vesicular shuttling while nucleomorph-encoded proteins require protein translocators in both of the two remaining membranes.

1.2.9. Protein import into the secondary plastids with four membranes and no CER

The other category of four membrane-bound plastids is found in the apicomplexans and the chlorarachniophytes. These plastids lack CER, meaning the outer most membrane is not continuous with the ER and ribosomes have never been observed. The phylum Apicomplexa is a group of obligate endoparasites with members such as *Toxoplasma* and *Plasmodium* that contain a non-photosynthetic secondary plastid termed an apicoplast (McFadden, Reith et al. 1996; Kohler, Delwiche et al. 1997) thought to be involved in fatty acid biosynthesis (Waller, Keeling et al. 1998), isoprene formation and haem synthesis (Ralph, Van Dooren et al. 2004). Chlorarachniophytes contain a nucleomorph between their two middle membranes which is a remnant of a green algal nucleus (Van

de Peer, Rensing et al. 1996), but to date has not yet been found to contain any protein translocator components (Gilson and McFadden 2002).

The leader sequence of proteins targeted to the plastids of this group is not structurally different from that directing proteins to the plastids containing a CER, as it is composed of a signal peptide followed by a transit peptide. Most of the work in this group has focused on protein targeting to apicoplasts because they can be transformed and have an important impact on human health (DeRocher, Hagen et al. 2000; van Dooren, Waller et al. 2000; Waller, Reed et al. 2000). The leader sequence contains a typical hydrophobic signal sequence, suggesting that the plastid-directed proteins enter the secretory system through the ER, while the transit peptide contains an abundance of asparagine, lysine and basic amino acids (Foth, Ralph et al. 2003). This transport system differs from that used by the CER-type plastids, in which the ER and the outer membrane of the plastid are connected, in that the apicoplast targeted proteins require a separate step of vesicular transport to arrive at the apicoplast. These proteins must somehow be sorted from the rest of the secretory proteins and get transported to the outermost membrane of the apicoplast. Two different routes for protein trafficking to the apicoplasts have been proposed to account for this. One proposed route for protein transport considers the apicoplast to be an alternate end point of the secretory pathway. As a consequence of this, one might expect proteins to be transported in vesicles from the ER to the Golgi where they can be sorted from other proteins by an unknown transit-peptide recognition factor. However, so far there is no evidence that supports a role for the Golgi in the transport process. In particular, protein transport to the apicoplast is not blocked by Brefeldin A (Joiner and Roos 2002).

In the other proposed route, the apicoplasts are proposed to lie prior to the point where proteins flowing through the secretory pathway are sorted. This considers the apicoplast as a part of the default pathway, and suggests that all proteins in the secretory pathway must then pass through the outer membrane space of the apicoplast. Proteins lacking the transit peptide would continue their passage via vesicle budding from the apicoplast outer membrane, while proteins possessing the transit peptide will be drawn in. Recently, a rule-based predictor tool named PlasmoAP (*Plasmodium falciparum* apicoplast-targeted proteins) has been designed in order to predict the apicoplast-targeted proteins from the

Plasmodium falciparum genome. Unlike the hydroxylated amino acid-rich transit peptides of higher plants, the apicoplast targeting sequences are rich in asparagine, lysine and basic amino acids (Foth, Ralph et al. 2003). It has been suggested that this positively charged transit peptide is electrophoretically pulled into the apicoplast lumen by a series of negatively charged transmembrane pores (possible duplicate of the Toc protein complex) (van Dooren, Schwartzbach et al. 2001; Foth, Ralph et al. 2003). This characterization provides a useful tool to screen out possible protein translocators in the apicoplast. For example, the hypothetical *Plasmodium* protein (NP_703634) shares 26% sequence identity over 272 amino acids with Tic22 of *Guillardia theta* and has an N-terminal hydrophobic signal peptide followed by a regions rich in asparagines and lysine. Clearly, this is a good candidate for a plastid translocation complex component in these organisms. So far, however, no other unambiguous translocator components have come to light in the Apicomplexan genome, although 466 proteins from the total 5282 proteins of *P. falciparum* are predicted to be targeted to the apicoplast (Foth, Ralph et al. 2003). The closest match lies with a hypothetical *Plasmodium* protein (gi 23619599) that shares weak similarity (1 e^{-7}) to Toc159 from pea and has a leader sequence appropriate for plastid targeting. Genomic data mining thus has considerable potential to identify translocator candidates, although all candidates will require rigorous testing to establish a real involvement in translocation.

1.2.10. Conclusions

Cells rely on protein translocators to maintain the functional identity of each of their different membrane-bound compartments. In simple systems, such as the two compartments of cyanobacteria, several protein translocators (the SecY and TatC complexes) and several types of targeting signals (hydrophobic regions in the leader sequence or other regions in the mature protein) are involved. In more complex systems, such as photosynthetic eukaryotes, the problem is even more acute as other compartments in the host could compete with those inside the plastid. Cells with primary plastids appear to have resolved this problem by conscripting cyanobacterial protein translocators (such as synToc75) and overlaying a transit signal rich in hydroxylated amino acids (such as the original synToc75 substrate) to the N-terminal end of plastid-directed proteins. This new protein translocation system for eukaryotes was distinct from the SecY and TatC systems used for targeting proteins to the thylakoids, allowing the elements of the thylakoid targeting mechanism used by the ancestral prokaryotic symbiont to be conserved. In an analogous manner, cells with secondary plastids have overlaid yet another targeting signal on to the N-terminal end of the protein. This latest system used the same hydrophobic signal and translocator complex initially used for protein export by the ancestral prokaryotic symbiont. The additional membranes separating the host cytoplasm from the thylakoids allowed this system to be used without any possible confusion as to the destination of the protein.

It seems likely, therefore, that a limited number of protein translocating systems have arisen throughout evolution. Genomic sequencing efforts should thus prove very informative with respect to determining which translocators will have homologs in the nuclear genomes of algae with secondary plastids. The characterization of the protein components to the import pathway will provide an unambiguous picture of which pathways are evolutionarily conserved and which have been derived *de novo*. However, some problems still remain to be resolved. First, for those plastids with CER, how do proteins get across the second membrane? And for those plastids without it, how do proteins get to the plastid from the ER? This later question is even more acute in the three-membrane bound plastids, where transport vesicles appear to have the bulk of the protein rather than a targeting signal in the cytoplasm. So, while we have come far in our

understanding of protein import into complex plastids, there is still a long way to go. Fortunately, getting there really is half the fun.

Table 1.2.1. Protein components to membrane translocation systems in bacteria and plastids

	E. coli		Chloroplast				
					Thylakoid membrane		
	SecY	Tat/ΔpH	Outer membrane	Inner membrane	Sec	Tat/ΔpH	
Signal	Hydrophobic	-RR-Hydrophobic	S/T-rich transit peptide	S/T-rich transit peptide	Hydrophobic	-RR-Hydrophobic	
Signal Receptors	SecY	TatB TatC	Toc33/34	Tic22	cpSecY	Hcf106 cpTatC	
Translocator Channel	SecY SecE SecG	TatA TatB TatC TatE	Toc75 Toc159	Tic20 Tic32? Tic62 Tic110	cpSecY cpSecE	Tha4 (TatA) Hcf106 (TatB) cpTatC	
Soluble Components	SecA		Toc159		cpSecA cpSRP54		
Accessory Proteins	SecD SecF	TatD	Toc64	Tic55 Tic40? IAP100?			
Energy	SecA Ribosome	ΔpH	Toc34? Toc159?	Chaperon		ΔpH	

Figure 1.2.1. Schematic representation of plastid evolution. A typical eukaryote, containing both a nucleus and mitochondria, is proposed to have engulfed a cyanobacterial-like cell in the primary endosymbiotic event that eventually gave rise to all plastids. This original endosymbiont, surrounded by two membranes and a peptidoglycan wall (dotted line), presumably contained thylakoids dotted with phycobilisomes. Three groups of extant primary plastids are distinguished, those of green alga and higher plants (which have lost their phycobilisomes), those of the red alga, and those of the glaucophytes (which have retained the peptidoglycan wall). All have lost the outer bacterial membrane. In the different secondary endosymbioses, a photosynthetic eukaryote (either a red or a green alga) instead of a cyanobacterial-like cell was engulfed by a new eukaryotic host. Extant secondary plastids are surrounded by either three or four membranes, and in some cases contain a residual nucleus termed a nucleomorph derived from the original eukaryotic host. In several cases the outer membrane of the secondary plastid is contiguous with the ER of the new host. No secondary plastids have phycobilisomes, although cryptophytes do have phycobilin pigments inside the thylakoid lumen.

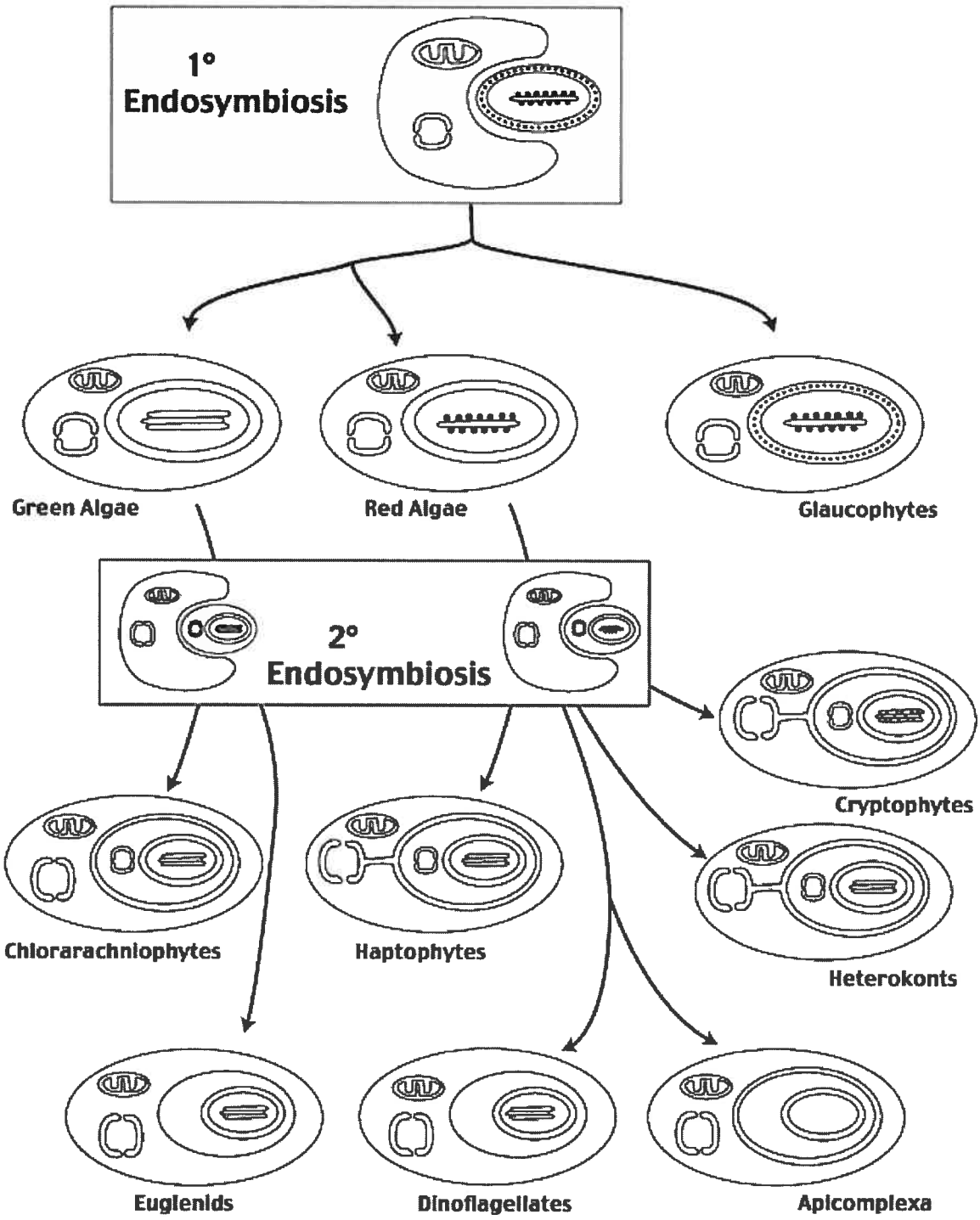
1°
Endosymbiosis
Green Algae
Red Algae
Glaucophytes
2°
Endosymbiosis
Cryptophytes
Chlorarachniophytes
Haptophytes
Heterokonts
Euglenids
Dinoflagellates
Apicomplexa

Figure 1.2.2. Schematic views of primary and secondary plastids and the known translocator components. The structure of known peptide leader sequences, and the compartment to which they are directed, is shown immediately below each schematic of the plastids or cyanobacteria. The sequences marked S/T are rich in the hydroxylated amino acids serine and threonine, N/K are rich in asparagine and lysine, Phob are rich in hydrophobic amino acids and the black triangles represent sites for proteolytic cleavage. The known protein translocators, and the membranes in which they are found, are shown where known for each group. The translocators include Toc complex components in the outer membrane, Tic complex components in the inner membrane, and the Tat and SecY pathways for import into the thylakoids. Chlorarachniophytes and cryptophytes contain a nucleomorph (NM), the remnants of the original endosymbiont nucleus in addition to the new host cell nucleus (N). A cyanobacterial cell is shown at top for comparison. The three groups of secondary plastids are those with four membranes lacking CER (top left), with four membranes with CER (right) and those with three membranes (bottom left).

Primary Plastids

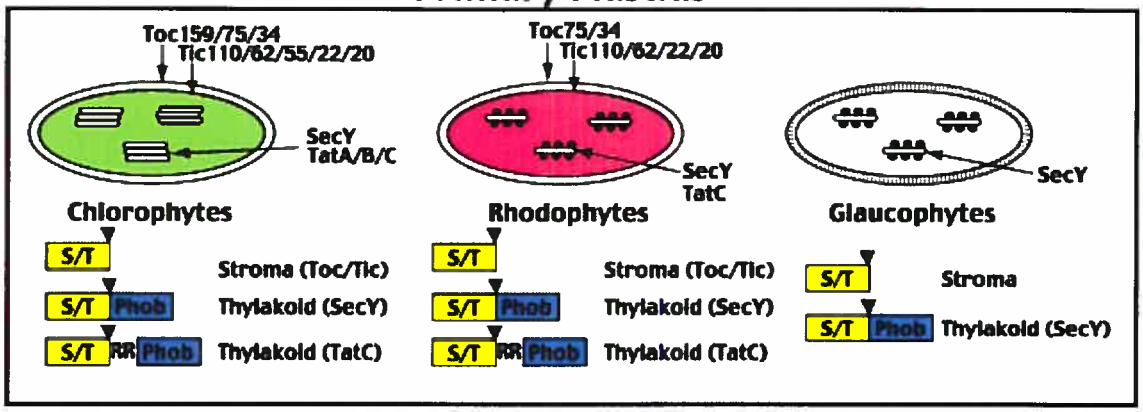

Secondary Plastids

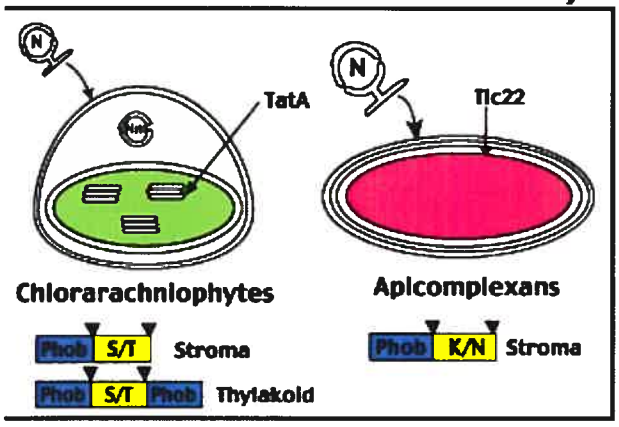

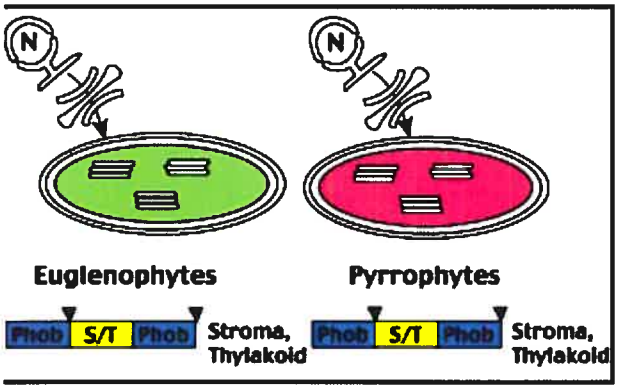

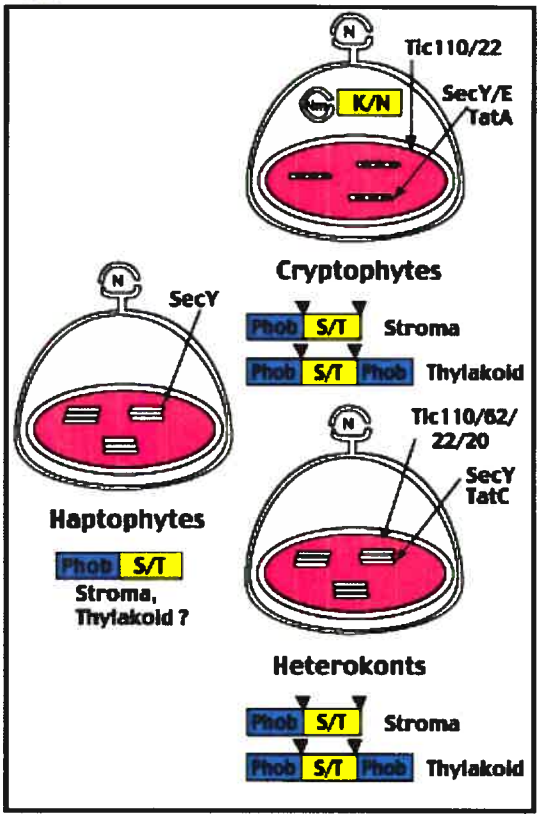

Chapter 2- publication #1

Circadian Changes in Ribulose-1,5-Bisphosphate Carboxylase/Oxygenase Distribution Inside Individual Chloroplasts Can Account for the Rhythm in Dinoflagellate Carbon Fixation

Nassoury, N., Fritz, L., Morse, D. 2001. Published in *Plant Cell.* 13, 923-934.

In this article we described a new mechanism for regulation of carbon assimilation in the context of cell biology. The observation that changes in sub-organelle localization of a protein are used to modulate its activity has never been reported prior to this work. We were able to show that the sequestration of Rubisco to one end of the plastids formed regions of distinct functions within one organelle (Carbon fixation vs. Oxygen evolution). This work formed part of the answer to the question raised by the discovery of a form II Rubisco in dinoflagellates.

All the experimental procedures were done by me except the double fluorescent labeling images that were taken by our collaborator Dr. Fritz, (Northern Arizona University) who has a well equipped microscopy lab and a special triple filter cube for simultaneous viewing of different colors of fluorescence after double labeling.

2.1. Abstract

Previous studies of photosynthetic carbon fixation in the marine alga Gonyaulax have shown that the reaction rates in vivo vary threefold between day and night but that the in vitro activity of ribulose-1,5-bisphosphate carboxylase/oxygenase (Rubisco), which catalyzes the rate-limiting step in this process, remains constant. Using protein gel blotting, we confirm that Rubisco protein levels are constant over time. We present simultaneous measurements of the rhythms of CO_2 fixation and O_2 evolution and show that the two rhythms are ~6 hr out of phase. We further show that the distribution of Rubisco within chloroplasts varies as a function of circadian time and that this rhythm in Rubisco distribution correlates with the CO_2 fixation rhythm. At times of high carbon fixation, Rubisco is found in pyrenoids, regions of the chloroplasts located near the cell center, and is separated from most of the light-harvesting protein PCP (for peridinin–chlorophyll *a*–protein), which is found in cortical regions of the plastids. We propose that the rhythm in Rubisco distribution is causally related to the rhythm in carbon fixation and suggest that several mechanisms involving enzyme sequestration could account for the increase in the efficiency of carbon fixation.

2.2. Introduction

Circadian rhythms are daily biochemical changes that are driven by circadian clocks but are not by themselves clocks. Biological clocks are characterized by transcriptional feedback loops that maintain their own oscillation (Dunlap 1999; Shearman et al. 2000) and that receive phasing information from changes in light intensity (Crosthwaite et al. 1997; Ceriani et al. 1999) or temperature (Liu et al. 1998) that allows them to synchronize their oscillations with natural environmental cycles. In contrast, circadian rhythms are changes in an organism's physiology or biochemistry that, although rhythmic under constant conditions, are incapable of independent oscillations and instead require the timing signals provided by circadian clocks.

A useful theoretical framework for understanding many biological rhythms is the notion that a central oscillator provides periodic regulatory signals that result in the control of a rate-limiting step (RLS) in a given biochemical pathway. Thus, understanding the regulation of the RLS is vital to understanding the clock's effect on organisms. For example, previous work on the bioluminescence rhythm in the dinoflagellate Gonyaulax has shown that both dinoflagellate luciferase (the reaction catalyst) and the luciferin (substrate) binding protein LBP contribute to the RLS of the nightly bioluminescence reaction. Cellular levels of both proteins vary seven- to 10-fold between day and night in phase with the 50- to 100-fold variations in bioluminescence capacity (Johnson et al. 1984; Morse et al. 1989a). In a vertebrate example, *N*-acetyltransferase catalyzes the RLS in vertebrate melatonin synthesis, and *N*-acetyltransferase levels correlate with the circulating melatonin rhythm (Gastel et al. 1998).

Rhythms are generally considered to reflect the differential expression of a target gene and may use components common to the clock's own transcriptional feedback loop, as with the vasopressin RNA rhythm (Jin et al. 1999), which appears linked to the rhythm in melatonin levels. On the other hand, transcriptional activators not involved directly in the clock mechanism also have been implicated in regulating target gene expression, as shown for the neuropeptide PDF (Renaud et al. 1983), which is believed to be linked to behavioral rhythms in Drosophila (Renn et al. 1999). It must be recognized, however, that changes in the amount of enzyme brought about by changes in gene expression are not the only way to regulate an enzyme's activity. In Bryophyllum, changes in

phosphoenolpyruvate activity appear to be due to post-translational modification (phosphorylation) of the enzyme (Nimmo et al. 1984).

In Gonyaulax, both oxygen evolution (Sweeney 1960) and carbon fixation (Hastings et al. 1961) are bona fide circadian rhythms. The oxygen evolution rhythm has been proposed to result from altered electron flux through photosystem II (Samuelsson et al. 1983). Although the control mechanism of this rhythm is not understood, it is possible that it may involve the soluble light-harvesting peridinin–chlorophyll *a*–protein (PCP), because this protein feeds energy primarily into photosystem II (Govindjee et al. 1979). Curiously, dinoflagellates are the only organisms known to use PCP in light harvesting, and the structure of this soluble protein is unlike that of any other light-harvesting protein (Norris and Miller 1994; Hofmann et al. 1996).

In addition to the unusual light-harvesting protein PCP, dinoflagellates also are the only known organisms whose chloroplasts contain a form II ribulose-1,5-bisphosphate carboxylase/oxygenase (Rubisco) (Morse et al. 1995; Rowan et al. 1996). The form II enzyme is composed of only large subunits and shares limited sequence identity with the form I enzyme (Narang et al. 1984). The lack of signal on protein gel blot analyses of dinoflagellate proteins using anti-form I Rubisco and the absence of a protein at the molecular weight expected for the small Rubisco subunit show that the form II enzyme is the only form of Rubisco found in dinoflagellates (Morse et al. 1995).

The form II Rubisco, like its form I homolog, catalyzes both the first carboxylation step in the Calvin cycle and the first oxygenation step in photorespiration. Oxygen is a competitive inhibitor of CO_2 binding to both forms of Rubisco, but the ratio of the reaction rate (v) with O_2 as a substrate and with CO_2 as a substrate (vO_2/vCO_2) in the form II enzyme in dinoflagellates and α-proteobacteria is five- and 10-fold greater, respectively, than the ratio in the form I enzyme in higher plants (Jordan and Ogren 1981; Whitney and Andrews 1998). Thus, the form II enzyme is more sensitive to competition by O_2 than is the form I enzyme, and both theoretical considerations (Whitney and Andrews 1998) and measurements of the growth of cyanobacteria engineered to express only the form II enzyme (Pierce et al. 1989) suggest that the form II Rubisco should not function efficiently in an oxygen-generating organelle.

Rubisco usually catalyzes the RLS in carbon fixation (Hartman and Harpel 1994); thus, it would appear to be a likely target for clock control of the carbon fixation rhythm. In previous studies, the in vitro activity of Gonyaulax Rubisco was shown to be constant (Bush and Sweeney 1972). As a caveat to this observation, however, dinoflagellate Rubisco is inactivated rapidly after extraction (Whitney and Yellowlees 1995), which may have compromised earlier measurements of Rubisco activity. To date, there are no indications that the activity of the form II enzyme can be modulated by a Rubisco activase, as is the case with the form I homolog (Hartman and Harpel 1994).

In the present study, we have confirmed the rhythmicity of the CO_2 fixation rhythm and measured its phase with respect to the O_2 evolution rhythm by measuring both simultaneously. We have used antibodies raised against dino-flagellate Rubisco to confirm that there are no changes in the cellular levels of Rubisco that could account for the rhythm of carbon fixation. We reasoned that if the amount or activity of Rubisco does not change as a function of time of extraction, differential substrate availability in vivo might be responsible for the biological rhythm. Thus, we used the anti-Rubisco and anti-PCP antibodies to document changes in the subcellular distribution of Rubisco that correlate with the rhythm in carbon fixation. The sequestration of Rubisco could produce an increase in CO_2 fixation if carbon-concentrating enzymes, none of which are yet known for dinoflagellates, were colocalized along with the Rubisco, or alternatively, if separation from the site of oxygen generation decreased the effective O_2 concentration near the oxygen-sensitive form II enzyme.

2.3. Materials and Methods

2.3.1. Antibody Preparation

All antibodies were raised in rabbits by Cocalico Biologicals (Reamstown, PA), using its standard operating protocol. The ribulose-1,5-bisphosphate carboxylase/oxygenase (Rubisco) antigen was prepared as a His-tagged fusion protein from a Rubisco cDNA (Morse et al. 1995) cloned into the pQE31 expression vector (Qiagen, Valencia, CA). The orientation of the insert was verified by polymerase chain reaction and restriction mapping. The insert was expressed in M15 cells and purified using nickel–nitrilotriacetic acid agarose resin affinity chromatography as described by the manufacturer (Qiagen). The anti-Rubisco titer was 1:20,000, as measured by ELISA, and the antibody was used at a dilution of 1:2000 for protein gel blots and 1:100 for immunocytochemistry. For ELISA, proteins were measured as OD_{490} after reaction with bicinchoninic acid (Pierce Chemical Co., Rockford, IL), whereas Rubisco was measured as OD_{650} after reaction with anti-Rubisco antibody, a peroxidase-labeled secondary antibody (Sigma), and the chromogenic substrate 3,3',5,5'-tetramethylbenzidine (Bio-Rad). Proteins for ELISAs were extracted in water using a beadbeater (BioSpec Products, Bartlesville, OK) and used immediately. For protein gel blots, primary antibodies were detected using either iodinated protein A (ICN Biomedicals Inc., Costa Mesa, CA) or the peroxidase-conjugated secondary antibody and a chemiluminescence substrate (Amersham).

The peridinin–chlorophyll *a*–protein (PCP) antigen was purified from *Gonyaulax polyedra* cells grown in f/2 medium (Morse et al. 1989b), using an ammonium sulfate precipitation method as described by Sharples et al. 1996, except that 100 mM Tris, pH 8, containing 10 mM EDTA and 50 mM DTT was used as the extraction buffer and a DEAE column replaced the cation exchange column. Brick-red fractions characteristic of peridinin were collected at each step of the purification, and the final DEAE eluate was purified further by preparative SDS-PAGE. The band at 32 kD was excised for immunization. The anti-PCP titer was 1:10,000, as measured by ELISA, and the antibody was used at a dilution of 1:1000 for protein gel blots and 1:100 for immunocytochemistry.

2.3.2. Microscopy

Cells during the middle of the day (6 hr after lights on, or light dark time 6) or night (6 hr after lights off, or light dark time 18) phase were harvested and fixed for immunocytochemistry by using standard methods. Fluorescent images of both fluorescein isothiocyanate (FITC)– and Texas red–labeled secondary antibodies (goat anti-rabbit conjugates) were captured with a Leitz Aristoplan light/fluorescence microscope (Wetzlar, Germany) equipped with a digital SPOT camera (Diagnostic Instruments, Sterling Heights, MI). Simultaneous fluorescence after double labeling was imaged through a triple filter cube (Chroma Tech, Brattleboro, VT) configured for UV (393/13 nm excitation, 458/15 nm emission), blue (485/16 nm excitation, 519/30 nm emission), and green (555/24 nm excitation, 602/40 nm emission) fluorescence. Captured images were imported directly into a personal computer operating with Windows 95 (Microsoft, Redmond, WA). Images were cropped and edited (for contrast and brightness only) in Adobe Photoshop 4.0 (Mountain View, CA). Cell samples taken in constant conditions were stained with anti-Rubisco antibody, and the position of the antibody was visualized with phase-contrast microscopy (to aid in visualization of the unstained plastids) after reaction with a peroxidase-conjugated secondary antibody (Sigma) and an enhanced 3,3' diaminobenzidine stain (Pierce Chemical Co.). Transmission electron microscopy was performed using a JEOL JEM 100S microscope operating at 80 kV. Immunostaining was performed as described (Fritz et al. 1990), with detection using 20-nm gold–conjugated secondary antibodies (Ted Pella, Redding, CA).

2.3.3. Photosynthetic Oxygen Evolution

Cell cultures of Gonyaulax (strain No. CCMP407; Provasoli-Guillard National Center for the Culture of Marine Phytoplankton, Boothbay Harbor, ME) were grown under a 12-hr-light/12-hr-dark (60 $\mu E \cdot m^{-2} \cdot sec^{-1}$ white fluorescent light) cycle at 18°C in f/2 medium as described by Guillard and Ryther 1962. O_2 evolution rhythms were measured from 200-mL cultures kept under constant white fluorescent light (60 $\mu E \cdot m^{-2} \cdot sec^{-1}$) by using an automated respirometer (Columbus Instruments, Columbus, OH). CO_2 fixation rhythms were measured for duplicate cultures by using conversion of ^{14}C-bicarbonate (ICN Biomedicals Inc., Costa Mesa, CA) to acid-insoluble material by five 10-mL aliquots of

cell culture under saturating white light (300 $\mu E \cdot m^{-2} \cdot sec^{-1}$). Hours under constant conditions can be converted to circadian time using a period length of 22 hr under these conditions. For instantaneous measurements of O_2 evolution and consumption rates, a 50-mL cell culture was concentrated to 1 mL by filtration on a 20-μm Nitex filter, and the O_2 concentration was monitored with a microelectrode for 20 min in darkness and then 20 min in white light (300 $\mu E \cdot m^{-2} \cdot sec^{-1}$). Cells in the concentrate were counted with a hemocytometer to correct for differences in cell number. Zero and full-scale end points for the calibration of these O_2 levels were set by a 10 mg/mL aqueous solution of sodium dithionite and by air-saturated water, respectively.

2.4. Results

2.4.1. Circadian CO_2 Fixation Is Phased Differently from O_2 Evolution

The two photosynthesis rhythms (CO_2 fixation and O_2 evolution) were measured simultaneously in cell cultures grown under constant conditions (Fig. 2.1). Both rhythms continue under conditions of constant light with an approximately threefold amplitude and similar periods (~22 hr under the light intensities used), thus representing bona fide circadian rhythms. However, the phases of the two rhythms are different, with maximum carbon fixation rates (Fig. 2.1, circles) preceding maximum oxygen evolution rates (Fig. 2.1, open squares) by ~6 hr. This suggests that different regulatory mechanisms may be involved in the control of these two photosynthesis rhythms. It is also noteworthy that the waveforms of the two rhythms differ as well, with carbon fixation approximating a sawtooth wave and oxygen evolution approximating a sine wave. Waveforms are an often overlooked aspect of biological rhythms that can be informative regarding the basic biochemistry underlying the rhythm. Thus, any explanation proposed for the rhythmicity of CO_2 fixation must be able to account for the sawtooth waveform.

2.4.2. CO_2 Fixation Rate Changes Are Not Due to Differing Rubisco Levels

To determine if the circadian rhythm in carbon fixation was due to changes in Rubisco gene expression, measurements of Rubisco levels over a daily period were required. We raised rabbit polyclonal antibodies to the dinoflagellate Rubisco and verified that these antibodies were specific by reaction with only a single protein on protein gel (immunoblot) analyses of whole-cell extracts (Fig. 2.2). As a control for use of the anti-Rubisco antibody in immunocytochemistry, we also prepared an antibody against the light-harvesting protein PCP. The anti-PCP antibody likewise is specific for its antigen on protein gel blot analyses. Control experiments either in the absence of primary antibody or using preimmune serum showed no reaction with Gonyaulax extracts (data not shown). The amount of immunoreactive Rubisco extractable from the cells at different times during a light/dark cycle was first assayed using protein gel blot analysis (Fig. 2.3A). A visual examination of the autoradiographs suggests that there are no marked changes in Rubisco protein levels, a conclusion supported by densitometric scans (Fig. 2.3D). This conclusion is supported by measurements of Rubisco levels at times corresponding to

maximum and minimum CO_2 fixation using ELISA (Fig. 2.3E). Because the amount of protein extracted for protein gel blots is approximately constant for the different times examined (Fig. 2.3C), and because the amount of anti-Rubisco antibody per microgram of protein does not vary between periods of maximum and minimum CO_2 fixation, we conclude that the threefold variation in the amplitude of the carbon fixation rhythm (Fig. 2.1) is not due to changes in the amount of Rubisco.

The same immunoblots also were tested for variations in PCP levels (Fig. 2.3B). PCP levels in cells grown under light/dark cycles vary up to twofold during the course of a day and thus provide a strong contrast to the measured Rubisco levels. Neither PCP nor Rubisco levels vary in cells extracted in constant conditions (data not shown).

2.4.3. Plastid Morphology Changes during the Light/ Dark Cycle

Gonyaulax plastids, viewed by light microscopy, undergo two distinct morphological changes. These changes are in (1) the proximity of the cortical end of the plastid to the plasma membrane and (2) the formation of specialized regions of the plastid, which are termed pyrenoids. The former can be observed in whole cells by using either fluorescence or visible light microscopy to visualize the endogenous fluorescence or absorbance, respectively, of chlorophyll. In cells taken in the middle of the day phase, the radially oriented chloroplasts are extended almost to the cell wall (Fig. 2.4A and Fig. 2.4B). In contrast, night-phase cells have shorter, more compact plastids. The cortical ends of the plastids are seen to be withdrawn from the cell periphery by both visible (Fig. 2.4G) and fluorescence (Fig. 2.4H) microscopy. Fluorescence microscopy also shows that the cytoplasmic region adjacent to the cell periphery of night-phase cells contains numerous scintillons that appear blue due to the endogenous fluorescence of the bioluminescence substrate luciferin.

The formation of pyrenoids cannot be observed in living intact cells and requires an examination of cell sections. To ensure that equivalent planes of sections were examined in all cases, we selected sections that contained two ends of the U-shaped nucleus. The U-shaped nucleus circles the midline of the alga, with the open end of the U corresponding to the site of flagellar attachment. The region of the cell within the U-shaped nucleus appears clear. In day-phase cells colored with aniline blue, pyrenoids are seen as slightly

bulbous inner regions of the chloroplasts (Fig. 2.4C, arrowheads) that surround this central clear area. Day-phase plastids often have a dumbbell appearance, with the inner expanded area comprising the pyrenoid; the outer expanded areas will be referred to as cortical regions. In contrast, sections from night-phase cells show none of these bulbous inner regions surrounding the central clear area (Fig. 2.4I), and the diameter of the plastids is relatively constant from the clear central region to the cell periphery.

2.4.4. Rubisco Is Localized in Pyrenoids in Day-Phase Cells

In many photosynthetic algae, pyrenoids contain form I Rubisco (McKay and Gibbs 1991). More recently, the form II Rubisco in the dinoflagellate Amphidinium also has been localized to pyrenoids (Jenks and Gibbs 2000). Because the formation of pyrenoids in both Euglena (Osafune et al. 1990), which contains form I Rubisco, and Gonyaulax (Schmitter 1971) is clock controlled, we reasoned that the form II Rubisco in Gonyaulax might be selectively sequestered into pyrenoids on a daily basis. Thus, we first determined whether Gonyaulax pyrenoids did, in fact, contain form II Rubisco.

Anti-Rubisco staining confirms that Rubisco is restricted to the pyrenoid region of day-phase plastids (Fig. 2.4D, arrowheads). In contrast, when plastids from night-phase cells are labeled similarly, Rubisco staining appears uniform over the entire surface of the plastid (Fig. 2.4J). As a control for the anti-Rubisco staining, we stained serial sections from both day-phase and night-phase cells with the anti-PCP antibody. In contrast to the anti-Rubisco staining, anti-PCP staining was less intense in the pyrenoids than in cortical regions of the day-phase chloroplasts (Fig. 2.4E). However, in night-phase cells, anti-PCP staining was distributed evenly over the surface of the plastid, as was found with the anti-Rubisco staining (Fig. 2.4K). No staining was observed for either day-phase or night-phase cells when preimmune serum replaced either the anti-Rubisco or the anti-PCP antibody (data not shown).

These observations suggested that the plastids of day-phase cells contained regions with different protein complements. To confirm this observation, we stained single sections sequentially with the anti-PCP antibody, a fluorescein isothiocyanate (FITC)–conjugated secondary antibody, the anti-Rubisco antibody, and a Texas red–conjugated secondary antibody. Double-labeled sections of day-phase cells show two distinctly colored regions,

indicating limited overlap between Rubisco and PCP (Fig. 2.4F). Cortical regions of the plastids are green, indicating that little Rubisco is present, whereas pyrenoids are reddish orange, indicating that some PCP is present. The yellow color of the cell wall and of the condensed chromosomes in the two ends of the U-shaped nucleus is due to nonspecific binding of approximately equal amounts of the secondary antibodies; thus, it is significant that little yellow is observed in the plastids. In contrast, when night-phase cell sections were stained sequentially with anti-Rubisco and anti-PCP antibodies, all regions of the plastids were similarly colored, and there were more regions with a yellow color than were found in day-phase plastids (Fig. 2.4L).

2.4.5. Quantitative Measurements of Protein Distribution

To confirm and quantitate the unequal distribution of Rubisco and PCP in day-phase cells, we used transmission electron microscopy (TEM) to count the number of gold-labeled secondary antibodies bound to the sections. In TEM, pyrenoids can be seen to contain widely spaced (0.2 μm) thylakoid membranes, which appear white because the samples were not treated with osmium to preserve their antigenicity. The amount of Rubisco staining in the pyrenoids (Fig. 2.5A), estimated by the number of gold particles per μm^2, is 15- to 20-fold greater than that found in chloroplast regions near the cell periphery (Table 2.1). Thylakoid membranes are not visible in the cortical regions of this plastid because the plane of the section runs parallel to the thylakoids (rather than perpendicular, as in the pyrenoid region). However, this section contains a cortical region of an adjacent plastid sectioned perpendicular to the thylakoids (0.07 μm spacing; immediately to the right of the pyrenoid in Fig. 2.5A). This finding confirms that the absence of Rubisco labeling is not related to the thylakoids themselves. Because pyrenoids typically represent one-third of the total area of chloroplasts, we calculate that ~90% of the cellular Rubisco is found within the pyrenoid. In contrast, after anti-PCP staining, gold particles can be detected throughout the length of the chloroplast (Fig. 2.5B), although the staining intensity (number of gold particles/μm^2) is two- to threefold greater in the cortical regions of the chloroplasts than in the pyrenoids (Table 1). Again, taking into account the larger proportional area of the cortical regions, we calculate that

these areas contain ~80% of the total PCP. No staining is observed if preimmune serum replaces either of the two antisera (data not shown).

Closer examination of the labeling patterns of anti-Rubisco and anti-PCP antibodies indicated that Rubisco was associated with the darker-stained stroma, whereas PCP was associated with the lighter-stained thylakoids. This difference in the suborganellar distribution of the two proteins was confirmed by higher magnification micrographs. In these, pyrenoid regions of day-phase plastids were examined, because the greater spacing between thylakoid membranes allowed a more accurate determination of gold particle distribution. We observed 10-fold more anti-Rubisco labeling over the stroma than over the thylakoids (Fig. 2.5C and Table 2.2). This staining is in good agreement with the observation that Rubisco is found in the pyrenoid stroma in many algae (McKay and Gibbs 1991) and with Rubisco distribution in the dinoflagellate Amphidinium (Jenks and Gibbs 2000). In contrast, more than half of the anti-PCP staining is associated unambiguously with the thylakoid membranes, and less than one-quarter of the label is found unambiguously in the stroma (Fig. 2.5D and Table 2.2). A thylakoid location of PCP is in agreement with the presence of the inner thylakoid membrane lipid digalactosyl diacyl glycerol in the crystal structure of the protein (Hofmann et al. 1996).

There is no difference in the suborganellar distribution of the two proteins in night-phase cells (data not shown), although these measurements are more difficult due to the fact that the thylakoid membranes are generally closer together than when pyrenoids are present (see below). There is also no difference in the amount of anti-PCP label per unit length of the thylakoid membranes inside the pyrenoid or in the cortical regions of the plastid (data not shown). Together, these observations suggest a possible link between the asymmetrical distribution of Rubisco and PCP in day-phase plastids. Because thylakoid spacing is two- to threefold greater in the pyrenoids than in more cortical regions of the plastids, a thylakoid protein might be expected to decrease in labeling by the same factor, exactly as observed (Table 2.1). It appears that an increase in the abundance of a stromal protein such as Rubisco occurs at the expense of a thylakoidal protein such as PCP.

TEM confirms that pyrenoids, as distinguished by the widely spaced thylakoid membranes, are absent from night-phase cell plastids. Instead, thylakoid spacing is constant everywhere, and there is a uniform density of gold particles over the surface of

the plastids after either anti-Rubisco (Fig. 2.5E) or anti-PCP (Fig. 2.5F) labeling. The plastid in Fig. 2.5E was chosen for its similar morphology to the plastid in Fig. 2.5F, despite a generally lower amount of labeling in this particular experiment.

2.4.6. Rubisco Distribution Correlates with Carbon Fixation Efficiency

To determine if the daily changes in the distribution of Rubisco or PCP within the plastid were correlated with either CO_2 fixation or O_2 evolution, respectively, we examined the anti-Rubisco staining of cell sections (Fig. 2.6) taken at different times. The specific times chosen are from the experiment shown in Fig. 2.1 (shaded circles). The sharp increase in carbon fixation rates correlates with the movement of Rubisco toward a developing pyrenoid, whereas the maximum ability of the cells to fix carbon correlates with complete pyrenoid formation. We observe that pyrenoids also are evident in cells when carbon fixation rates are decreasing, but note that at these times, the rate of O_2 evolution is increasing. These observations suggest that the increased O_2 evolution may have a detrimental effect on carbon fixation. Finally, when carbon fixation rates are at a minimum, pyrenoids are not observed and Rubisco is spread out over the surface of the plastid.

2.5. Discussion

We have shown that in the dinoflagellate Gonyaulax, Rubisco and PCP are found in different regions of the day-phase plastid and are spread over the surface of the plastid during the night phase (Fig. 2.4 and Fig. 2.5). Because PCP represents a marker for light-harvesting reactions and Rubisco represents a marker for carbon fixation, the separation of these two proteins suggests that day-phase plastids have specialized regions for the light and dark reactions. We also have shown that the sequestration of Rubisco into pyrenoids correlates with an ability of the cells to fix carbon more efficiently than when the proteins are distributed evenly over the plastids (Fig. 2.1 and Fig. 2.6). Because there is no rhythm in the amount of Rubisco that can account for the CO_2 fixation rhythm (Fig. 2.3), we propose that the changes in the subcellular distribution of Rubisco might contribute to the biological rhythm of CO_2 fixation. There is precedence among dinoflagellates for the idea that changes in the subcellular localization of an enzyme can regulate the rate of the reaction it catalyzes. For example, the luciferase-containing organelles responsible for bioluminescence in the dinoflagellate *Pyrocystis fusiformis* have been shown to move from a central location in the cytoplasm to the cell periphery, in phase with the onset of bioluminescence (Widder and Case 1982). Interestingly, the amount of luciferase in this alga is constant over time (Knaust et al. 1998), as are the levels of Rubisco in Gonyaulax (Fig. 2.3). However, luciferase distribution in Pyrocystis changes within the cytoplasm, whereas Rubisco localization in Gonyaulax changes within an organelle.

Many circadian changes have been noted in the ultrastructure of dinoflagellate chloroplasts. These include the packing of chloroplasts near the cell surface, the maximum length of the plastids, the spacing between thylakoid membranes in the region of the pyrenoids, and the daily formation of the bulbous centrally located pyrenoids (Herman and Sweeney 1975; Rensing et al. 1980). Although we have not measured all of these parameters simultaneously with the measurements of the two photosynthetic rhythms, some seem more likely than others to be related to changes in O_2 evolution. However, we have measured the pyrenoid formation rhythm and found a good correlation between it and the CO_2 fixation rhythm. Given the presence of Rubisco in the pyrenoid

and the potential of this enzyme to act as the RLS of carbon fixation, it seems likely that the microenvironment surrounding the Rubisco is important for its activity.

If Rubisco sequestration into pyrenoids is implicated in carbon fixation, is PCP abundance in cortical regions of the plastids implicated in oxygen evolution? We have observed that the rhythm in PCP distribution appears to mirror the rhythm in Rubisco distribution, presumably due to the wider spacing between thylakoids found in the pyrenoids (Fig. 2.5) and the different suborganellar locations of the two enzymes (Table 2). We also observed that the onset of the two physiological rhythms is ~6 hr out of phase (Fig. 2.1). Because the phases of the PCP and Rubisco distribution rhythms are similar and the phases of the oxygen evolution and carbon fixation rhythms are different, it seems unlikely that PCP distribution plays a role in the oxygen evolution rhythm. We suggest that the changes in PCP distribution represent instead a consequence of Rubisco distribution changes.

We have shown that changes in the in vivo activity of Rubisco, as measured by the rate of carbon fixation, cannot be due to changes in the amount of protein (Fig. 2.3). We also have shown that there are no differences in the distribution of various Rubisco isoforms, as determined by two-dimensional electrophoresis (Markovic et al. 1996), suggesting that the enzyme does not undergo post-translational modifications during the daily period. To date, there is no evidence that Rubisco activase can act on the form II Rubisco (Hartman and Harpel 1994) or that dinoflagellates contain the form I enzyme (Morse et al. 1995). Therefore, it seems probable that the changing reaction rates in vivo reflect changes in substrate concentrations.

The metabolic consequence of the competition between O_2 and CO_2 for the active site of Rubisco is that the net rate of carbon fixation depends on the concentration of both rather than on the concentration of CO_2 alone. In C_4 plants and many algae, the vO_2/vCO_2 ratio is biased toward carbon fixation by CO_2-concentrating mechanisms (CCM) (Badger et al. 1998). CCM in the dinoflagellate Symbiodinium depends on the energy derived from photosynthetic electron transport to move inorganic carbon into the cell against a concentration gradient (Badger et al. 1998). However, in Gonyaulax, the phase of the electron transport rhythm, as measured by O_2 evolution, lags behind the CO_2 fixation rhythm by 6 hr (Fig. 2.1). Therefore, CO_2 concentration by this mechanism cannot

explain how CO_2 fixation rates increase sharply at times when O_2 evolution rates remain low (Fig. 2.1, circadian time 20 to 22). Of course, our data do not rule out the presence of a CCM in Gonyaulax, and it is possible that carbon-concentrating enzymes may be sequestered into pyrenoids at the same time as the Rubisco. Unfortunately, there is insufficient information available regarding CCM in dinoflagellates to investigate this possibility fully. On the basis of the fact that the onset of carbon fixation precedes the onset of oxygen evolution, we conclude that the possibility that Rubisco movement and the accompanying increase in carbon fixation rates could be due to an increase in photosynthetic electron transport can be excluded.

It is also possible that the sequestration of Rubisco into pyrenoids affects its activity without involving CO_2 concentrations. For example, a decrease in the relative reaction rates using either O_2 or CO_2 as a substrate (vO_2/vCO_2 ratio) could be achieved by a decrease in the oxygen tension as well as by an increase in the CO_2 concentration. In this regard, it is interesting that in *Amphidinium carterae,* the pyrenoid persists during the dark phase (Matthys-Rochon 1979), and that the amount of Rubisco in the pyrenoid increases as a function of the light intensity (Jenks and Gibbs 2000). These findings suggest that Rubisco in this organism may be sequestered in response to increased oxygen tension, a situation clearly different from that in Gonyaulax, in which pyrenoid formation occurs rhythmically as a circadian clock–controlled process under constant light (Fig. 2.6).

Is it reasonable that a spatial separation of Rubisco and PCP could decrease the local oxygen tension and thus increase the rate of carbon fixation? The net oxygen concentration in the region of the pyrenoids is not known, but it will be a function of the diffusion rate into the cell, the photosynthetic oxygen evolution rate, and the respiration rate. We have measured the mean oxygen consumption rate of cells in darkness as 62% (SD = 11, n = 15) of the oxygen evolution rate of illuminated cells (300 $\mu E \cdot m^{-2} \cdot sec^{-1}$ cool-white light), averaged from several different times during a light/dark cycle. These values represent the high end of the range reported previously for this organism (30 to 60%; Prezelin et al. 1977). Given the spherical geometry of the cells, more photosynthetically produced oxygen should diffuse out into the medium than in toward the cell center. Thus, assuming the same respiration rate in light and darkness and the same amount of oxygen

diffusing inward as outward, the measured respiration rate could serve to decrease the oxygen tension in the area of the pyrenoids. Presumably, this respiration occurs in the many mitochondria that are found distributed throughout the cytoplasm from the pyrenoids out to the cell periphery (Schmitter 1971).

What is the mechanism responsible for the separation of Rubisco and PCP? We hypothesize that aggregates of Rubisco in day-phase plastids fill the stroma and push apart the thylakoids to form pyrenoids. Because the PCP labeling along each thylakoid is constant but the thylakoids are approximately three times more densely packed in the plastid periphery, the rhythm in PCP distribution is derived directly from pyrenoid formation. One model to explain this fact could involve active recruitment of Rubisco to a developing pyrenoid, perhaps using prokaryotic-type cytoskeletal elements known to be present in plastids (Lutkenhaus and Addinall 1997; Osteryoung et al. 1998). A second possibility is that thylakoid membranes are brought into close physical association in cortical regions of the plastid, which forces Rubisco down toward the cell center in a manner similar to the extrusion of toothpaste from a toothpaste tube. However, there is little day/night variation in the distance between thylakoids in cortical regions of the plastid (Rensing et al. 1980), suggesting that the latter possibility is unlikely.

Irrespective of the mechanism of protein sequestration, our results show that the sequestration of Rubisco into pyrenoids is the result of a bona fide circadian rhythm. This rhythm correlates with the rhythm in carbon fixation, and we propose that there is a causal link between the two. A link is plausible if the separation of Rubisco from the site of oxygen generation reduces the internal oxygen tension in the region of the pyrenoids and thus reduces competition by oxygen for the active site of the form II Rubisco in dinoflagellate plastids.

Table 2.1. PCP and Rubisco Distribution within Day-Phase Plastids[a]

	Label Density (Gold Particles/μm^2)	
Location within Plastid	PCP	Rubisco
Cortex	19 ± 6 (5998)	3 ± 2 (1629)
Pyrenoid	8 ± 0.3 (629)	41 ± 12 (3136)
Pyrenoid/cortex	0.5 ± 0.12	11 ± 4

[a] Values shown are mean ±SD (number of gold particles).

Table 2.2. Suborganellar Distribution of PCP and Rubisco[a]

Location within Plastid	Percentage of Total Label	
	PCP	Rubisco
Thylakoid	54 ± 6	10 ± 4
Undetermined	30 ± 6	10 ± 4
Stroma	16 ± 4	80 ± 8

[a] More than 1000 gold particles were counted for each antibody. The location of gold particles touching both stroma and thylakoid membranes was scored as undetermined because of the size of the primary and secondary antibodies as well as the gold particles.

Figure 2.1. Rhythms of CO_2 Fixation and O_2 Evolution Are Phased Differently.
The circadian rhythms of O_2 evolution (open squares) and CO_2 fixation (large, shaded circles) have the same period but differ in phase and waveform. Real time (in hours from the end of the last dark period) is shown at the bottom, and circadian time (based on a 22-hr period with 0 corresponding to dawn) is shown at the top. Large shaded circles in the CO_2 fixation rhythm represent times when samples of the cultures were fixed and embedded for subsequent immunolabeling experiments.

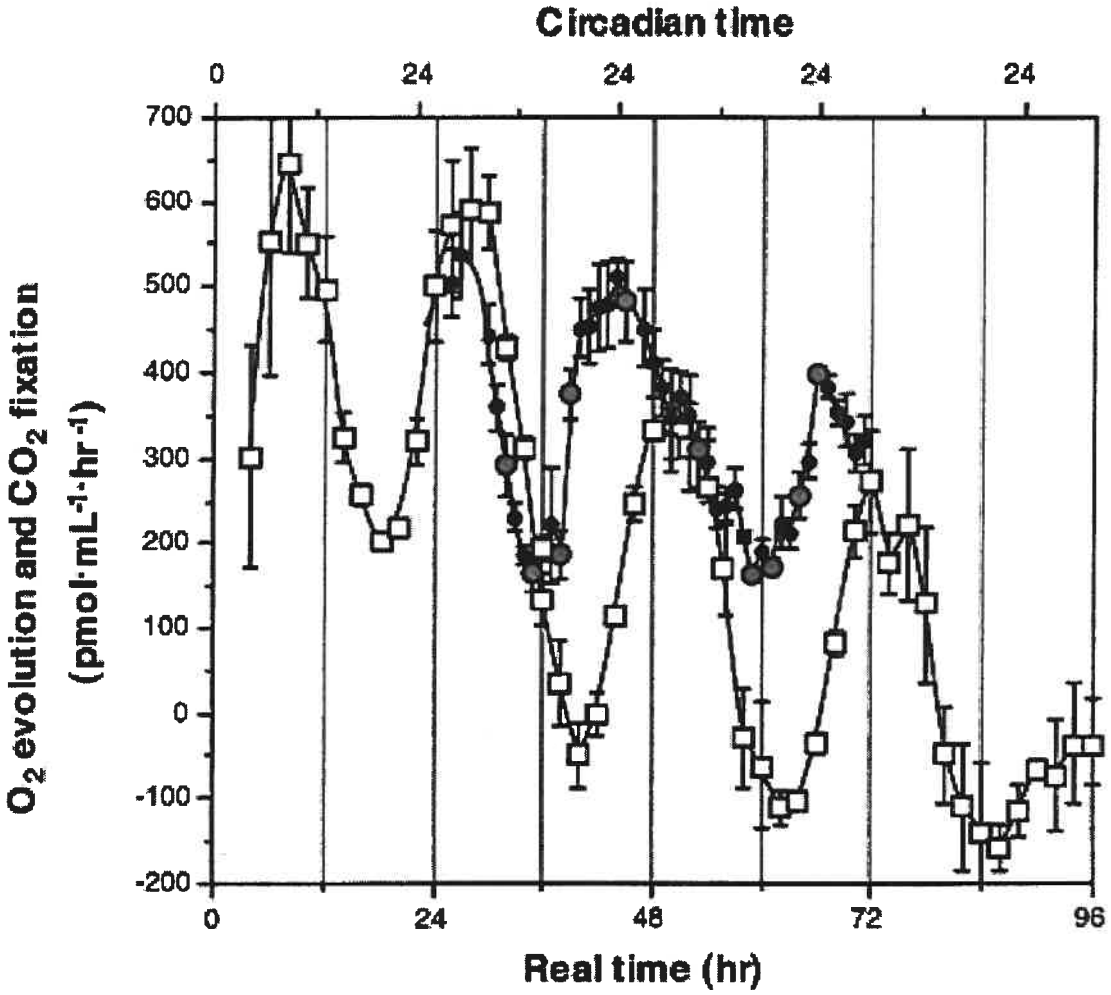
Circadian time
0
24
24
24
24
700
600
500
400
300
200
100
0
-100
-200
O_2 evolution and CO_2 fixation
(pmol·mL^{-1}·hr^{-1})
0
24
48
72
96
Real time (hr)

Figure 2.2. Specificity of Anti-Rubisco and Anti-PCP Antibodies on Protein Gel Blots. Crude extracts of Gonyaulax proteins stained with Coomassie Brilliant Blue after SDS-PAGE (lane second from left) show that Rubisco (55 kD) and PCP (32 kD) are major proteins in the cell and that only single proteins are recognized on protein gel blots by anti-Rubisco (Anti-RuBisCO, lane second from right) and anti-PCP (lane at right) antibodies. Molecular mass markers (in kilodaltons) are shown at left.

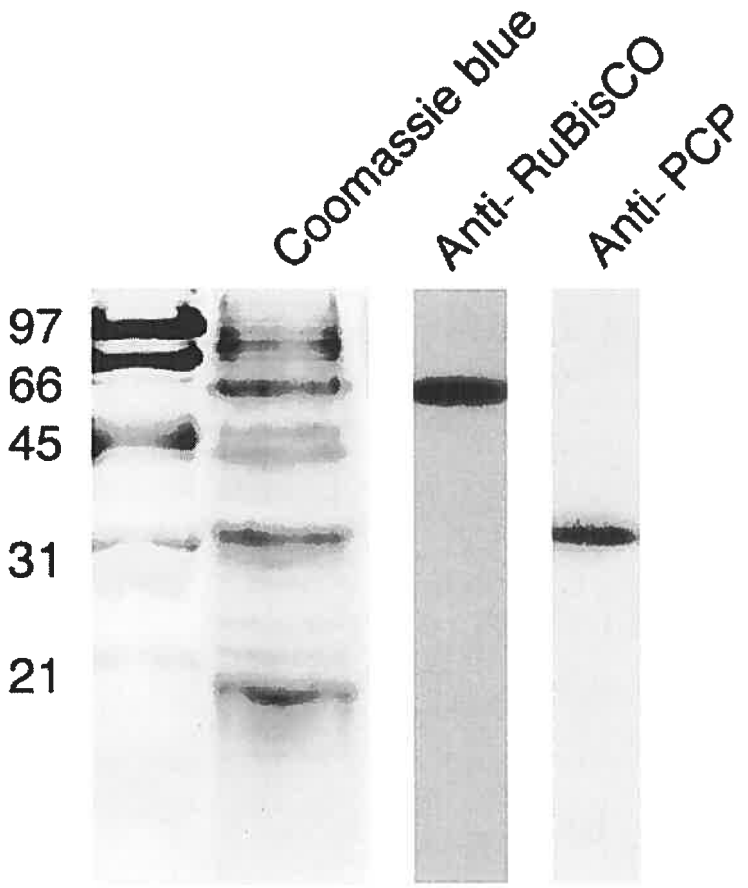
Coomassie blue
Anti- RuBisCO
Anti- PCP
97
66
45
31
21

Figure 2.3. Rubisco Levels Are Constant during the Daily Cycle.

Protein gel blots of extracts taken from 50 mL of Gonyaulax cell culture during 1 day (closed bar, dark period; open bar, light period). Numbers correspond to the time at which protein samples were taken.

(A) to **(C)** Anti-Rubisco staining **(A)** is constant, whereas anti-PCP staining **(B)** shows an approximately twofold variation. Ponceau red staining **(C)** was used as a control for protein load. Numbers at right indicate molecular weight.

(D) Densitometric scans of the anti-Rubisco staining in **(A)**.

(E) The cellular levels of Rubisco at times corresponding to either maximum (filled circles) or minimum (open circles) CO_2 fixation rates were determined by plots of immunologically reactive protein in ELISAs as a function of total soluble protein. Only the linear region of the dilution curve is shown. Error bars in **(D)** and **(E)** indicate ±SD.

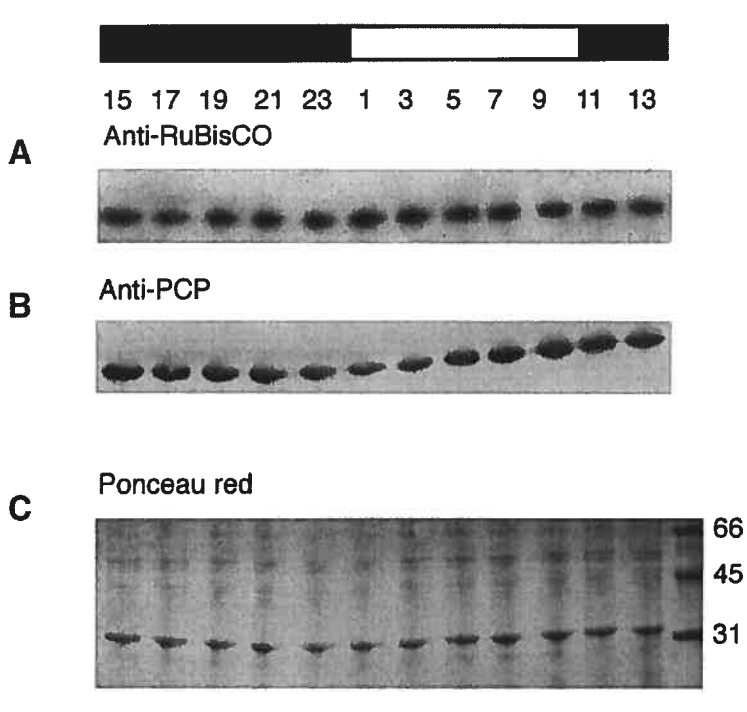
15 17 19 21 23 1 3 5 7 9 11 13
A
Anti-RuBisCO
B
Anti-PCP
C
Ponceau red
66
45
31

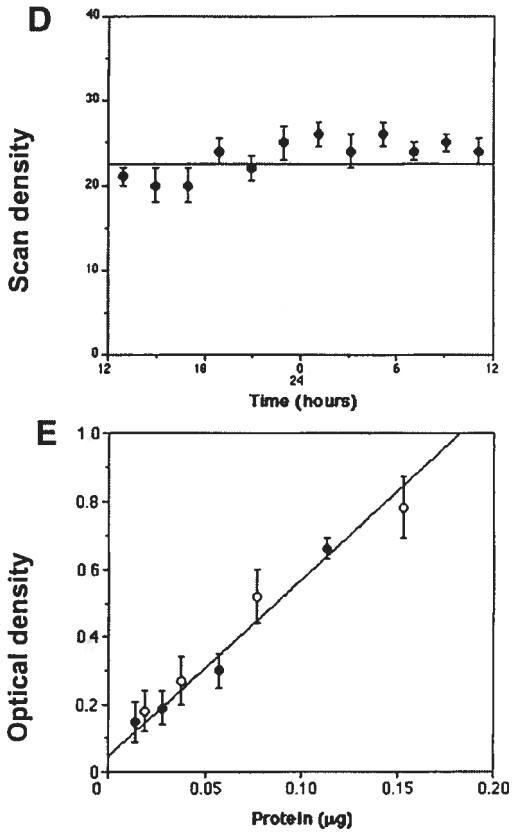
D
Scan density
Time (hours)
E
Optical density
Protein (µg)

Figure 2.4. Rubisco and PCP Distribution Is Different in Night- and Day-Phase Cells. Cells were taken during either the middle of the light period (light dark time 6; **[A]** to **[F]**) or the middle of the night phase (light dark time 18; **[G]** to **[L]**). Whole cells were examined by either UV fluorescence (**[A]** and **[G]**) or visible light (**[B]** and **[H]**). Cell sections were stained with aniline blue (**[C]** and **[I]**), anti-Rubisco antibody (**[D]** and **[J]**), or anti-PCP antibody (**[E]** and **[K]**). Antibody binding was visualized using fluorescently labeled secondary antibodies. To visualize the distribution of both proteins, serial sections were stained with the two antibodies separately (**[D]** and **[E]**, **[J]** and **[K]**). Alternatively, single sections were stained sequentially with anti-PCP antibody, an FITC-conjugated secondary antibody (green), anti-Rubisco antibody, and a Texas red–conjugated secondary antibody (**[F]** and **[L]**). A greenish yellow fluorescence due to nonspecific binding of both secondary antibodies in approximately equal amounts can be seen in the cell wall and in the permanently condensed chromosomes in both ends of the U-shaped nucleus. Arrowheads in **(C)** to **(F)** point to pyrenoid regions of the plastids. Cells are ~35 μm in diameter.

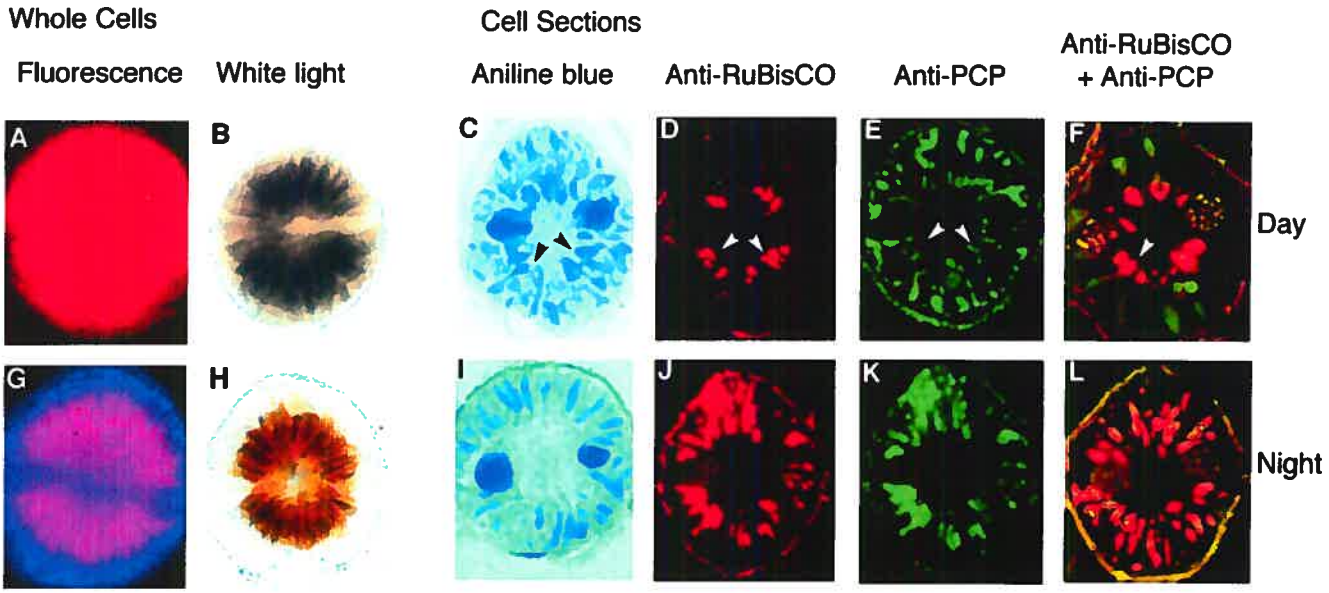
Whole Cells
Cell Sections
Fluorescence
White light
Aniline blue
Anti-RuBisCO
Anti-PCP
Anti-RuBisCO + Anti-PCP
A
B
C
D
E
F
Day
G
H
I
J
K
L
Night

Figure 2.5. Rubisco and PCP Are Found in Different Compartments.

Sections of cells from day-phase cells ([**A**] to [**D**]) and night-phase cells ([**E**] and [**F**]) were stained with anti-Rubisco antibody ([**A**], [**C**], and [**E**]) or anti-PCP antibody ([**B**], [**D**], and [**F**]). Antibody binding was visualized with gold-labeled secondary antibodies for TEM. Micrographs are oriented with the cortical (Cor) regions of the plastids at the top (Cell Wall) and the pyrenoid (Pyr) regions of day-phase plastids, with their widely spaced thylakoid membranes, at the bottom. Higher magnification of the pyrenoid regions places the anti-Rubisco labeling over the stroma (**C**) and the anti-PCP labeling over the thylakoids (**D**). Sections of night-phase cells show a uniform distribution of label after staining with either anti-Rubisco (**E**) or anti-PCP (**F**) antibody. Pyrenoid regions, with their widely spaced thylakoid membranes, are not observed in night-phase cells. Bars = 1 μm in all electron micrographs.

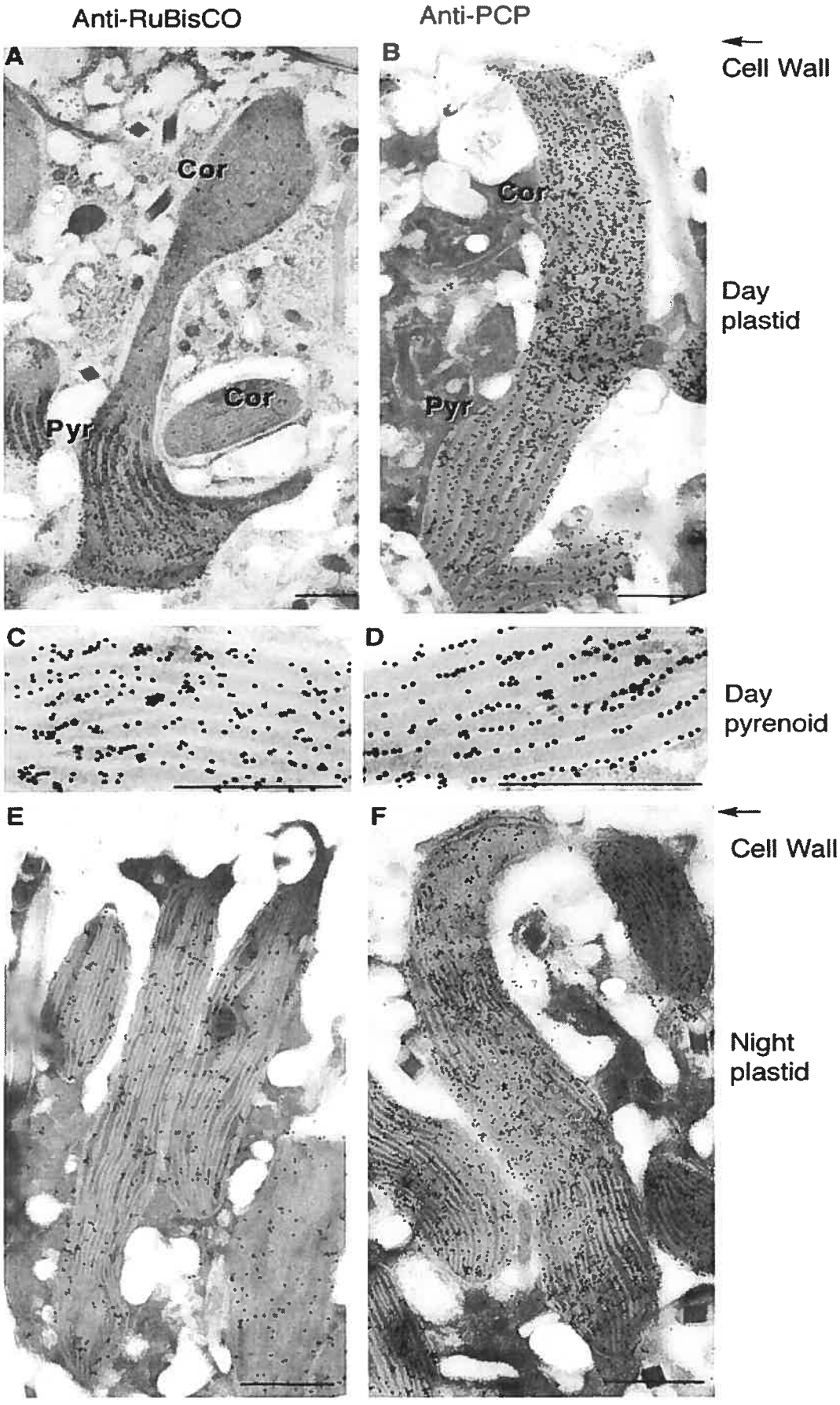
Anti-RuBisCO
Anti-PCP
A
B
Cor
Cor
Cor
Pyr
Pyr
Cell Wall
Day plastid
C
D
Day pyrenoid
E
F
Cell Wall
Night plastid

Figure 2.6. Rubisco Distribution in Plastids Correlates with the Circadian Rhythm in Carbon Fixation.

Cells fixed at times corresponding to decreasing, minimum, increasing, and maximum CO_2 fixation rates were sectioned and stained with anti-Rubisco antibody and a peroxidase-conjugated secondary antibody. The sampling times, indicated as circadian time (CT), are those corresponding to the large, shaded circles in Fig 2.1. Similar circadian times from the two circadian cycles are aligned vertically. Dark areas surrounding the clear central area correspond to anti-Rubisco staining in the pyrenoids (arrowheads). The decrease in CO_2 fixation rates at CT10 and CT11, despite the presence of pyrenoids, suggests that increasing O_2 evolution rates (see Fig. 2.1) are detrimental to CO_2 fixation.

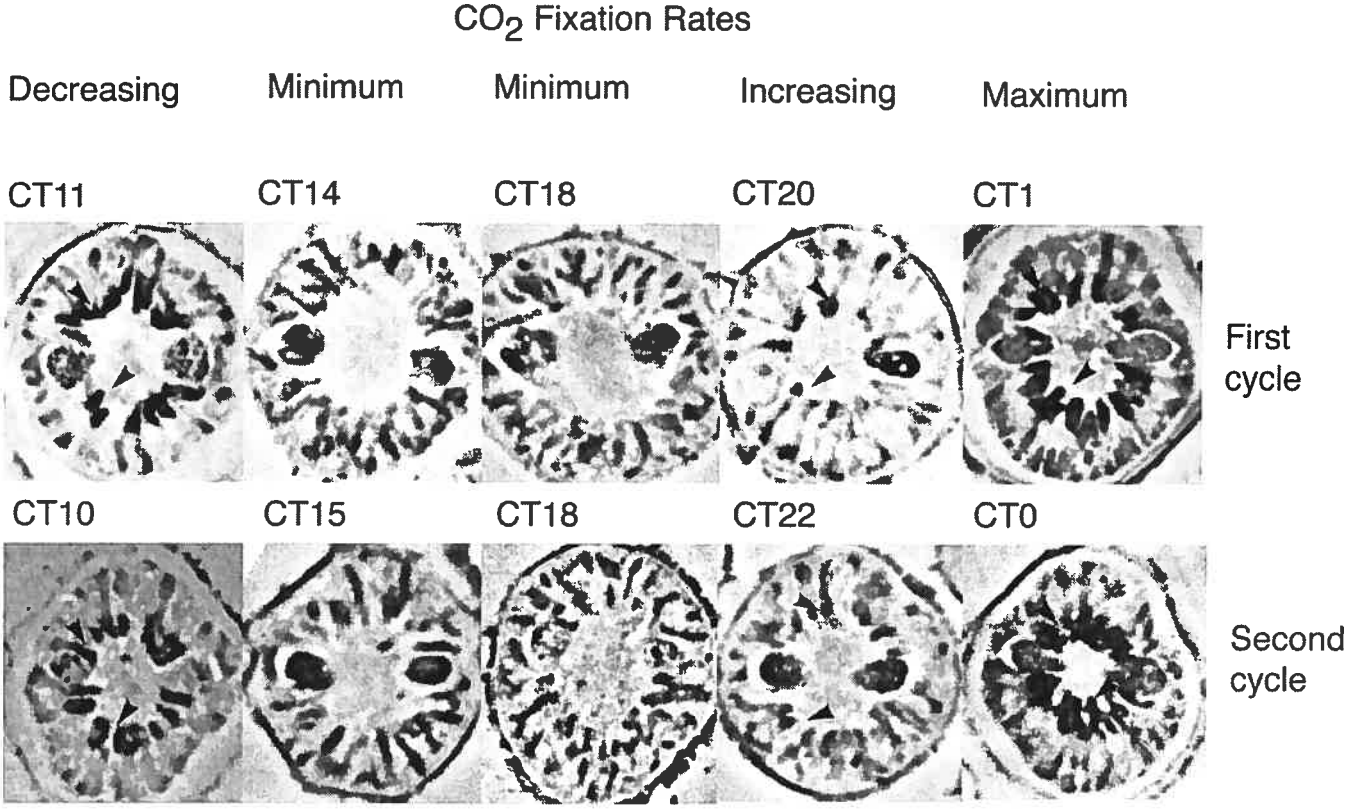
CO_2 Fixation Rates
Decreasing
Minimum
Minimum
Increasing
Maximum
CT11
CT14
CT18
CT20
CT1
First cycle
CT10
CT15
CT18
CT22
CT0
Second cycle

2.6. Acknowledgments

We thank L. Pelletier and T. Bertomeu for technical assistance, Drs. D. Layzell and G. Espie for helpful discussions, and Drs. S. Gibbs and M. Cappadocia for critical reviews of the manuscript. We gratefully acknowledge the financial support of the Natural Sciences and Engineering Research Council of Canada (D.M.) and Northern Arizona University organized research (L.F.).

CHAPTER 3- PUBLICATION #2

Plastid ultrastructure defines the protein import pathway in dinoflagellates

Nassoury, N., Cappadocia, M., Morse, D. (2003). Published in. *J. Cell Sci.* 116:2867-74.

This part of my Ph.D. work illuminates parts of the mechanism of protein targeting to the triple membrane bound organelles of dinoflagellates. Our results show that proteins arrive at the plastid with a small membrane-bound plastid transit sequence located inside the transport vesicle. This mechanism is akin to that of the phylogenetically distant Euglena (whose plastids are surrounded by three membranes) rather than to the phylogenetically related Apicomplexa (whose plastids are surrounded by four membranes). This study represent an example of the importance and the significant role that ultrastructure of an organelle can impose on the intracellular trafficking of the cell.

All the experimental procedures were done by me and Dr. Cappadocia supervised the plant transformations experiments.

3.1. Abstract

Eukaryotic cells contain a variety of different compartments that are distinguished by their own particular function and characteristic set of proteins. Protein targeting mechanisms to organelles have an additional layer of complexity in algae, where plastids may be surrounded by three or four membranes instead of two as in higher plants. The mechanism of protein import into dinoflagellates plastids, however, has not been previously described despite the importance of plastid targeting in a group of algae responsible for roughly half the ocean's net primary production. Here, we show how nuclear-encoded proteins enter the triple membrane-bound plastids of the dinoflagellate *Gonyaulax*. These proteins all contain an N-terminal leader sequence with two distinct hydrophobic regions flanking a region rich in hydroxylated amino acids (S/T). We demonstrate that plastid proteins transit through the Golgi in vivo, that the first hydrophobic region in the leader acts as a typical signal peptide in vitro, and that the S/T-rich region acts as a typical plastid transit sequence in transgenic plants. We also show that the second hydrophobic region acts as a stop transfer sequence so that plastid proteins in Golgi-derived vesicles are integral membrane proteins with a predominant cytoplasmic component. The dinoflagellate mechanism is thus different from that used by the phylogenetically related apicomplexans, and instead, is similar to that of the phylogenetically distant *Euglena*, whose plastids are also bound by three membranes. We conclude that the protein import mechanism is dictated by plastid ultrastructure rather than by the evolutionary history of the cell.

Key words: Dinoflagellate, Plastid, Nuclear-encoded protein, Protein import, Signal peptide

3.2. Introduction

Protein targeting towards the proper subcellular compartments is vital for the cell. For compartments surrounded by two membranes, nuclear-encoded proteins contain an N-terminal leader sequence that allows their targeting and post-translational translocation through both envelope membranes (Bruce, 2000; Strub et al., 2000; Vothknecht and Soll, 2000). In the case of higher plant chloroplasts, the acquisition of a chloroplast transit sequence allows the return to the plastid of proteins encoded by genes that were present in the original prokaryotic endosymbiont and were subsequently transferred to the eukaryotic host cell nucleus (Martin and Schnarrenberger, 1997; Martin et al., 1998). In some algae, however, plastids may be surrounded by either three or four membranes. These are thought to result from secondary endosymbioses (where a host cell acquires an eukaryotic endosymbiont already equipped with plastids), a hypothesis supported by differences in the molecular phylogeny of plastid and nuclear genes (Delwiche and Palmer, 1996; Morden et al., 1992). The transfer of genes with a chloroplast transit sequence from the nucleus of the primary endosymbiont to the nucleus of the secondary endosymbiont requires additional signals for correct targeting, which has led to the suggestion that the final composition of the leader sequence might recapitulate the evolutionary history of the plastid (McFadden, 1999). This is supported by analyses of leader sequences of plastid-directed proteins in the four membrane-bound plastids of haptophytes, crysophytes, apicomplexans and diatoms, all of which contain an N-terminal hydrophobic signal peptide (to target proteins to the ER) followed by a transit sequence which can direct proteins synthesized in vitro to purified plant plastids (van Dooren et al., 2001).

Several mechanisms are known for directing proteins to four membrane-bound plastids. In one mechanism, such as that used by haptophytes and diatoms, ribosomes are attached directly to the outer plastid membrane. After passage of the first (outermost) membrane, termed the chloroplast ER (Gibbs, 1981), proteins either cross the second membrane through large pores, or traverse the subsequent intermembrane space inside transport vesicles (van Dooren et al., 2001). In contrast to this mechanism, targeting to the four membrane-bound plastids of the apicomplexans does not involve ribosomes bound to the outer membrane, and indeed, many aspects of the mechanism are still unknown (van

Dooren et al., 2001). It is known that plastid proteins enter the ER membrane system using an N-terminal signal peptide, since constructs lacking the signal peptide produce a cytoplasmic protein (Waller et al., 2000). It is also known that a transit peptide, exposed after cleavage of the signal peptide, is required for entry into the plastid, as proteins lacking this transit peptide are secreted from the cell (Waller et al., 2000). However, several mechanisms have been suggested for targeting proteins to the outermost plastid membrane from the ER (van Dooren et al., 2001). One proposal is that all proteins entering the ER eventually pass through the outermost plastid compartment, and those destined to remain in the plastid bind to a receptor for the transit peptide. Alternatively, proteins may be specifically targeted to the outer plastid membrane directly from the Golgi. While the observation that plastid directed proteins lacking a transit peptide are secreted suggests passage through the Golgi, it must be stressed that this has not been directly shown.

Intriguingly, nuclear-encoded proteins destined for the triple membrane-bound plastids of *Euglena* clearly transit through the Golgi (van Dooren et al., 2001). Details of the mechanism differ, however, as in *Euglena* the plastid-directed leader sequences contain two hydrophobic regions separated by an S/T-rich region reminiscent of a plastid transit sequence (Henze et al., 1995; Kishore et al., 1993). In vitro studies have demonstrated that the plastid directed proteins remain inserted in the ER membranes, unlike the apicomplexans where the plastid proteins are soluble inside the ER (Kishore et al., 1993; Osafune et al., 1990; Sulli et al., 1999; Sulli and Schwartzbach, 1996). The second hydrophobic region present in the *Euglena* leaders is absent in apicomplexan leaders (Foth et al., 2003).

In contrast to the above, there are no reports describing the transport mechanism used by nuclear-encoded plastid proteins in dinoflagellates. This is an unfortunate gap in our understanding of protein import pathways as dinoflagellates, along with diatoms, constitute the bulk of the phytoplankton, and the oceans are responsible for roughly half the primary production of the biosphere (Field et al., 1998). The dinoflagellates contain members with several types of plastids, of which those containing the carotenoid peridinin are the most prevalent. The next most abundant type of plastids contains fucoxanthin, and these are proposed to share a common ancestor with the peridinin-

containing plastids (Yoon et al., 2002). Both types of plastids are surrounded by three membranes, and may thus employ a similar mechanism for protein import. On the one hand, this mechanism might be expected to be similar to that of apicomplexans because of their close phylogenetic relationship to the dinoflagellates (Sogin et al., 1996). On the other hand, protein import into dinoflagellate plastids might also be similar to that in *Euglena*, because the leader sequences of dinoflagellate plastid-directed proteins (Fagan et al., 1998; Le et al., 1997) are similar to those used by *Euglena.*

To distinguish between these two possibilities, we have characterized the import pathway into peridinin-containing plastids of the dinoflagellate *Gonyaulax polyedra.* We have studied import of two proteins for which we have previously raised antibodies (Nassoury et al., 2001), the carbon fixing enzyme Ribulose bisphosphate carboxylase/oxygenase (Rubisco) and the soluble light-harvesting peridinin-chlorophyll *a*-protein (PCP). Dinoflagellate Rubisco is unusual, in that it is a form II enzyme and is formed only of large 55 kDa subunits (Morse et al., 1995). This enzyme is synthesized as a polyprotein, which must be processed to form the mature large subunits by cleavage of small linker peptides (Rowan et al., 1996). The mechanism and location of this processing event is unknown, although the final destination of the protein is the stroma, as determined by immunolocalization (Nassoury et al., 2001). The soluble PCP is not a polyprotein, and it is located in the thylakoids, also as determined by immunolocalization (Nassoury et al., 2001). The synthesis of both proteins is under control of the circadian clock in vivo, and their expression times differ slightly. When the algae are grown under a 12:12 light:dark (LD) regime, Rubisco is synthesized from about midnight to midday (LDT 18 to 6), while PCP is synthesized from dawn to dusk (LDT 0 to 12) (Markovic et al., 1996). We found that nuclear-encoded proteins passed through the Golgi on route to the plastid, as has been shown for *Euglena* (Schiff et al., 1991). Furthermore, we show that the dinoflagellate plastid-directed protein leader sequences are functionally similar to those found in *Euglena.* We suggest that the second hydrophobic region present in the leader is a mechanistic requirement dictated by the triple membrane architecture of the plastids.

3.3. Materials and Methods

3.3.1. Luciferase constructs

The PCP leader sequence was amplified by PCR from a complete genomic clone using the oligonucleotides 5'-agccATGGGCCGCTCTCGT-3' and 5'-aaccatggtGTCGGCGAAGGCTGC-3'. The restriction site *Nco*I (lower case) was incorporated into primers to assist cloning of the product into pSP-luc+fusion vector (Promega Biotech) in-frame at the 5' end of the luciferase coding sequence. The construct containing the complete PCP leader sequence and luciferase (1-2 LUC) was then cloned into the *Bam*HI and *Hin*dIII sites of the vector pBluescript for further manipulations. For in vivo transformation, the 30 nucleotide 5'UTR of the *S. chacoense* S_{11}-RNase gene (Saba-El-Leil et al., 1994) was inserted at the *Hin*dIII site of pBluescript located at the 5' end of the PCP leader sequence by two sequential PCR amplifications. The first amplification used oligonucleotides 5'-TGTTCAAACTGCAAAATGGGCCGCTCTCGTAC-3' and T3 on the 1-2 LUC construct. For the second, this fragment was purified and re-amplified using oligonucleotides 5'-ataagcttGTACGATGAAACTAAATTGTTCAAACTGCAAA-3' and T3. The resulting DNA fragment was then digested by *Hin*dIII and *Bam*HI and cloned back into pBluescript. A deletion construct lacking the first hydrophobic region of the leader sequence (2LUC) was generated by PCR amplification from the 1-2 LUC using 5'-ggatatcatgGCCACGCGCTGCCTCCA-3' which corresponds to the 5' end sequence following the first signal peptidase site in the leader sequence of PCP and 5'-aggatatcTTTGCAGTTTGAACAT-3' which corresponds to the 3' end of the 5'UTR of the *S. chacoense* S_{11}-RNase gene. The restriction site *Eco*RV (lower case) was incorporated into primers to assist cloning as well as to provide an ATG start codon. The amplification product was digested with *Eco*RV and re-ligated, resulting in a plasmid missing the first hydrophobic core of the leader sequence. All PCR amplifications were done using proofreading DNA polymerase and all constructs were sequenced at each step. Constructs cloned separately into *Kpn*I and *Sac*I sites of the vector pBIN19 containing the 35 S double enhancer were introduced into the highly regenerable G4 line of the wild potato

Solanum chacoense by *Agrobacterium*-mediated transformation as described (Matton et al., 1997).

3.3.2. In vitro translation and processing experiments

Constructs 1-2LUC and 2LUC were translated using a T7 TnT-coupled rabbit reticulocyte system (Promega Biotech) containing ^{35}S-methionine (ICN) in the presence or absence of 4 µl canine pancreatic microsomal membranes (Promega) as described by the supplier. Protease protection assays were performed by incubating the translation mix with 0.1 mg/ml trypsin in the presence or absence of 0.5% Triton X-100. Sedimentation of membrane-bound translation products was performed by centrifugation in an airfuge using an A-100/30 fixed angle rotor for 1 hour at 100,000 *g*. Translation products were visualized by autoradiography after separation on 12% SDS polyacrylamide gels and electrophoretic transfer onto nitrocellulose membranes.

3.3.3. Immunocytochemistry and transformation

Gonyaulax cells were cultured and prepared for electron immunocytochemistry as described, using antibodies directed against a *Gonyaulax* Rubisco expressed from a cDNA in bacteria or PCP purified by column chromatography from the algae as described (Nassoury et al., 2001). A 20 nm gold-labeled goat anti-rabbit was used for detection (Ted Pella). A similar procedure was followed for immunolabeling of *S. chacoense* cells, except that a commercial anti-luciferase (Promega Biotech) was used as a primary antibody. A 20 nm gold-labeled rabbit anti-goat was used for detection (Ted Pella).

3.3.4. Sequence analysis

The sequences used for multiple alignments were obtained from GenBank using the accession numbers (top to bottom in Fig. 3.2) X94549, U93077, AF298221, AJ009670, AF028561, D14702, X89768, L21904, X15743, X66617 and S53593. Sequences for hydrophobicity plots (in Fig. 3.4) were AF087139, AF028561 and L21904. All analyses were performed using MacVector software, including ClustalW multiple alignments and neighbour-joining phylogenetic analyses. Bootstrap values are given for 10,000 trees.

3.4. Results

3.4.1. Nuclear-encoded plastid proteins transit through the Golgi

We first used immunocytochemistry to localize nuclear-encoded plastid proteins at times during the light-dark cycle when protein synthesis rates are high (Markovic et al., 1996). In one series of experiments, an antibody directed against the stromal protein Ribulose bisphosphate carboxylase/oxygenase (Rubisco) (Nassoury et al., 2001) was used. Cells were first harvested at dawn, also termed LDT 0 (the start of the light phase in a 12:12 light: dark cycle), a time when the in vivo synthesis rate of Rubisco is high (Markovic et al., 1996). There is label not only over the chloroplast, as expected, but also over the Golgi (Fig.. 3.1A,B). To confirm this result, we also examined the labeling patterns obtained with an antibody directed against the thylakoid protein peridinin-chlorophyll *a*-protein (PCP) (Nassoury et al., 2001). Again, sections were prepared from cells harvested at LDT 0, when the in vivo synthesis rate of PCP is high (Markovic et al., 1996). The immunostaining shows that both the chloroplast and the Golgi are labeled (Fig. 3.1C,D). Thus, identical results are obtained with plastid proteins located in two different sub-organellar compartments. Furthermore, as Rubisco is encoded as a polyprotein (Rowan et al., 1996) while PCP is not (Le et al., 1997), different types of nuclear-encoded plastid protein transit through the Golgi in dinoflagellates. We conclude that all nuclear-encoded plastid proteins will arrive at the outer plastid membrane in the form of Golgi-derived vesicles as observed in *Euglena* (van Dooren et al., 2001).

3.4.2. The plastid targeting sequence contains a signal peptide

To rule out the possibility that the observed Golgi labeling was a non-specific response to the antibodies, we immunolabelled sections from cells isolated at midday (LDT 6) with the anti-Rubisco. At this time in their daily cycle, the in vivo synthesis rate of Rubisco is low (Markovic et al., 1996). We observed a constant labeling of the plastid (Fig. 3.1C), in agreement with previous results showing no difference in the total Rubisco levels detected on Western blots and by enzyme-linked immunosorbent assay at different times over the daily cycle (Nassoury et al., 2001). However, no label was found over the Golgi, confirming that the labeling seen at time of high synthesis rates was indeed due to the

presence of Rubisco. This control experiment was also performed using cells isolated at midnight (LDT 19) and the anti-PCP antiserum. At this time, PCP synthesis rates are low (Markovic et al., 1996), and again, no labeling of the Golgi was observed (Fig. 3.1F). We conclude that both proteins must enter the Golgi from the ER at times of high synthesis rates.

Targeting to the ER typically requires the presence of an N-terminal hydrophobic signal peptide. Indeed, such a signal, followed by an AXA-type signal peptidase site, is found in the leader sequences of plastid directed proteins for both dinoflagellates and *Euglena*. In *Euglena*, the two hydrophobic regions have been proposed to act as start and stop signals for translocation across the ER membrane (Sulli et al., 1999). This topology results in a membrane-bound protein with the first signal peptidase site inside the ER lumen and the bulk of the protein outside.

We thus tested if dinoflagellate plastid leader sequences acted similarly to those studied in *Euglena*. For our in vitro analyses, we chose to examine the leader sequence of the thylakoid protein PCP. The leader sequence of this protein is virtually identical to that of the stromal protein glyceraldehyde-3-phosphate dehydrogenase (GAP) (Fagan et al., 1999), suggesting that the information to distinguish between stromal and thylakoid locations might be found within the coding sequence of the mature PCP. To avoid potentially conflicting signals, the complete PCP leader sequence, encoding both hydrophobic regions and the S/T-rich regions separating them (Le et al., 1997), was thus fused with a luciferase reporter gene. These constructs were transcribed and translated in vitro and the protein products analyzed by SDS PAGE. The size of the protein produced is as predicted when the transcripts are translated in the absence of canine microsomes, and is smaller when translated in the presence of canine microsomes. As expected, the processed form is larger than luciferase alone (Fig. 3.2A). We conclude that the size change upon addition of microsomes is consistent with cleavage of the signal peptide at the expected site.

This cleavage of the signal peptide following the signal peptide suggested that the first hydrophobic region is inserted into the microsomal membrane with the N-terminus in the cytoplasm. If so, then the second hydrophobic region should act as a stop transfer signal, and the final topology of the protein, after cleavage by the signal peptidase, would be a

single pass membrane protein with its C-terminal end in the cytoplasm. To test this, we digested with trypsin the protein produced in the presence of microsomes. This treatment reduced the level of radiolabelled protein, and no further decrease in the amount of protein could be obtained by inclusion of Triton X-100 in the digestion (Fig. 3.2A). This indicated that the small amount of signal resisting digestion did not represent luciferase inside the microsomes. The topology of the protein deduced from this experiment is unambiguous and is illustrated at right (Fig. 3.2A).

3.4.3. The leader contains a functional plastid transit sequence

These results also suggested that the second hydrophobic region might act as a signal peptide if the first hydrophobic region was deleted, as has been observed in *Euglena* (Sulli et al., 1999). We thus prepared and translated a construct lacking the first hydrophobic region. The new construct showed no size decrease upon addition of microsomes, and the protein product was sensitive to trypsin digestion (Fig. 3.2B). To test the possibility that the hydrophobic region was inserted into the membrane, the labeled protein was centrifuged at 100,000 *g* for one hour following the translation. The labeled protein is found in the pellet, suggesting that the protein is either membrane bound or is tightly associated with the microsomal membrane. A likely topology for the protein, based on both these results and by analogy to results obtained with *Euglena*, is illustrated in the schema at right (Fig. 3.2B).

The topology of the plastid-directed proteins deduced from the in vitro experiments described above suggests that plastid precursor proteins may arrive at the plastid anchored in the membrane of a transport vesicle with their S/T-rich region inside the vesicle lumen. Fusion of the vesicle with the outer plastid membrane would make the S/T-rich sequence available to protein translocators spanning the inner two plastid membranes. We thus predicted that S/T-rich sequence would be equivalent to the transit sequence of higher plant plastid proteins. To test this, we asked if the translocators in the double membrane-bound plastids of higher plants could recognize this sequence in vivo. In vivo experiments allow a potential import into plastids to be evaluated in the context of competition with other compartments, unlike in vitro tests where only import into isolated pea chloroplasts is assessed (DeRocher et al., 2000; Wastl and Maier, 2000).

We prepared a reporter gene construct containing the leader sequence lacking the first hydrophobic region. This gene fusion, containing a *Solanum chacoense* 5'UTR and driven by the constitutive 35S promoter, was used to transform the wild potato *S. chacoense* (Matton et al., 1997). Leaves of eight transformed plants were screened and two selected for analysis on the basis of high signal with the antibody. The anti-luciferase antibody detects only the luciferase and has no reaction with untransformed plants and plants with low expression of the transgene (Fig. 3.3C). However, in the highly expressing plants, the subcellular location of the fusion protein was clearly the chloroplast. The presence of the reporter in the plastids confirms that the S/T-rich region acts as an authentic plastid targeting sequence in higher plants as well (Fig. 3.3A, B). To quantify the immunolabeling, five random pictures were taken from each sample, and the number of gold beads determined for plastid, vacuolar and cytoplasmic compartments. The label density in the plastids of transformed plants is 5- to 10-fold greater than that in other compartments within the same plant, and over 10-fold greater than the background labeling observed in the plastids of untransformed plants (Fig. 3.3D). Presumably, this conservation of function reflects the common evolutionary ancestor to all extant plastids. We have not observed staining in the ER or nuclear membranes in these experiments. However, we cannot completely rule out some ER targeting, as we did not detect any signal above background in plants transformed with a luciferase reporter fused to the full-length leader sequence. If proteins directed to the ER membrane in this manner were unstable, for example, a direct comparison of the staining intensity in the two compartments would be impossible. In any event, it is clear that the S/T-rich region acts as an authentic transit peptide in higher plants.

3.5. Discussion

In this report we have addressed the protein import pathway used by dinoflagellates to allow entry of nuclear-encoded proteins into their triple membrane-bound plastids. We have shown that plastid-directed proteins transit through the Golgi in vivo (Fig. 3.1), and that plastid-directed proteins are directed to microsomes in vitro (Fig. 3.2). Protease sensitivity of these proteins indicates they have a topology similar to that found in *Euglena* (Sulli et al., 1999), where the bulk of the protein is cytoplasmic and the S/T-rich region of the leader is in the ER lumen. Lastly, we demonstrate that this S/T-rich region is a functional transit sequence, as it can direct the luciferase reporter into the plastids of higher plants (Fig. 3.3). This represents the first reported in vivo demonstration that an algal plastid transit sequence can function in higher plants. Taken together, these experiments characterize the key elements in dinoflagellate plastid protein targeting mechanisms, and thus fill a large gap in our understanding of protein entry into the plastids derived from secondary endosymbioses.

Similar to the leader sequences used to target other complex plastids, the dinoflagellate leader contains a hydrophobic N-terminal signal peptide and an internal plastid transit sequence. Unlike most other leader sequences, the dinoflagellate sequences contain a second hydrophobic region at the C-terminal end. This unusual feature is also found in *Euglena*, as shown by an alignment of five dinoflagellate sequences and six *Euglena* sequences (Fig. 3.4A). This alignment is color coded for visualization of the hydrophobic character (blue boxes). An AXA-type signal peptidase site follows the first hydrophobic regions (arrow) here manually aligned for comparison. The serine/threonine-rich regions (yellow boxes) that constitute the plastid transit sequence separate the two hydrophobic regions (Fig. 3.4A). Since *Euglena* and the dinoflagellates share a triple bound plastid architecture, we suggest that the C-terminal hydrophobic region, and the unusual protein topology that results from its insertion in the membrane of the transport vesicles, are required by the organelle's structure.

It is instructive to consider the dinoflagellate targeting mechanism in the light of the phylogenetic relationships between the different algal classes. First, it is generally accepted that a close phylogenetic relationship exists between apicomplexans and dinoflagellates (Fast et al., 2002; Sogin et al., 1996). This relationship can be illustrated

by the molecular phylogeny of glyceraldehyde-3-phosphate dehydrogenase (GAP). Many examples of these trees are available in the literature, and the neighbor-joining tree shown here (Fig. 3.4B) is illustrative of much larger taxonomic samplings (Fast et al., 2001). These trees show the close relationship between apicomplexan and dinoflagellate hosts, as well as the relationship between euglenoids and trypanosomes. An interesting feature of the GAP phylogeny is the clustering of plastid directed sequences in the apicomplexans and the dinoflagellates (Fig. 3.4B) (Fast et al., 2001). This phylogeny is supported by some plastid sequences (Fast et al., 2002; Wilson et al., 1996; Zhang et al., 2000), but not by a *tufA* phylogeny (Kohler et al., 1997) or the presence of a green algal-like mitochondrial *cox2* gene in the apicomplexan nucleus (Funes et al., 2002) that suggest green algal ancestry for the apicoplast. In any event, plastids from dinoflagellates and *Euglena* have had different evolutionary origins, even though both have three membranes and a second hydrophobic region in the leader sequences (Fig. 3.4B). In the model discussed below, we consider the case where dinoflagellate and apicomplexan plastids share a common ancestor. However, it is important to note that similar conclusions can also be reached in other scenarios, provided the plastids of dinoflagellates initially had four bounding membranes.

One possible evolutionary scheme, based on the GAP phylogeny shown (Fig. 3.4B), would involve uptake of a red algal symbiont by the common ancestor to both dinoflagellates and apicomplexans (Fig. 3.4C). Genes that had been transferred to the red algal nucleus, either before or after this secondary endosymbiotic event, would then be transferred to the new host cell nucleus. Given the ability of the dinoflagellate S/T-rich transit sequences to still function in higher plants (Fig. 3.3), any sequences transferred to the new host nucleus presumably included this plastid transit sequence. To re-enter the plastids, now bounded by four membranes, a signal peptide would have to be acquired in addition to the transit peptide (McFadden, 1999). Thus, according to this scheme, plastid-directed proteins in the last common ancestor for the apicomplexans and dinoflagellates would be expected to have both a signal peptide and a transit peptide in their leaders. The divergence of the dinoflagellates, and the loss of one bounding membrane around their plastids, must then have been accompanied by the selection of modifications in the C-terminal end of the leader sequence with an accentuated hydrophobicity. This new

hydrophobic region, common to the sequence of plastid-directed nuclear proteins of dinoflagellates and *Euglena* (Fig. 3.4A), thus appears to be an essential element for targeting nuclear-encoded proteins to triple membrane-bound plastids.

The scheme above posits a transfer of genes to the nucleus of the new host cell before loss of the outermost plastid membrane. So far, however, it has not been possible to date the timing of these events. An alternative model, in which membrane loss occurred prior to gene transfer, would require hydrophobic signal peptide-like sequences to be inserted both before and after the transit peptide. A third model, where genes were transferred from the plastid genome directly to the new host nucleus, is not favored because of the fact that the reduced gene content of most extant plastids shows considerable overlap (Palmer and Delwiche, 1996). In any event, the peptide leader sequence does not recapitulate the gene transfer process, as at least part of the leader is defined not by phylogeny but by the mechanistic requirements of protein targeting to triple membrane-bound plastids.

What mechanistic requirement may be filled by the second membrane-spanning region in the dinoflagellate leader? One possible role may be to present the plastid transit sequence to the protein translocators in the inner (second) membranes. However, it may also act as a recovery mechanism should any of the plastid proteins be misdirected to the plasma membrane, as soluble proteins secreted from the cell would be irretrievably lost. Indeed, as little is known about the targeting mechanism that delivers proteins specifically to the plastid, this now represents the next challenge in elucidating the protein import mechanisms in dinoflagellates and *Euglena*.

Figure 3.1. Nuclear-encoded plastid proteins transit through the Golgi. *Gonyaulax* cell sections were treated with antibodies raised against two nuclear-encoded plastid proteins, Rubisco and peridinin-chlorophyll *a*-protein (PCP). In one series of experiments, cells were harvested and fixed at LDT 0 (by convention, the start of the light phase), a time when both proteins are actively synthesized in vivo. As a control for the specificity of the Golgi labeling, cells were also harvested and fixed at times when Rubisco or PCP were not actively synthesized in vivo (LDT 6 and 19, respectively). Sections were stained with either anti-Rubisco (A-C) or anti-PCP (D-F) as a primary antibody and a 20 nm gold-conjugated goat anti-rabbit as a secondary antibody. The Golgi is indicated by arrows in all pictures, and all scale bars represent 1 μm. Note that Rubisco and PCP have different sub-organellar locations (stroma and thylakoid lumen, respectively) within the plastids (P). The thylakoid membranes appear white, as osmium tetroxide was not used during fixation to preserve the antigenicity of the proteins.

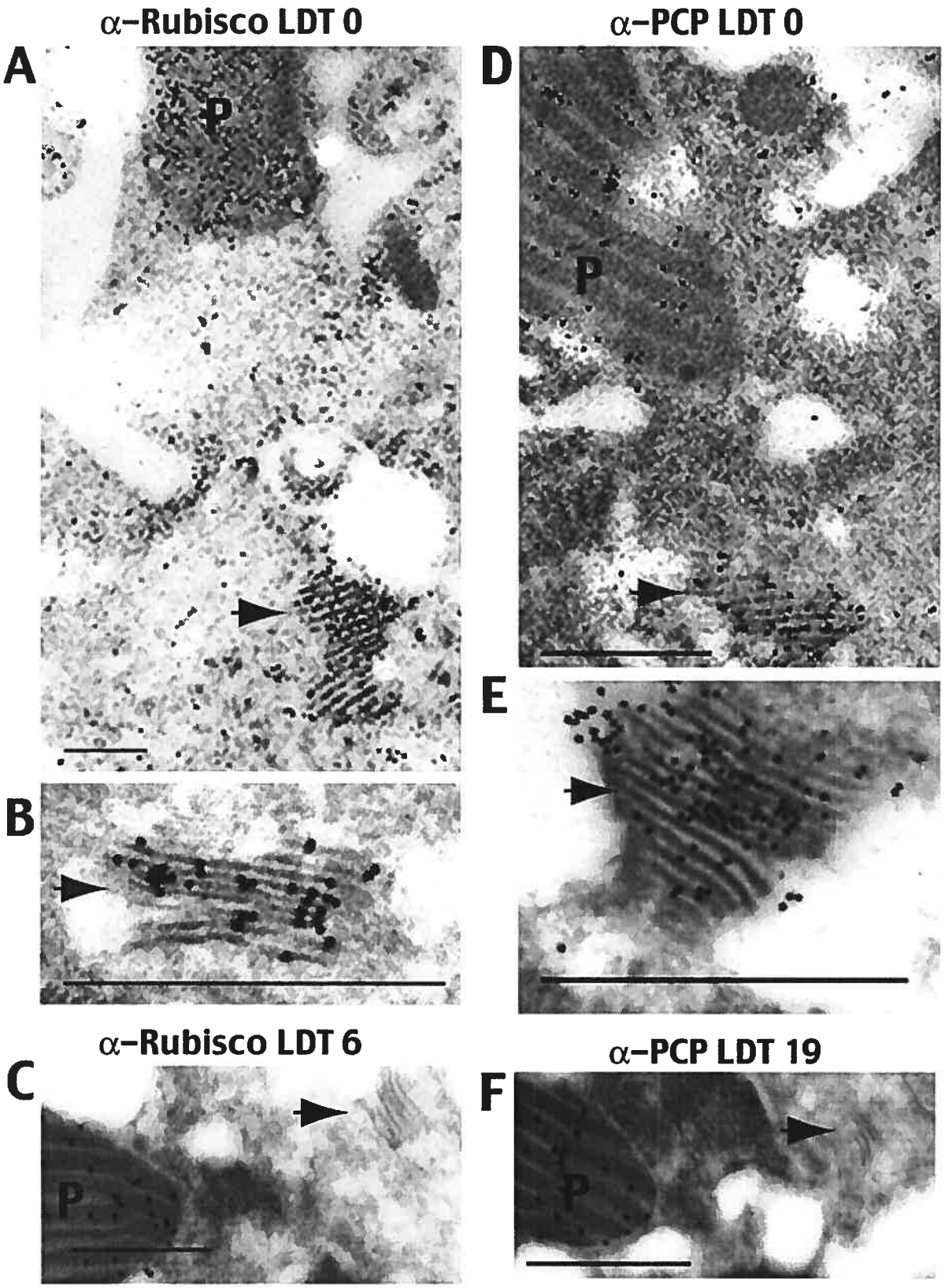
α-Rubisco LDT 0
α-PCP LDT 0
A
D
P
P
B
E
α-Rubisco LDT 6
α-PCP LDT 19
C
F
P
P

Figure 3.2. The PCP leader contains a signal peptide that targets a reporter gene to canine microsomes in vitro. (A) A schematic view of the G. polyedra PCP leader used (top) shows two hydrophobic regions (numbered black boxes) separated by an S/T-rich region (white box) fused to luciferase (line). The small arrow indicates the potential AXA signal peptidase site. This construct was transcribed and translated in vitro in rabbit reticulocyte lysates (RRL) with the additions as illustrated. A smaller protein is produced after translation in the presence of canine microsomes, confirming cleavage after the first hydrophobic region. The topology of the protein, deduced from its susceptibility to trypsin digestion, is shown schematically on the right (small arrow indicates cleavage by the signal peptidase inside the vesicle). Note that the bulk of the protein remains outside the microsomal membrane. (B) A schematic view of the luciferase reporter fused with a modified G. polyedra PCP leader (top) lacking the first hydrophobic region. This construct was also translated as above. Most of the translation product is found in the pellet (P) rather than the supernatant (S) after ultracentrifugation, suggesting that it may be inserted into the microsomal membrane as found in Euglena. The predicted topology is again shown schematically on the right.

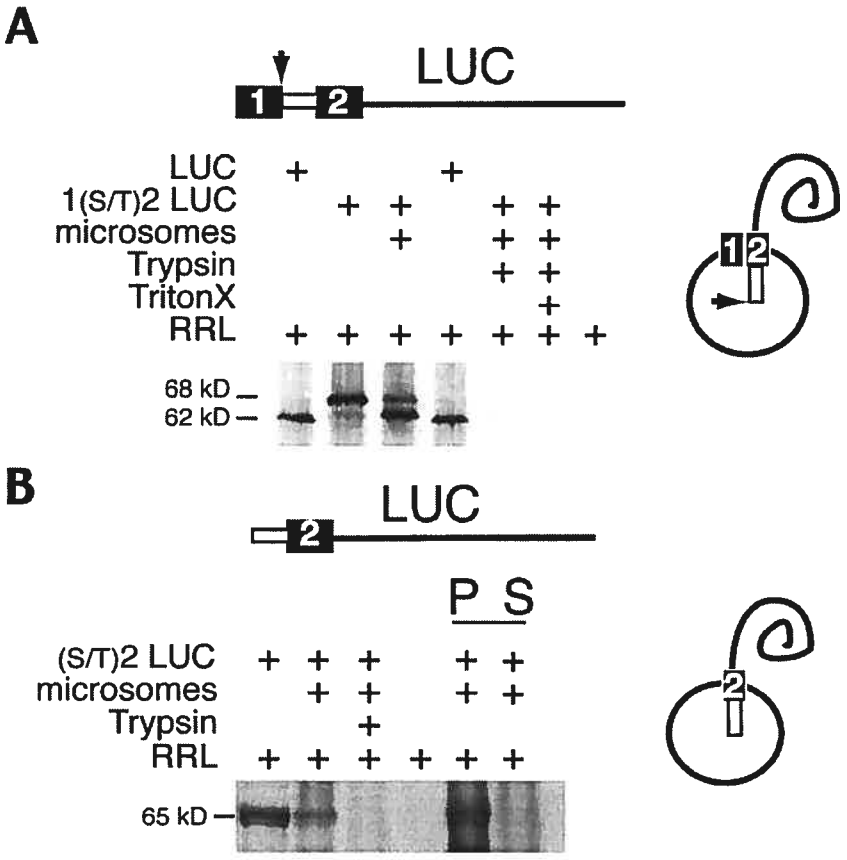
A
LUC
1
2
LUC
1(S/T)2 LUC
microsomes
Trypsin
TritonX
RRL
68 kD
62 kD
1
2
B
LUC
2
P S
(S/T)2 LUC
microsomes
Trypsin
RRL
65 kD
2

Figure 3.3. Targeting to higher plant plastids by the S/T-rich region in the PCP leader. The luciferase reporter construct lacking the first hydrophobic region (as described in Fig. 3.2B) was fused with a *Solanum chacoense* 5'UTR and introduced into a highly regenerable genotype (G4) of *S. chacoense*. Two independent transformants expressed high levels of luciferase in the chloroplasts (A,B), as shown by immunoelectron microscopy using a commercial anti-luciferase as a primary antibody and a 20 nm gold-conjugated rabbit anti-goat as a secondary antibody. Label is observed over the plastid (P) but not the cell wall (CW), vacuole (V) or nucleus (N). Untransformed plants (C) show only background labeling. (D) Quantification of the label density is shown as number of gold beads per μm^2 for the two transformed plants above as well as for an untransformed control. Bars, 1 μm.

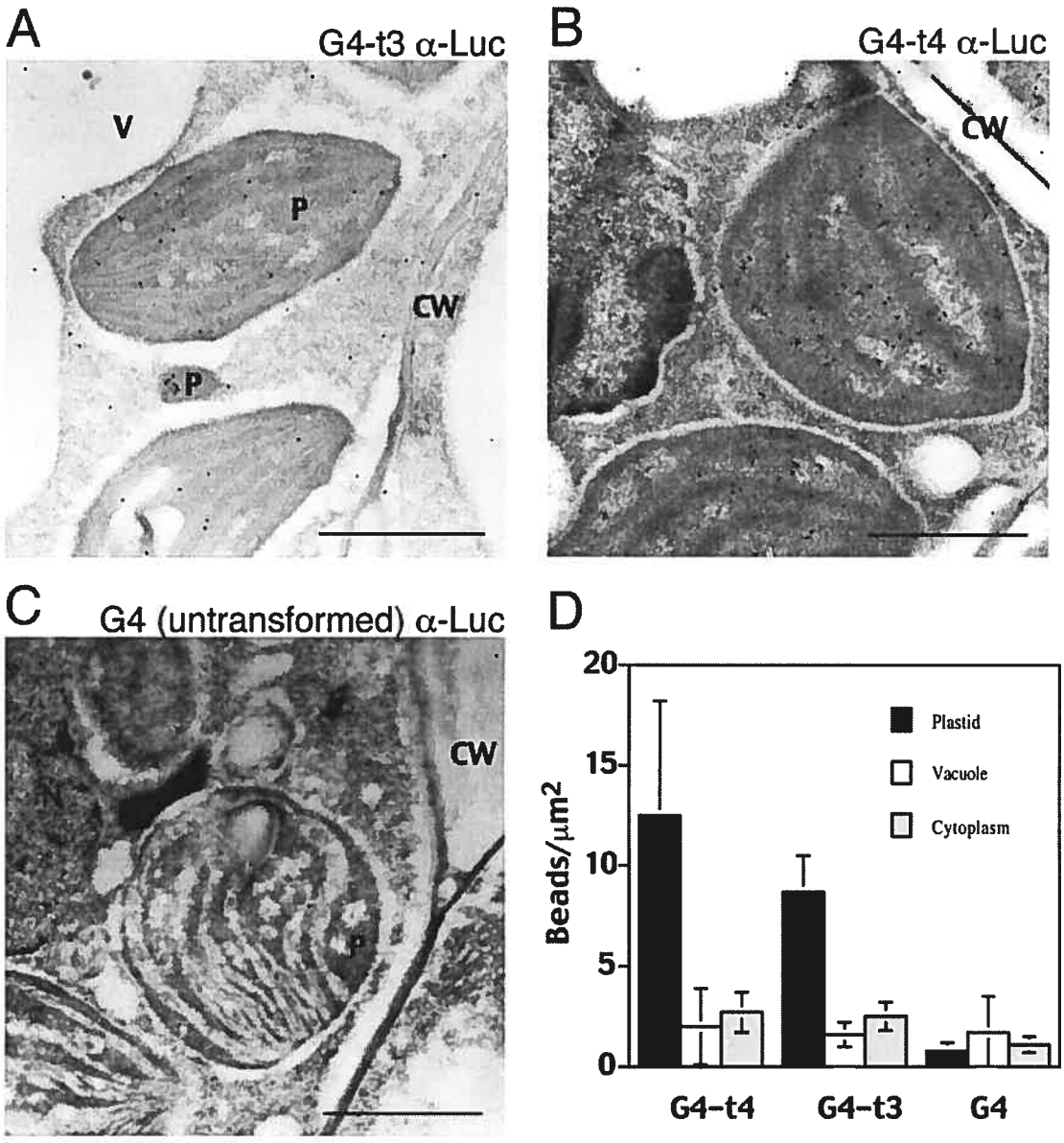
A
G4-t3 α-Luc
V
P
CW
P
B
G4-t4 α-Luc
CW
C
G4 (untransformed) α-Luc
CW
D
20
15
10
5
0
Beads/μm2
Plastid
Vacuole
Cytoplasm
G4-t4
G4-t3
G4

Figure 3.4. The leader sequence is defined by plastid ultrastructure rather than by its phylogeny. (A) Alignment of signal peptides from (top to bottom) five dinoflagellate (*Amphidinium carterae, Symbiodinium* sp and *Gonyaulax polyedra*) and six *Euglena gracilis* plastid-directed, nuclear-encoded proteins. Two conserved hydrophobic regions (blue) are interspersed with polar (yellow), acidic (red) or basic (green) residues. Gaps (white) were introduced to align the hydrophobic regions. The AXA signal peptidase site is at the end of the first hydrophobic region (arrow). (B) A phylogenetic reconstruction using glyceraldehyde-3-phosphate dehydrogenase sequences shows significant bootstrap support for the apicomplexan *Toxoplasma* and the dinoflagellate *Gonyaulax* as sister clades, using both plastid and cytoplasmic isoforms, as well as strong bootstrap support excluding *Euglena*. Numbers at the nodes indicate bootstrap support (10,000 trees). (C) Plastid evolution. Dinoflagellates and apicomplexans share a common ancestor both for the host cell and the plastid, and are unrelated to either Euglenoids or their plastids. Gene transfer from the endosymbiont nucleus to the new host cell nucleus must be accompanied by addition of a peptide signal, which allows the plastid-directed proteins to pass the new membranes. (D) Representative hydrophobicity plots of signal peptide sequences from the apicomplexan ribosomal protein S9 (RPS9), showing only a single hydrophobic region, as well as from a dinoflagellate and a Euglenoid glyceraldehyde-3-phosphate dehydrogenase (GAP), showing two distinct hydrophobic regions. All plots are to the same scale, with hydrophobicity increasing above the midline.

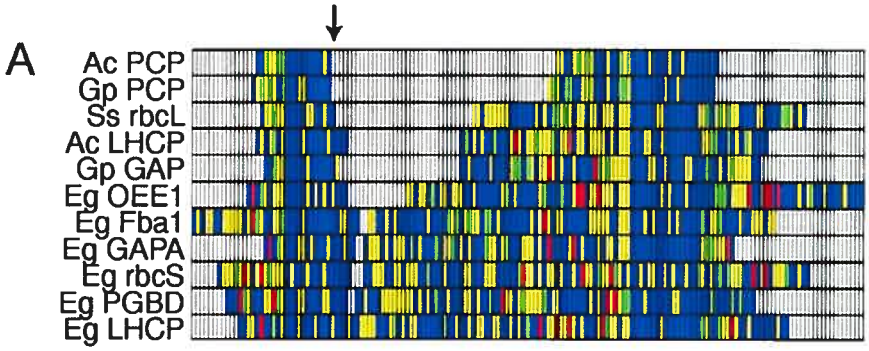
A
Ac PCP
Gp PCP
Ss rbcL
Ac LHCP
Gp GAP
Eg OEE1
Eg Fba1
Eg GAPA
Eg rbcS
Eg PGBD
Eg LHCP


B
membranes
hydrophobic regions
100
100
100
78
100
98
99
73
Euglena plastid 3 2
Arabidopsis plastid 2 0
Trypanosoma cytoplasm
Euglena cytoplasm
Toxoplasma plastid 4 1
Gonyaulax plastid 3 2
Pyrenomas plastid 4 1
Gonyaulax cytoplasm
Toxoplasma cytoplasm
Arabidopsis cytoplasm

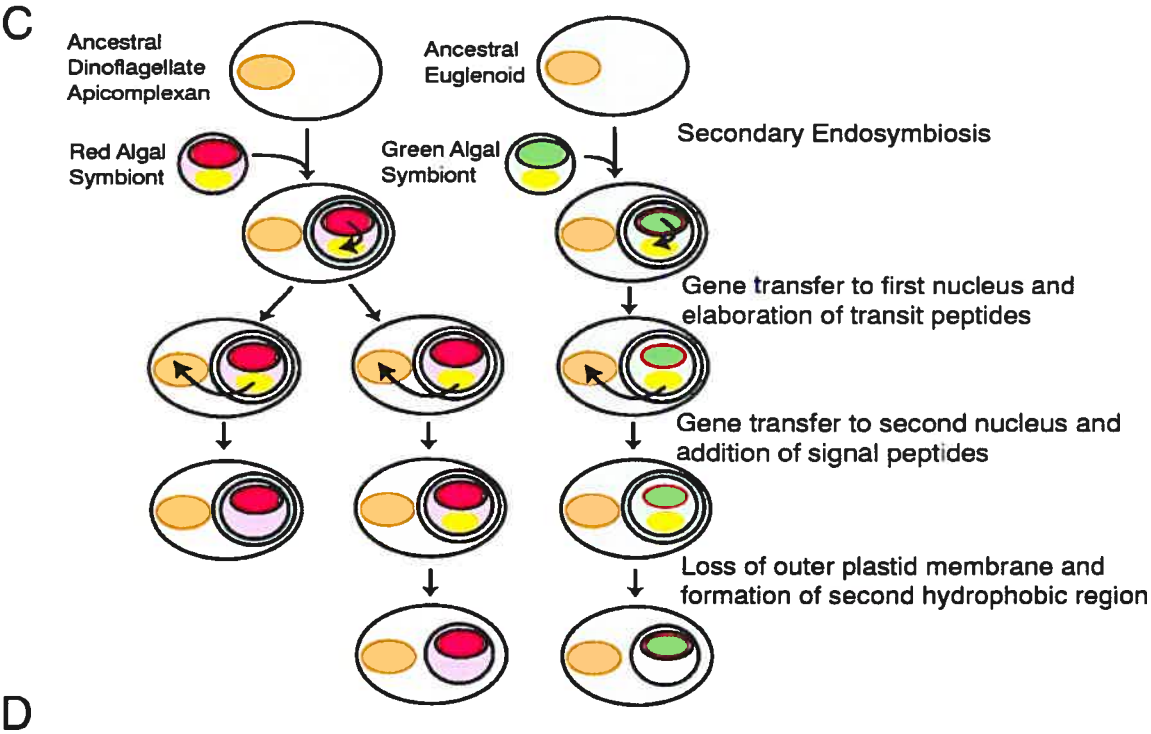
C
Ancestral Dinoflagellate Apicomplexan
Ancestral Euglenoid
Red Algal Symbiont
Green Algal Symbiont
Secondary Endosymbiosis
Gene transfer to first nucleus and elaboration of transit peptides
Gene transfer to second nucleus and addition of signal peptides
Loss of outer plastid membrane and formation of second hydrophobic region

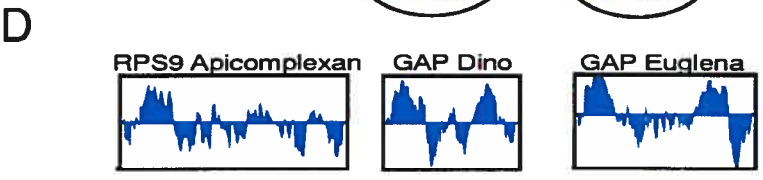
D
RPS9 Apicomplexan
GAP Dino
GAP Euglena

3.6. Acknowledgements

We thank L. Pelletier for technical assistance with the electron microscope, G. Laublin for expertise in plant transformation and tissue culture, K. K. Rashidan for technical assistance with the airfuge, S. Gibbs for helpful discussions and interpretation of the immunoelectron micrographs, and D. T. Luu for critical review of the manuscript. We also thank two anonymous reviewers for thoughtful comments and effective suggestions on figure organization. This work has been supported by the National Sciences and Engineering Research Council of Canada (to D.M. and M.C.).

CHAPTER 4- PUBLICATION #3

A Brefeldin A sensitive step in dinoflagellate photosynthetic carbon fixation

Nassoury, N., Y. Wang and D. Morse (*submitted*)

In this part of my Ph.D. work we took advantage of the inhibitory effects of Brefeldin-A on the Golgi function and tried to obtain information regarding the circadian oscillation in pyrenoid formation by inhibiting protein import into plastid. We suggest that newly synthesized proteins and perhaps Rubisco itself could act as the timing signal for the plastid remodeling. In agreement with our speculation of a correlation between the appearance of pyrenoids and the carbon fixation ability of the cells, by inhibiting the pyrenoid formation with BFA, the carbon fixation rhythm was noticeably affected. These experiments not only represent the first report of BFA action in dinoflagellates but also accentuate the likely impact of enzyme location in regulating circadian rhythms.

For this article all the experimental procedures were realized by me and Yunling Wang has performed the 2-D protein gels.

4.1. Abstract

The rate of carbon fixation in the dinoflagellate *Gonyaulax* is regulated by a circadian clock to rise from a minimum at midnight to a maximum at the start of the light period. The increase correlates with recruitment of the rate limiting step enzyme Rubisco to one end of the plastid forming a specialized region termed a pyrenoid. Newly synthesized Rubisco transits through the Golgi on its way to the triple membrane bound *Gonyaulax* plastid, and we show that the vesicular transport inhibitor Brefeldin A (BFA) blocks both the increase in carbon fixation rates and the formation of pyrenoids. We show that Rubisco synthesis is rhythmic and occurs concurrently with pyrenoid formation, and that Rubisco entry into chloroplasts is blocked by BFA. Rubisco synthesized in the presence of BFA accumulates in polyvesicular structures termed BFA bodies. Rubisco recruitment to the pyrenoid involves a specific timing signal rather than ongoing Rubisco synthesis as Brefeldin A treatments after the onset of Rubisco synthesis retard but do not block pyrenoid formation. BFA acts as a specific inhibitor of photosynthetic carbon fixation, as it has no effect on circadian timing of bioluminescence or cell division rhythms. These experiments represent the first report of BFA action in dinoflagellates and underscore the importance of enzyme location in regulating circadian rhythms.

4.2. Introduction

Dinoflagellates are eukaryotic protists that display a number of singular features, including a nuclear envelope that remains intact during mitosis and an extranuclear spindle (Fritz and Treimer, 1983), a complete lack of histones (Rizzo, 1991) and the presence of permanently condensed chromosomes (Bhaud et al., 2000; Spector et al., 1981). The plastids are surrounded by three membranes (Gibbs, 1981), use the carotenoid peridinin as an accessory light harvesting pigment (Jeffrey et al., 1975), contain their genome in single gene minicircles (Barbrook and Howe, 2000; Zhang et al., 1999), and employ a targeting mechanism for nuclear-encoded plastid-directed proteins which involves transit through the Golgi (Nassoury et al., 2003).

Despite these many unusual features, dinoflagellates are a useful model system for the study of the biochemical basis underlying circadian rhythms. The reason for this is that many processes with defined rate limiting steps (RLS) are clock controlled, and thus the regulatory links between oscillation of a molecular clock and the observed biochemical or physiological rhythms can be examined in detail. The rhythm in bioluminescence, for example, correlates with the cellular levels of both the substrate (Bode et al., 1963; Morse et al., 1989) and the reaction catalyst (Johnson et al., 1984) of the light producing reaction. Protein levels are regulated at the synthesis level using a translational control mechanism (Mittag et al., 1994).

Control over photosynthetic carbon fixation initially appeared to fit inside the bioluminescence paradigm for clock control over rhythmic behavior. For example, synthesis of Rubisco, the enzyme catalyzing the RLS of carbon fixation in all organisms, is synthesized rhythmically (Markovic et al., 1996). However, although the peak of *in vivo* protein synthesis rates (Markovic et al., 1996) and photosynthetic carbon fixation rates (Nassoury et al., 2001) have a similar phase, levels of Rubisco do not alter appreciably over the course of the daily cycle (Nassoury et al., 2001). Accessory proteins such as Rubisco activase (Hartman and Harpel, 1994) are unlikely to modulate enzyme activity because dinoflagellates use a form II Rubisco (Morse et al., 1995) for which no activase proteins have yet been described. It was thus interesting to find that instead of changes in protein amount, the suborganellar localization of Rubisco changed in phase with the rhythm of carbon fixation rates (Nassoury et al., 2001). In particular, when

carbon fixation rates are high, Rubisco is located in a centrally located, specialized region of the plastid termed a pyrenoid, whereas the light harvesting protein PCP is found primarily in regions of the plastid close to the periphery of the cell (Nassoury et al., 2001). This separates the sites of oxygen production and carbon fixation to opposite poles of individual plastids and suggests that plastids form regions of specialized function to optimize performance. The change in Rubisco distribution is believed to affect the reaction rate by altering the delicate balance between binding of the substrate CO_2 and the competitive inhibitor O_2 to the active site of the enzyme.

The mechanism whereby Rubisco distribution in the plastid is altered is still unknown. However, the observation that plastid-directed nuclear-encoded proteins transit through the Golgi (Nassoury et al., 2003) has suggested a unique approach to testing the involvement of Rubisco synthesis in pyrenoid formation. This approach exploits the inhibition of vesicular transport by the small hydrophobic fungal metabolite Brefeldin A (BFA). BFA is a potent inhibitor of secretion whose effects appear linked to vesicular transport, since one of the main effects of BFA treatment is the loss of COPI coats from the Golgi (Kreis et al., 1995). This reagent should thus be a more specific inhibitor of Rubisco synthesis than the general protein synthesis inhibitors such as anisomycin or cycloheximide. The effects of these reagents are difficult to interpret because of their complex phase shifting effects on the internal time of the circadian clock (Taylor et al., 1982).

Vesicular transport between subcellular compartments such as the ER and Golgi is regulated by small Ras-like GTPases called ADP-ribosylation factors (ARFs) that act as coat recruitment factors when associated with a membrane (Schekman and Orci, 1996; Serafini et al., 1991). The membrane association occurs following a conformational change when GDP on the soluble ARF-GDP is exchanged for GTP, and the site of ARF activation thus determines the site of coat recruitment. ARF activation is catalyzed by membrane-bound guanine nucleotide exchange factors (GEFs) that accelerate the replacement of GDP with GTP (Helms and Rothman, 1992). Interestingly, the GEFs associated with the Golgi membrane are particularly sensitive to inhibition by BFA (Donaldson et al., 1992). BFA stabilizes binding between the ARF-GDP and a ~ 200 amino acid Sec7 domain in the GEF (Moss and Vaughan, 1999; Peyroche et al., 1999).

The crystal structure of the ARF1-GDP-Sec7-BFA complex shows that BFA binds at the protein-protein interface and obstructs the conformational changes in ARF1 required for Sec7 to free the GDP molecule (Mossessova et al., 2003).

The effects of BFA are rapid, typically within minutes, and are characterized by disassembly of the Golgi complex and a redistribution of its contents into the endoplasmic reticulum (ER) (Dascher and Balch, 1994). The visualization of GFP-labeled proteins specific for different compartments is admirably suited to study of all aspects of vesicular transport system dynamics (Lippincott-Schwartz et al., 2000). The collapse of the Golgi compartment after BFA treatment is thought to result from the release of COPI from the Golgi membranes (Presley et al., 2002) which may permit interactions between the vSNAREs and tSNAREs on Golgi stack and ER membranes. A rapid release of COPI coats from the Golgi into the cytosol has also been shown in tobacco cells (Ritzenthaler et al., 2002) suggesting that BFA-induced loss of COPI coats from the Golgi is a general characteristic of drug action. Clearly these phenotypes must be observed in order to ensure that BFA is having the correct effect in dinoflagellates. However, as a caveat to the exquisite specificity of BFA discussed above, it must be noted that as organisms diverge more substantially from mammalian cells, it is possible that other sec7 domain containing GEFs might be present. Thus, there are potential effects of blocking the activation of monomeric GTPases involved in signal transduction, nuclear protein transport, or cytoskeleton organization (de Lanerolle and Cole, 2002) that must be evaluated when phylogenetic relationships with model organisms become more distant.

In the present study we report that BFA blocks vesicular transport of Rubisco to the Golgi in dinoflagellates, and this constitutes the first report of BFA action in this group of protists. We show that no newly synthesized Rubisco enters the plastid after BFA treatment, and that instead, Rubisco becomes associated with a newly formed polyvesicular structure termed a BFA body. This blockage in Rubisco transport to the plastids completely blocks the normal rise in carbon fixation rates, the formation of pyrenoids, and the associated accumulation of Rubisco in the pyrenoid, thus providing further support for the role of pyrenoids in augmenting carbon fixation rates. However, when BFA is applied after the onset of Rubisco synthesis, pyrenoid formation is slowed

by not blocked. We conclude that transport of newly synthesized nuclear-encoded proteins to the plastid provides a circadian timing signal for pyrenoid formation.

4.3. Materials and Methods

4.3.1. Cell growth and viability measurements

Cell cultures of *Gonyaulax polyedra* (strain number 1936, Provasoli-Guillard Center for Culture of Marine Phytoplankton, Boothbay Harbor, Maine) were grown under a 12h light/12h dark (60 umol m^{-2} sec^{-1} white fluorescent light) at 16°C in f/2 medium as described (Guillard and Ryther, 1962). During the typical 24 hour cycle, the start of the light phase is termed LD 0, while the onset of darkness is called LD 12. For treatment of the cultures with BFA (Sigma), a 10mg/ml stock solution was made in dimethyl sulfoxide and was further diluted to working solution of 1mg/ml in dimethyl sulfoxide before use. For each BFA concentration experiment, either BFA or solvent alone was added at different concentrations at middle of the night phase and samples were taken at hourly intervals for six hours and after 24h for determination of the percent viable cells by staining with the vital dye Evan's blue (Crutchfield et al., 1999).

4.3.2. Metabolic labeling and electrophoresis

For each sample, a 100 ml aliquot of cell culture was removed and concentrated to 1 ml using a 20 um Nylon filter. The samples were pretreated with 1ul of 100 uM chloramphenicol in ethanol for 10 minutes prior to labeling with 200 uCi of ^{35}S-methionine for 20 minutes in the dark at 16°C. The cells were then washed three times with fresh f\2 medium to remove excess radiolabel and five times with 0.4 M sucrose to remove the salt. The cell pellet was resuspended in 200ul 4% Chaps and the cells mechanically disrupted using a mini-beadbeater (Biospec Products, Bartlesville, OK). The extract was clarified by centrifugation at 14,000 xg for 10 minutes at 4°C, and the protein precipitated from the supernatant by addition of 1ml acetone at -20°C. The protein pellet recovered by centrifugation was washed 10 times with cold 70 % acetone before resuspension in UC buffer (7 M Urea, 2 M thiourea, 4% CHAPS, 0.02 M DTT, 0.5% pH 4-7 IPG buffer (Amersham-Pharmacia Biotech)). The samples were centrifuged at 14,000 xg for 15 minutes and the supernatant allowed to rehydrate an pH 4-7 IEF strip (Amersham-Pharmacia Biotech) overnight at 20 °C. The samples were focused at 500 V for 1h, 1000 V for 1 h and 8000 V for 6 h. The strips were then equilibrated for 15 min in

10 mL Equilibration Buffer (50 mM Tris-HCl pH 8.8, 6 M urea, 30 % glycerol, 2 % SDS, Bromophenol blue), 15 minutes with 10 mg/mL DTT, and a final 15 minute incubation in 10 mL Equilibration buffer containing 25 mg/mL iodoacetamide and 10 mg/mL DTT. The strips were then electrophoresed on a standard SDS-Polyacrylamide gel as a second dimension. The gels were stained with Coomassie Blue, dried using a gel drier and exposed to film at -80 °C for 7 days.

4.3.3. Immunoelectron microscopy

Cells were harvested and washed with 0.4 M phosphate buffer and fixed with 3% Gluteraldehyde in 0.4 M phosphate buffer for 30 minutes, washed 3 times in PBS and water, followed by standard dehydration procedures and embedded in LR White resin as recommended by the manufacturer. Immunostaining and electron microscopy were preformed as previously described (Nassoury et al., 2001).

4.3.4. Carbon fixation measurements

CO_2 fixation rates were measured from conversion of $NaH^{14}CO_3$ to acid-insoluble material. For each assay, 1 uCi radiolabeled bicarbonate was added to each of five 10 mL aliquots of cell culture. The cultures were preincubated under saturating white light (300 umol $m^{-2}sec^{-1}$) for three minutes, the carbonate added, and the exposure to bright light continued for a further 15 minutes, over which time radiolabel incorporation is linear. The cells were recovered on GF/A filters, washed twice with 10 mL f/2 medium and exposed to HCl vapor overnight. Radioactivity was measured in a LKB scintillation counter after addition of scintillation cocktail.

4.4. Results

4.4.1. Brefeldin A blocks increases in CO_2 fixation rates and pyrenoid formation

Gonyaulax is quite sensitive to Brefeldin A (BFA), with an LD_{50} after 24 hours of 0.3 ug/mL. BFA concentrations of 0.1 ug/mL were lethal to roughly 20% of cells in the population after 24 hours, while concentrations of 0.03 ug/mL or lower did not cause cell death after 24 hours. The concentrations of 0.1 and 0.3 ug/mL were thus employed as intermediate and high levels of the drug in subsequent studies. The toxic concentrations of BFA for dinoflagellates appear intermediate between toxic levels observed for mammalian cells ($LD_{50} \approx 0.01$ ug/mL) and protists such as *Toxoplasma* (10 ug/mL).

To determine the effects of BFA concentrations on chloroplast function, we first measured carbon fixation rates *in vivo* using incorporation of $H^{14}CO_3^-$ (Fig. 4.1). As previously shown for samples in constant light (Nassoury et al., 2001), carbon fixation rates in control cultures under LD cycles also increase roughly three-fold from a minimum at mid-night (LDT 18 on a LD 12:12 cycle) to a maximum roughly six hours later (LDT 0). In contrast, carbon fixation rates in cultures treated with either 0.1 or 0.3 ug/mL BFA did not increase to the same extent. In samples treated with 0.1 ug/mL BFA, carbon fixation rates increased roughly in parallel with control cultures for two hours, but after 6 hours total treatment with the drug had carbon fixation rates roughly double the values at LD 18. The effect in cells treated with 0.3 ug/mL BFA was even more pronounced, with carbon fixation rates after six hours treatment almost the same as that found at LD 18. These results indicate that carbon fixation rates in *Gonyaulax* are indeed sensitive to BFA and are suggestive of a dose response effect to the inhibition.

In untreated control samples, circadian increases in carbon fixation rates are accompanied by formation of a pyrenoid, a specialized region in the plastid that is distinguished by widely spaced thylakoid membrane stacks and most of the plastid's Rubisco (Nassoury et al., 2001). For untreated cells, plastids at LD18 have no pyrenoids and Rubisco is spread evenly over the plastids in cell sections as determined by staining with anti-Rubisco and immunogold labeling (Nassoury et al., 2001). At LD 24, however, pyrenoids are fully formed and have a label density (gold beads per um^2) 11 ± 4 times greater than peripheral regions (Fig. 4.2 A). To test if the effects of BFA on carbon fixation rates were

accompanied by alterations in the normal progression of chloroplast ultrastructure, cells samples were taken at LD 24 after six hours BFA treatment. In cells treated with 0.1 ug/mL BFA, pyrenoids can be observed, although their total area appears generally smaller than that of pyrenoids in control cells (Fig. 4.2B). Furthermore, considerable Rubisco can be observed outside the pyrenoid regions by immunogold labeling, with a gold particle distribution in pyrenoids only 3 ± 1 times greater than in peripheral regions of the plastid. Clearly, these intermediate doses of BFA impair but do not block pyrenoid formation.

At higher doses of BFA (0.3 ug/mL), the effect on plastid ultrastructure is much more pronounced. First, in stark contrast to the elongated plastids seen in both control cells and in cells treated with 0.1 ug/mL BFA, the chloroplasts appear as shortened, almost circular structures (Fig. 4.2C). Each of these fragments is much smaller than that in the control plastids, suggesting that the chloroplasts have been fragmented. Second, the widely-spaced thylakoid membrane stacks characteristic of pyrenoids are never observed, even when plastids close to the nucleus are examined (Fig. 4.2D). Lastly, all plastids are all uniformly labeled with the antibody, independent of their position in the cell, indicating that Rubisco movement within the plastid did not occur before fragmentation of the plastids. Taken together, these observations indicate a clear dose dependent effect of BFA on the plastid ultrastructure and strengthen the correlative link between the presence of pyrenoids and efficient carbon fixation rates.

4.4.2. Brefeldin A treatment blocks Rubisco entry into the plastids

We have previously demonstrated that Rubisco import into *Gonyaulax* plastids involves transit through the Golgi (Nassoury et al., 2003). This suggested that the inhibition of both CO_2 fixation and pyrenoid formation by BFA might involve a block in the vesicular transport system carrying newly synthesized Rubisco from the Golgi to the plastid. To test this experimentally, we first examined the cells for evidence of impaired Rubisco transport in BFA treated cells. Cells treated with 0.3 ug/mL Brefeldin A were found to contain an unusual inclusion body, termed a BFA body, which was never observed in untreated cells (Fig. 4.3 A). This roughly spherical structure is located in the central region of the cell close to the nucleus, the location of the Golgi apparatus in untreated

cells (Schmitter, 1971). The BFA body contains electron dense and electron lucent regions, consistent with the presence of both proteins and lipids. At an ultrastructural level, it appears similar to the BFA bodies described in pancreatic ß-cells (Orci et al., 1993).

The addition of BFA to the cell cultures was not expected to inhibit protein synthesis but rather the transport of newly synthesized proteins from Golgi to the plastid. If the BFA body were indeed derived from the Golgi, we reasoned that nuclear-encoded plastid-directed proteins should be present in the BFA compartment. Immunoelectron microscopy using the anti-Rubisco clearly showed numerous colloidal gold particles decorating the electron dense region of the BFA bodies (Fig. 4.3C, D). Labeling was never observed over the electron lucent regions, consistent with higher protein content in the electron-dense regions. We interpret these results as confirmation that transport of the newly synthesized nuclear-encoded Rubisco protein normally destined for the plastid was indeed blocked.

The presence of Rubisco in the BFA body indicates that it should be derived from either the ER or the Golgi. If the site of action of BFA in dinoflagellates was similar to that demonstrated in animal cells, one would expect inhibition of Golgi-derived vesicular transport, including inhibition of the retrieval mechanism normally used to return ER proteins that have escaped to the Golgi. This predicts that plastid proteins would not accumulate in the ER membranes, including those forming the nuclear envelope if this compartment was contiguous with the ER. Indeed, no label was observed over the nuclear envelope (Fig. 4.3 B, solid arrow). These results suggest that the BFA body may represent a swollen and aggregated Golgi apparatus that has fused because of an inability to properly return the appropriate components of the vesicular fusion machinery to the ER.

The label density (gold beads/um^2) after anti-Rubisco labeling was also used to estimate the relative amount of Rubisco present in the BFA compartment and in the plastid (Fig. 4.3 C). The overall average of label density in the BFA compartment was roughly 2.5 fold greater than that found in the plastid (Table 4.1). Despite the fact that the BFA body has considerably less volume than the plastids, clearly this structure contains a substantial amount of plastid-directed protein. If the amount of Rubisco in the BFA body is

proportional to the amount of label, then the proportion of total cellular Rubisco in the structure can be estimated by simply multiplying the relative volumes of the BFA body and the plastids. This estimate suggests that roughly 10 % of the total cellular Rubisco may be found in the BFA body after a 6 hour treatment with the drug (Table 4.1).

The dose dependence of BFA on plastid morphology observed in figure 4.2 suggested that retargeting of newly synthesized Rubisco to the BFA body might also exhibit a dose dependence. To test this, we measured the relative label in the BFA body and in plastids after a six hour treatment with 0.1 ug/mL BFA. These analyses are complicated by the presence of partly formed pyrenoids, which do tend to accumulate Rubisco. However, the label density found in the BFA label is one third that found in the pyrenoids and roughly equal to that found in peripheral regions (Table 4.2). Clearly, both represent less label density than the 2.5 fold increase found in the BFA body after a 6 hour treatment with 0.3 ug/mL BFA. As an alternative to this experiment, the label densities were also measured after a two hour treatment with 0.3 mg/mL BFA. Again, the label density in the BFA body is reduced compared to the 6 hour 0.3 ug/mL BFA treatment. We conclude from these data that Rubisco accumulation in the BFA body is dependent on both the concentration and the duration of the BFA treatment.

To confirm that protein import into the plastid had indeed been inhibited by BFA, we also labeled cells *in vivo* with ^{35}S-methionine at various times between LD 18 and LD 24. Rubisco is synthesized as a polyprotein in dinoflagellates and must be proteolytically cleaved to the mature 55 kDa large subunit from a ~ 200 kDa precursor (Rowan et al., 1996; Zhang and Lin, 2003). The likely location for this processing is the plastid itself, as Rubisco and PCP are both transported to the plastid via the Golgi, and the unusual leader sequence of nuclear-encoded plastid-directed proteins produces an intermediate with the bulk of the protein in the cytoplasm (Nassoury et al., 2003). The incorporation of radiolabel into the 55kDa processed form of the protein thus reflects protein import into the plastid. In order to resolve the Rubisco from other proteins, crude extracts of radiolabeled proteins were subjected to two-dimensional gel electrophoresis. Western blot analysis confirmed the identity of a group of three major protein isoforms at 55 kDa as Rubisco (Fig. 4.4 A). In untreated cells, incorporation of radiolabel into the 55 kDa Rubisco could be observed in samples labeled between LD 20 and LD 24 (Fig. 4.4B).

However, no radiolabel was detected in the mature Rubisco subunits at LD 24 after a six-hour treatment with 0.3 ug/mL BFA (Fig. 4.4 B). Taken together, these experiments show that pyrenoid formation and recruitment of plastid Rubisco to the region of the pyrenoid does indeed require new protein synthesis, and that the action of BFA in blocking pyrenoid formation and the increase in carbon fixation rates occurs by inhibition of protein import from the Golgi.

4.4.3. Rubisco import acts as a timing marker for initiating pyrenoid formation

To further probe the relationship between Rubisco synthesis and pyrenoid formation, cells were treated with BFA at LD 22, two hours following the onset of Rubisco synthesis. We reasoned that if new Rubisco synthesis served as a timing marker for the onset of increased carbon fixation rates, then pyrenoids should still form when protein import was blocked. Alternatively, if continued Rubisco synthesis was necessary to sustain the pyrenoids, then these structures should collapse following a block in protein import. When the cells treated at LD 22 with BFA were observed at LDT 24, pyrenoids were formed as judged by the increased spacing between thylakoid membranes (Fig. 4.5 A, C). However, recruitment of Rubisco to the region of the pyrenoid is incomplete, as peripheral regions of the plastids still contain substantial levels of Rubisco (Fig. 4.6B). Counts of the label density in the pyrenoid show that the enrichment is less than 3 fold that in peripheral regions of the plastid after this two-hour BFA treatment (Table 4.2). Rubisco import to the plastid has been interrupted, as confirmed by the presence of BFA bodies that contain substantial levels of anti-Rubisco label (Fig. 4.5 C, D). Interestingly, after this 2 hour 0.3ug/mL BFA treatment the ratio of label density in the pyrenoid compared to the periphery is very similar to that observed with the 6 hour 0.1 ug/mL BFA treament (Table 4.2). This suggests the recruitment of Rubisco to the pyrenoid may be related to the amount of newly synthesized Rubisco entering the plastid.

To distinguish between a reduced rate of pyrenoid formation and an initiation of pyrenoid breakdown, cells treated with BFA at LD 22 were also examined at LDT 2. In these samples, pyrenoids can be clearly seen (Fig. 4.5 E), and contain Rubisco enriched by a factor of roughly 10 fold as determined by anti-Rubisco staining (Fig. 4.5 F). At LD 2 in these BFA treated cells, the level of Rubisco recruitment has proceeded to the same

extent as for control cells observed at LD 24. We interpret these results to indicate that pyrenoid formation is initiated by a timing signal provided to the plastid between LDT 18 and LDT 22. This signal is likely to be a protein imported into the plastid from the Golgi, as inhibition of vesicular transport after some signal has entered the plastids can retard pyrenoid formation. It also seems likely that the protein acts catalytically in Rubisco recruitment, as blockage of vesicular transport after LD 22 retards but does not block pyrenoid formation. Finally, we conclude that continued Rubisco synthesis is not necessary for maintenance of the pyrenoids.

4.4.4. BFA does not block pyrenoid breakdown

The preceding results suggested that pyrenoid formation might be regulated by import of newly synthesized proteins into the plastids. However, the disappearance of the pyrenoids is also a circadian controlled process. To determine if a specific signal imported from the Golgi was implicated in pyrenoid breakdown, BFA was administered to the cells at LD 12, two hours before pyrenoids have disappeared (Fig. 4.6 A). However, in both treated and untreated cells the plastid morphology is the same at LDT 14 (Fig. 4.6 B, C). For both, the plastids have been pulled back from the cell wall and no pyrenoids are present. This indicates that inhibition of vesicular traffic is unable to retard chloroplast movement in the cell and the decrease in thylakoid spacing, and suggests that any timing signals required for pyrenoid breakdown may impact the plastid using other mechanisms. Although formally possible that pyrenoid breakdown may be due to lack of new protein import at this time in the LD cycle, this seems unlikely given that the pyrenoid do not disappear when new protein import is blocked at LD 22.

4.4.5. BFA does not affect the timing of cell division or bioluminescence glow rhythms

The results showing that the timing of BFA application is important for inhibition of pyrenoid formation suggested the possibility that the effects of the drug could be an indirect result of an effect on the circadian clock. To test this, two other circadian rhythms were monitored following application of the drug. In one, the timing of the bioluminescence glow peak was measured, and this timing was not significantly altered

even by high doses of BFA (Fig. 4.6 A). In a second, the timing of cell division was monitored. In control cells, mitosis is gated to LD 1, as seen by the characteristic paired cells when the cell cultures are examined microscopically. In BFA treated cells, the timing of entry into M-phase was not altered, as paired cells were first observed at LD 1. However, the BFA-treated cells were not able to complete mitosis, as paired cells were also observed at LD 2 and LD 3. This behavior is unlike the control cells in which the paired cells have completed mitosis and have produced many small, recently divided cells. We interpret this later result as indicative of the requirement for vesicular transport during the formation of new cell walls analogous to the BFA-induced disruption of the terminal phase of cytokinesis in the embryonic blastomeres of BFA-treated *C. elegans* embryos (Skop et al., 2001). Taken together, these experiments indicate that BFA exerts its effect on the carbon fixation mechanism directly rather than by an indirect effect on the circadian timing of the rhythm.

4.5. Discussion

Circadian rhythms represent the observed outputs of the circadian timers common to most eukaryotic cells. Studies using DNA microarray technology have contributed greatly to our understanding of observed rhythms by documenting the numerous changes in gene expression that can be directly regulated by the circadian oscillator (Morse and Sassone-Corsi, 2002). These studies, however, imply that changes in gene expression will regulate the activity of biochemical pathways by altering the amounts of enzymes catalyzing the rate-limiting step (RLS) in the pathway. In this context, regulation of the circadian rhythm of carbon fixation in the dinoflagellate *Gonyaulax* is somewhat unusual. Instead of changes in enzyme amounts, the carbon fixation rhythm appears due to changes in the suborganellar distribution of the RLS catalyst Rubisco. This conclusion is based on the observations that the amount of Rubisco remains constant over the daily cycle while Rubisco accumulation in pyrenoids increases in concert with the increase in carbon fixation rates (Nassoury et al., 2001). The experiments described here support the view that Rubisco distribution is intricately linked to the distribution of the enzyme within the plastid, as BFA treatment blocks both the normal circadian increase in carbon fixation rates (Fig. 4.1) and Rubisco recruitment to the pyrenoids (Fig. 4.2). The molecular mechanism whereby changes in Rubisco distribution affect CO_2 fixation rates is not yet known, although we have previously proposed that the changes in Rubisco distribution alter the relative levels of the substrate CO_2 and the competitive inhibitor O_2. The concentrations of substrate and inhibitor affect the $\upsilon CO_2/\upsilon O_2$ ratio that in turn determines the activity of the enzyme (Jordan and Ogren, 1981). Interestingly, the thylakoid membranes contain the major light harvesting protein PCP (Hofmann et al., 1996), so that as Rubisco accumulates in the pyrenoid, and the spacing between the thylakoid membranes increases, the relative amount of PCP in the pyrenoid decreases. Our calculations show that the pyrenoid contains roughly 90% of the plastid Rubisco yet less than 20 % of the plastid PCP (Nassoury et al., 2001). Thus, Rubisco recruitment to the pyrenoid has the added benefit of reducing the impact of the O_2 generating machinery.

Previous experiments have indicated that the amount of Rubisco does not change appreciably over the course of the daily cycle (Bush and Sweeney, 1972; Nassoury et al.,

2001). However, the experiments reported here with BFA suggest that new protein synthesis may still be important in regulating the asymmetric distribution of Rubisco in the pyrenoids. This conclusion derives from the observations that BFA blocks the import of Rubisco into the plastids (Fig. 4.4) and the formation of pyrenoids (Fig. 4.2). Importantly, both effects are dose dependent, as a lower dose or a shorter treatment time were found to reduce not only Rubisco enrichment in the pyrenoid but also the relative label density in the BFA body (Table 4.2). These data thus point to a link between the amount of Rubisco that has entered the plastid and pyrenoid formation. The mechanism whereby newly synthesized Rubisco might signal pyrenoid formation is not yet known, and it is still possible that an accessory protein, synthesized and imported at the same time as Rubisco, acts as the functional signal for this process. Interestingly, independent of the identity of the actual signaling molecule, it appears the site of protein entry from the Golgi defines the site of pyrenoid formation. Pyrenoids only form in regions of the plastid near the Golgi apparatus, through which the newly synthesized Rubisco passes on its way to the plastid (Nassoury et al., 2003).

The inhibition of the carbon fixation rhythm effect by BFA is much more specific than inhibition by general protein synthesis inhibitors. We show that BFA treatment has no effect on the rhythm of either bioluminescence glow or cell division (Fig. 4.7). This indicates that the effects of BFA on the carbon fixation rhythms are not secondary effects resulting from an impact of the drug on the clock mechanism, since the phases of photosynthesis, bioluminescence and cell division are tightly coupled under normal growth conditions (McMurry and Hastings, 1972). In sharp contrast to the effects of BFA, the general protein synthesis inhibitors anisomycin (Taylor et al., 1982) or cycloheximide (Dunlap et al., 1980), shift the phase of the circadian clock by up to twelve hours. At least for cycloheximide pulses, the ultrastructural changes observed in plastid morphology all appear to be consistent with changes in the phase of the circadian clock (Rensing et al., 1980). Thus these effects are clearly a secondary effect of changes in overall circadian timing. It would be of interest to examine if RNAi could inhibit Rubisco synthesis, as this would provide the most specific tool possible for determining the role of new protein synthesis in the regulation of pyrenoid formation. To date, no studies have yet reported tests of RNAi in algae.

The exposure of cells to high concentrations of BFA at LD 18 does illustrate one unexpected and potentially secondary effect. This effect is seen as the production of large numbers of smaller, almost spherical plastids from the normal elongated plastid morphology after exposure to high concentrations of BFA (Fig. 4.2). This finding is especially interesting in that this unusual plastid morphology is not observed when BFA is given at LD 22 (Fig. 4.5). While the effect may be due to the accumulated effect of the long time spent with the drug, we believe the effect may instead be related to the timing of the plastid elongation. Normally, the chloroplasts become more elongated until they extend out to the cell periphery at a time roughly between LD 20 and LD 22 (Rensing et al., 1980). It seems reasonable to assume that if BFA was able to influence changes in plastid morphology that this might occur at the time plastid morphology is normally changing, and that BFA given after the change has already taken place might be ineffective. Interestingly, circadian changes in plastid morphology in the dinoflagellate *Pyrocystis* can be inhibited by cytochalsin D, which depolymerizes the actin cytoskeleton (McDougall, 2002). One possible connection between the actin cytoskeleton and BFA lies in the recently described Arfaptin, capable of binding Arf-GTP as well as Rac-GTP or Rac-GDP in mammalian cells (Tarricone et al., 2001). A blockage of Arf activation by BFA would thus free Arfaptin for Rac binding, which could then result in alteration of the actin cytoskeletal conformation.

BFA works quickly to inhibit vesicular transport in mammalian cells (Dascher and Balch, 1994), and in *Gonyaulax* we observe that BFA-bodies are well formed and stain strongly with the anti-Rubisco after only a two hour BFA treatment. This suggests that BFA may be similarly fast-acting in dinoflagellates. If the inhibition were complete as well as fast acting, then the BFA body should contain all the Rubisco synthesized subsequently to administration of the drug. To estimate the amount of Rubisco found in the BFA body, we first estimated the relative volume of the BFA body and the plastids. We assumed the chloroplasts to be cylinders and the BFA body to be a sphere, and estimate from this that the BFA body may have a volume of ~ 4 % that of the plastids (Table 4.1). The concentration of Rubisco in the BFA body, however, based on the gold particle density after anti-Rubisco labeling, could be ~ 2.5 times greater than in the plastids. This suggests that after a six hour BFA treatment the BFA body might contain up to 10 % of

the total cellular Rubisco. This is not unreasonable, given that the generation time of the cells under our growth conditions is roughly five days, and that Rubisco is only synthesized for roughly twelve hours each day (Markovic et al., 1996). The 6 hours of BFA treatment could thus represent one-tenth the total Rubisco synthesis. Our estimate is remarkably similar to what would be expected from complete inhibition of new protein import into the plastid. We have also noted that the relative amount of label in the BFA body is dependent on the BFA concentration used, with a 0.1 ug/mL treatment reducing the proportion of Rubisco label relative to the plastid (Table 4.2). This effect can be mirrored by reducing the length of time the cell are exposed to 0.3 ug/mL BFA, as this treatment is has a BFA body label density virtually indistinguishable from that produced by the longer, less concentrated dose (Table 4.2). Taken together, these results suggest that the 0.1 and 0.3 ug/mL BFA doses used here probably represent intermediate and complete inhibition of Golgi transport, respectively.

The ability of BFA to inhibit Rubisco import into the plastids was directly tested by *in vivo* labeling of protein with ^{35}S-methionine. Here, two-dimensional electrophoresis and autoradiography was used to specifically examine the incorporation of radiolabel into the 55 kDa Rubisco. The Rubisco in *Gonyaulax* is encoded as a polyprotein, which is ~ 200 kDa in other dinoflagellates (Rowan et al., 1996; Zhang and Lin, 2003). Incorporation into the mature 55 kDa large subunit was taken as a measure of protein import since only the N-terminal end of the polyprotein has the sequence necessary for directing the protein to the plastid. The targeting sequence directing proteins to the triple membrane bound plastids of *Gonyaulax* is similar to that used to target proteins to the triple membrane bound plastids of *Euglena*; characterized by two hydrophobic regions flanking a typical transit peptide, it is unlike that used in any other system (Nassoury et al., 2003). Furthermore, at times when Rubisco is actively synthesized, anti-Rubisco labeling increases in the Golgi but not in the cytoplasm. It thus seems likely that processing of the Rubisco polyprotein will occur as the polyprotein is translocated into the plastid stroma. Unlike untreated cells, where Rubisco begins to be imported at LD 20, cells treated with BFA do not incorporate radiolabel into the Rubisco large subunit. The synthesis of the Rubisco itself is not inhibited, however, as anti-Rubisco staining accumulates in the BFA body (Fig. 4.3).

This signal responsible for Rubisco recruitment and the formation of the spaced thylakoid stacks characteristic of the pyrenoid is supplied to the plastid between LD 18 and LD 22, as blockage of vesicular traffic by BFA at LD 22 slows but does not stop Rubisco recruitment to the pyrenoid from peripheral regions of the plastid (Fig. 4.5). This later result is also important in that it suggests pyrenoid maintenance does not depend on continued Rubisco synthesis. As a corollary of this, the disassembly of pyrenoids at the end of the day phase in cells treated with BFA will also not be due to a lack of new Rubisco synthesis. Since the breakdown of pyrenoids, unlike their formation, is not retarded by application of BFA (Fig. 4.6), this may suggest that either the signal is provided to the plastids prior to LD 12 or that the signal does not involve a protein imported into the plastid from the Golgi.

It is worth at this point to compare the mechanisms used for regulating the carbon fixation and bioluminescence rhythms. The bioluminescence capacity of the cells increases when the levels of both the reaction catalyst luciferase (Johnson et al., 1984) and the substrate binding protein LBP (Morse et al., 1989) increase and assemble into discrete organelles termed scintillons (Fritz et al., 1990). Scintillon formation begins at the time of LBP synthesis, and double immunolabeling experiments shows that small prescintillons can be detected as aggregates of both luciferase and LBP in the cytoplasm near the nucleus (Nicolas et al., 1991). These small prescintillons aggregate and move out toward the periphery of the cell where they become active as mature scintillons when they come in contact with the vacuolar membrane. The changes in bioluminescence capacity thus reflect changes in protein synthesis, protein amount and protein distribution within the cytoplasm. By comparison, we show here that changes in carbon fixation capacity reflect changes in protein synthesis and protein distribution in the chloroplast. In both cases, changes in levels of gene expression (at the translational level) initiate changes in protein localization that ultimately are observed as the rhythm. While the mechanism modulating Rubisco distribution may be subtler, the basic theme of enzyme localization appears conserved in these two rhythms.

Table 4.1.

The BFA body at LD 24 contains roughly 10 % the total cellular Rubisco [a]

	Volume (μm^3)	Labeling (Exp 1) (gold beads/μm^2)	Labeling (Exp 2) (gold beads/μm^2)
Plastids	400[b]	60 ± 5	30 ± 5
BFA compartment	15 [c]	175 ± 45	75 ± 17
BFA/plastid ratio	4 %	2.9	2.5

[a] The fraction of total cellular Rubisco in the BFA body is calculated from the product of its volume relative to the plastid and its label density relative to the plastid.

[b] Total cellular plastid volume was calculated from the number of organelles (~ 60 per cell) and the volume of one plastid (calculated as a cylinder of base 1 um and height 8 um).

[c] Volume of the BFA body was calculated as a sphere of diameter 3 um.

Table 4.2.

BFA body labeling and Rubisco enrichment in pyrenoids are dependent on BFA dose

	0.1 µg/mL BFA LD18 (gold beads/µm^2)	0.3 µg/mL BFA LD22 (gold beads/µm^2)
BFA body [a]	17 ± 2	29 ± 3
Pyrenoid	49 ± 5	60 ± 19
Periphery	18 ± 2	27 ± 9
BFA/Plastid (Periphery)	0.9 ± 0.2	1.1 ± 0.5
Pyrenoid/Periphery	2.7 ± 0.6	2.2 ± 1.5

[a] All cells were harvested at LD 24

Figure 4.1. BFA blocks CO_2 fixation

In the absence of BFA, rates of ^{14}C-CO_2 fixation in *Gonyaulax* cultures increase from midnight (LDT 18) to dawn (LD 24). This normal nightly increase can be blocked by either 0.1 or 0.3 μg/mL concentrations of BFA to cell cultures at LD 18.

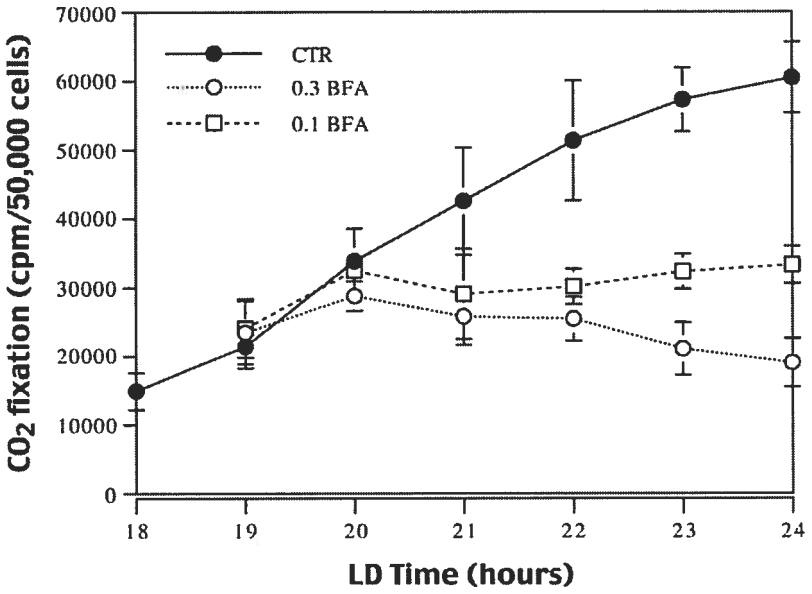
70000
60000
50000
40000
30000
20000
10000
0
CTR
0.3 BFA
0.1 BFA
CO_2 fixation (cpm/50,000 cells)
18
19
20
21
22
23
24
LD Time (hours)

Figure 4.2. BFA blocks formation of pyrenoids inside the plastids
The Rubisco distribution in chloroplasts is observed by anti-Rubisco followed by immunogold labeling. (A) In control cells at dawn, label is seen primarily in pyrenoids, regions of the plastid with widely spaced thylakoid membranes that are furthest from the cell periphery. (B) Cells treated with 0.1 ug/mL BFA contain chloroplasts roughly similar in shape and size to those in control cells, except that less anti-Rubisco staining is concentrated in regions corresponding to the pyrenoid. (C, D) Chloroplasts in cells treated with 0.3 ug/mL BFA have lost their typical elongated morphology and none of the smaller plastids have the expanded thylakoid membranes characteristic of pyrenoids. Scale bars are 1 um.

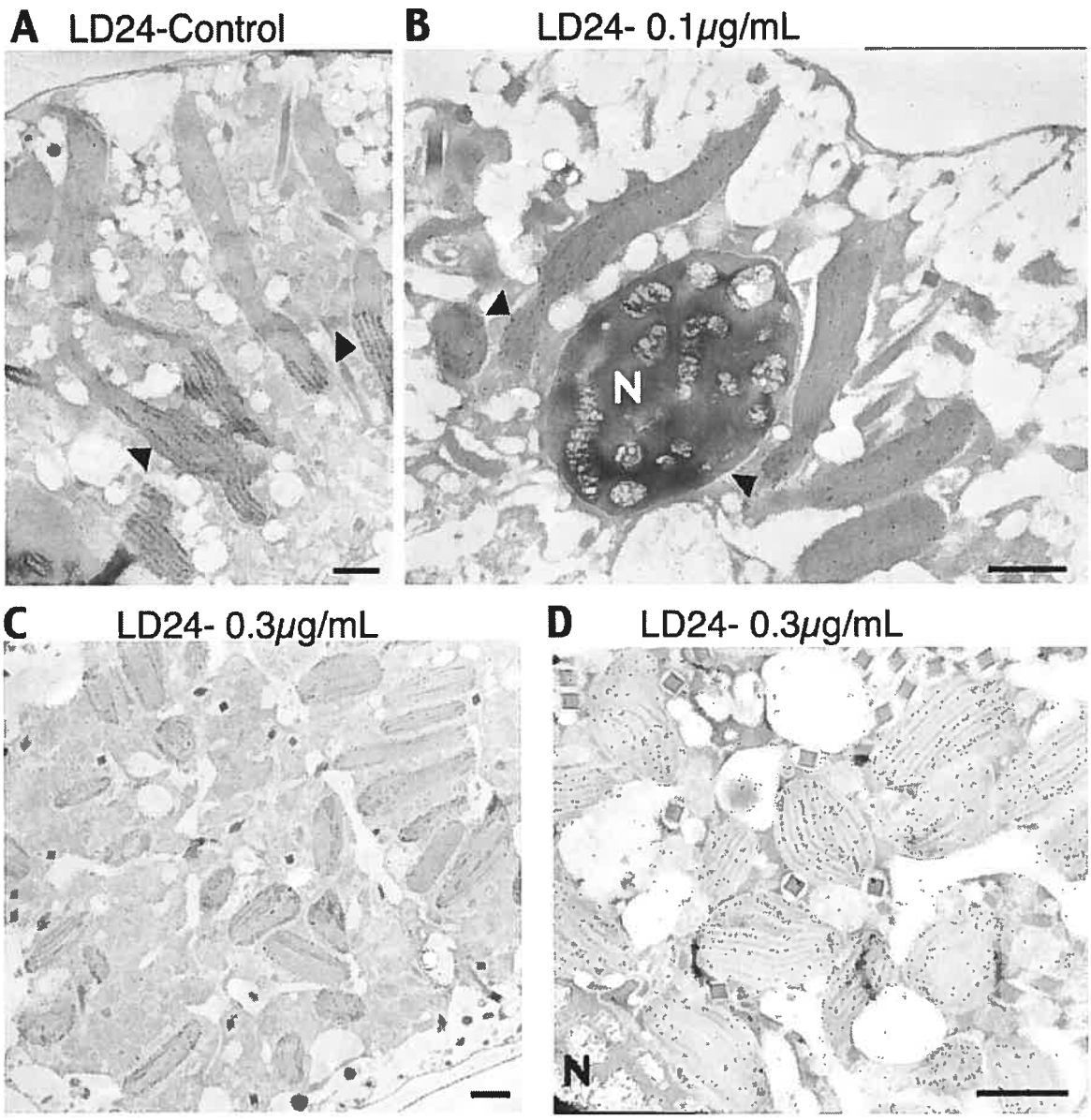
A LD24-Control
B LD24- 0.1μg/mL
N
C LD24- 0.3μg/mL
D LD24- 0.3μg/mL
N

Figure 4.3. BFA bodies contain membrane and nuclear-encoded plastid-directed proteins (A) Cells at LD 24 treated with 0.3 ug/mL BFA for 6 hours show a novel polyvesicular structure termed a BFA body (B) in the central region of the cell between the nucleus (N) and the plastids (P), a region corresponding to the normal location of the Golgi apparatus. (B) Staining of cell sections with anti-Rubisco and immunogold label indicates that Rubisco has not accumulated in the nuclear envelope (closed arrow) or in the membrane surrounding the plastid (open arrow). (C, D) Anti-Rubisco staining is associated with the electron dense regions of the BFA body, which show a label density much greater than that in the surrounding plastids.

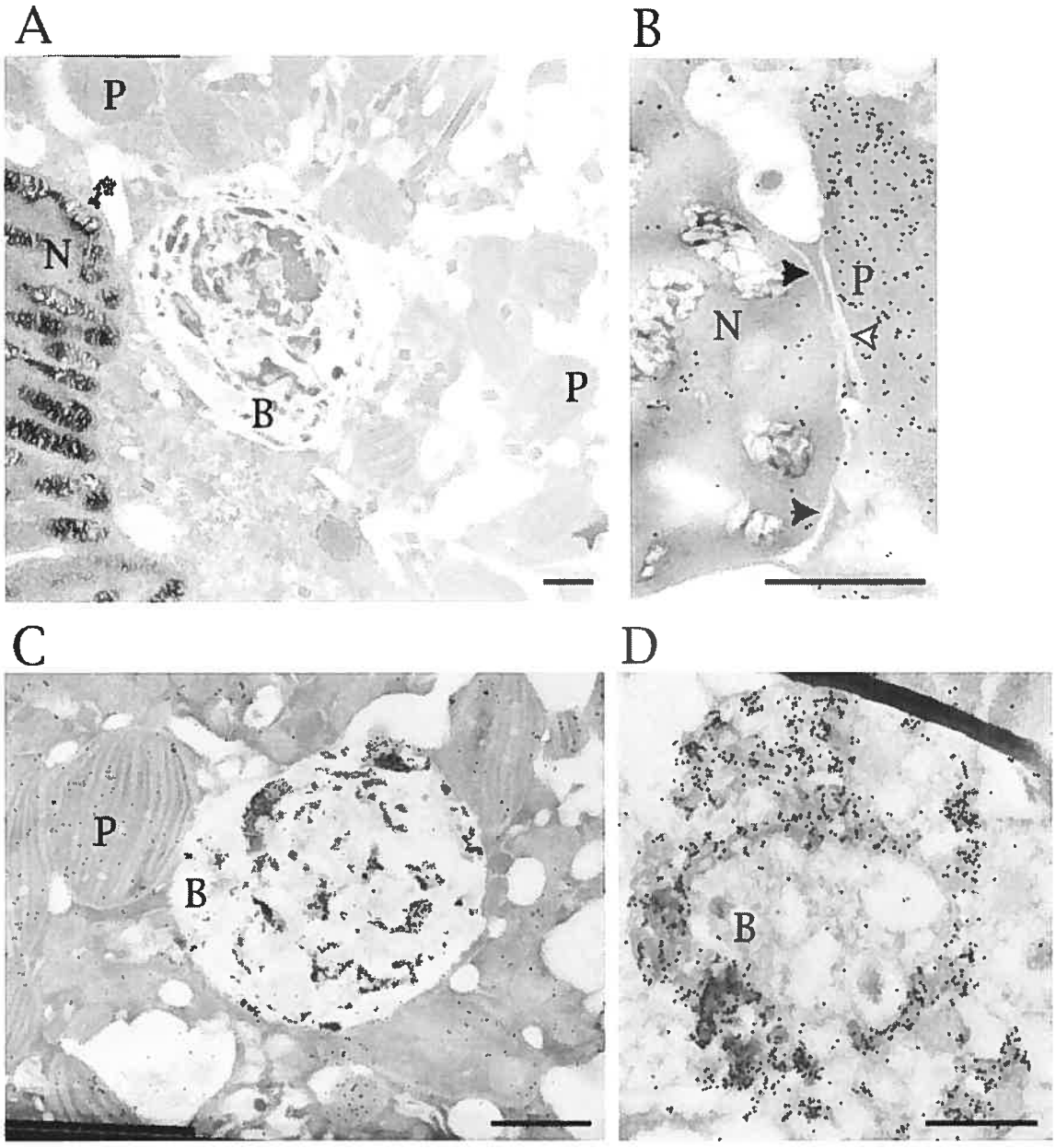
A
P
N
B
P
B
N
P
C
P
B
D
B

Figure 4.4. BFA blocks synthesis of nuclear-encoded plastid-directed proteins (A) Rubisco can be resolved from other protein components in the cells by two dimensional gels. The identity of the protein isoforms in the boxed area as Rubisco can be confirmed by anti-Rubisco staining on Western blots. (B) *In vivo* metabolic labeling with ^{35}S-methionine shows that amount of signal after autoradiography (AR) in the position associated with the Rubisco as determined by Coomassie blue staining (CB) depends on the time of labeling. No label is associated with the 55 kDa Rubisco isoforms at LD 18 in untreated cells, or at LD 24 in cells treated for six hours with 0.3 ug/mL BFA no radiolabel is incorporated into the 55 kDa Rubisco.

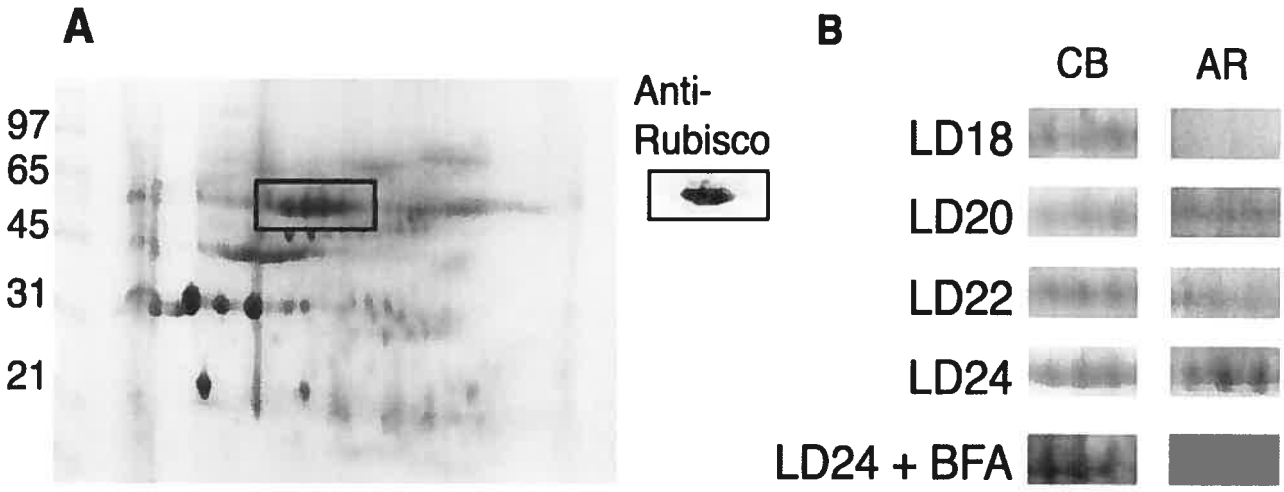
A
97
65
45
31
21
Anti-
Rubisco
B
CB
AR
LD18
LD20
LD22
LD24
LD24 + BFA

Figure 4.5. Addition of BFA after the onset of Rubisco synthesis delays Rubisco accumulation but does not stop pyrenoid formation

(A-D) In cells at LDT 24, after a two hour exposure to 0.3 ug/mL BFA, pyrenoids can be observed in plastids that have maintained their normal elongated morphology. The distribution of Rubisco, determined by anti-Rubisco and immunogold staining, shows that considerable marker is found in peripheral regions of the plastid. BFA bodies form after two hours BFA treatment, indicating the drug has had the expected effect on vesicular transport, and the BFA bodies contain Rubisco as shown by immunogold labeling. (E, F) In cells at LD 2, after a four hour exposure to 0.3 ug/mL BFA, pyrenoids are formed and plastid morphology is normal. The gold particle distribution inside the plastids, determined after anti-Rubisco staining, indicates that Rubisco accumulation in the pyrenoid is complete.

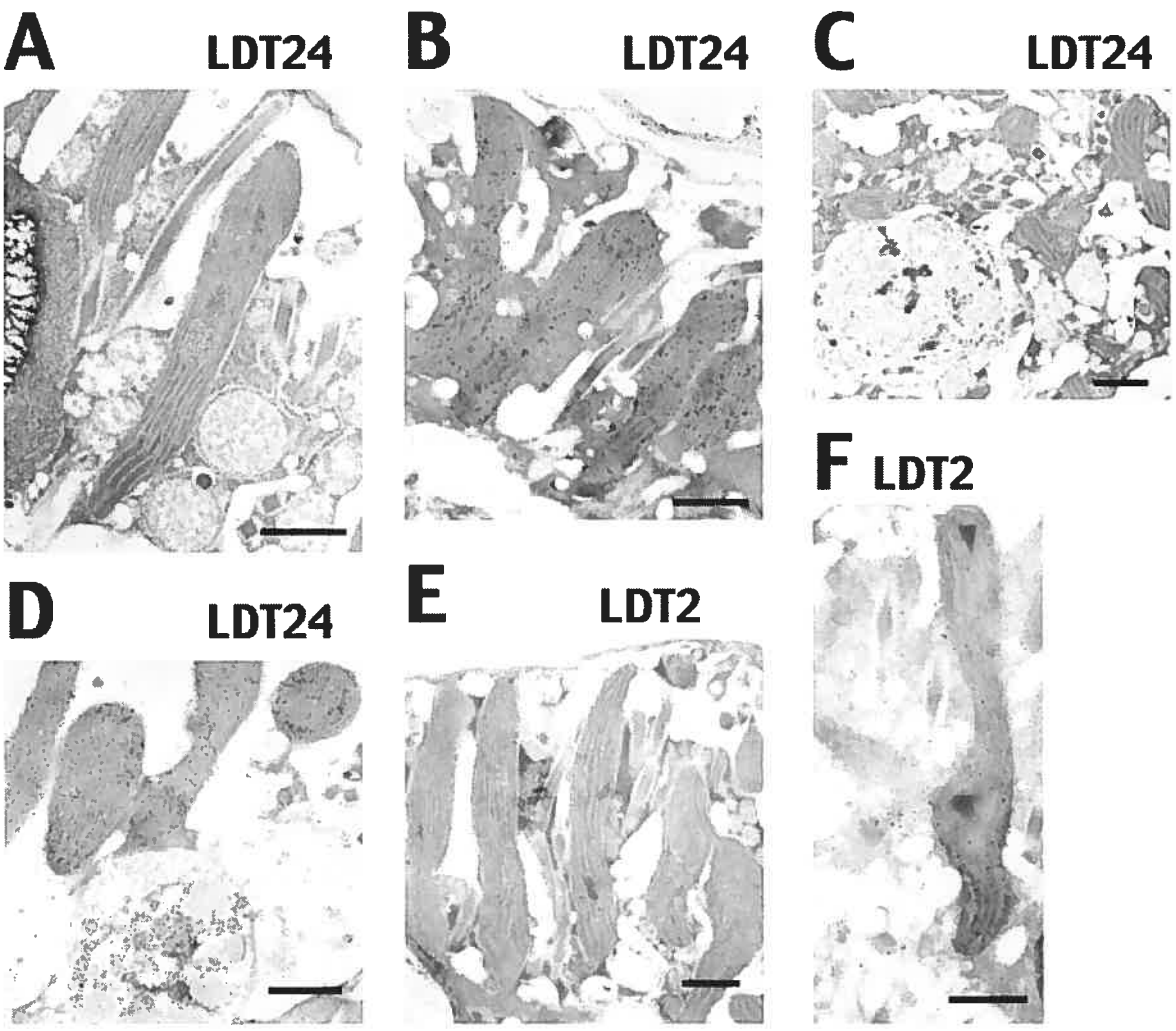
A
LDT24
B
LDT24
C
LDT24
D
LDT24
E
LDT2
F
LDT2

Figure 4.6. BFA does not inhibit pyrenoid breakdown

(A, B) In control cells, pyrenoids are still present in plastids at LD 12 but have disappeared by LDT 14. (C) The disappearance of pyrenoids is not inhibited by a two hour treatment with 0.3 ug/mL BFA.

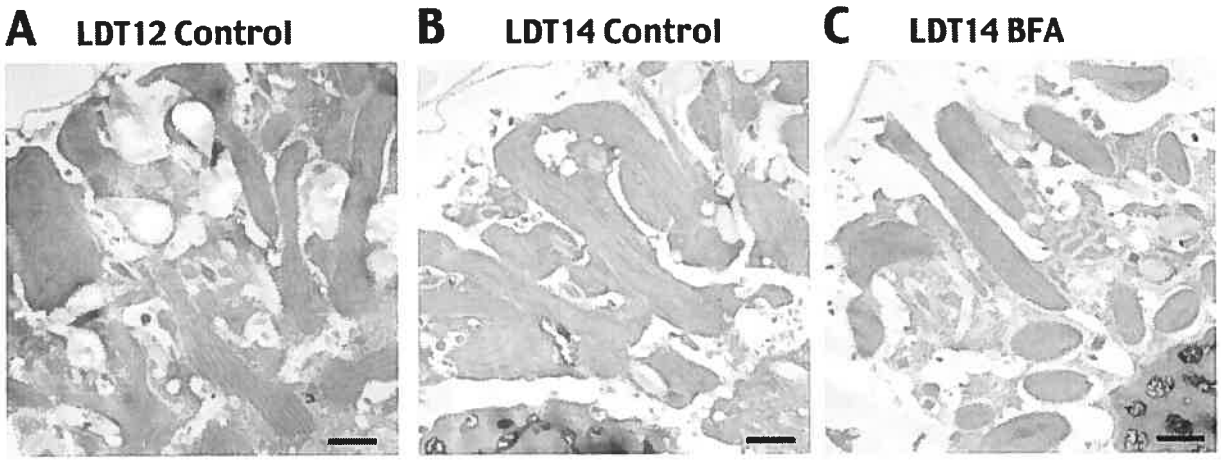
A
LDT12 Control
B
LDT14 Control
C
LDT14 BFA

Figure 4.7. BFA does not affect the timing of cell division or bioluminescence rhythms (A) Chart paper trace recordings of cells placed adjacent to a photomultiplier tube show luminescence emission as both flashes (vertical spikes) and glow (base line). The peak in bioluminescence glow occurs at roughly LD 22 in both control cell cultures and those to which 0.3 ug/mL BFA was added at LD 18. (B) Mitosis can be observed microscopically by the presence of characteristic paired cells (circles). Normally gated by the circadian clock to one hour after dawn (LDT 1), paired can be seen at this time both in control cultures and cultures to which 0.3 ug/mL BFA was added at LD 18. Treated cultures contain paired cells at later times and lack the many smaller cells indicating completion of mitosis.

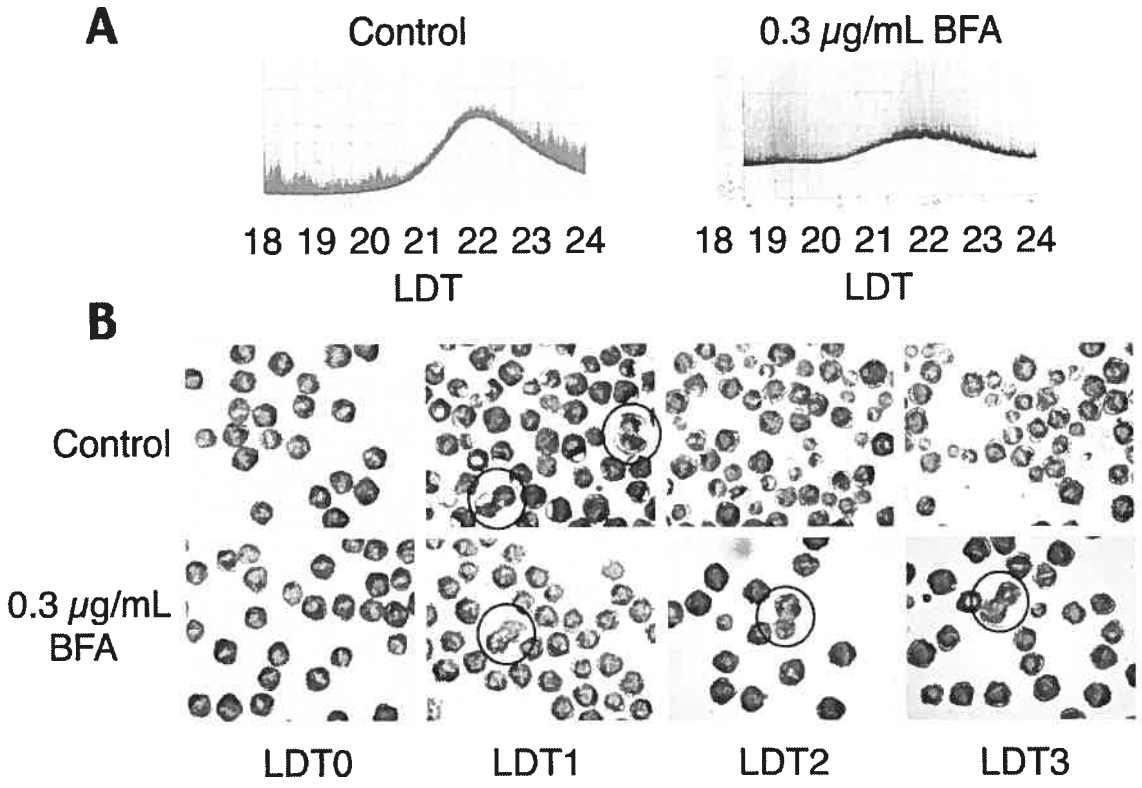
A
Control
0.3 μg/mL BFA
18 19 20 21 22 23 24
LDT
18 19 20 21 22 23 24
LDT
B
Control
0.3 μg/mL BFA
LDT0
LDT1
LDT2
LDT3

Figure 4.8. Schematic model of BFA inhibition of Rubisco import into plastids Rubisco is normally synthesized on membrane bound ribosomes and transported to the Golgi where it is targeted to the chloroplasts. The import of newly synthesized protein correlates with development of the pyrenoid and movement of Rubisco from the peripheral regions of the plastid to regions close to the Golgi. BFA treatment blocks Golgi to plastid transport and when BFA is given before the onset of Rubisco synthesis completely inhibits pyrenoid formation and Rubisco movement.

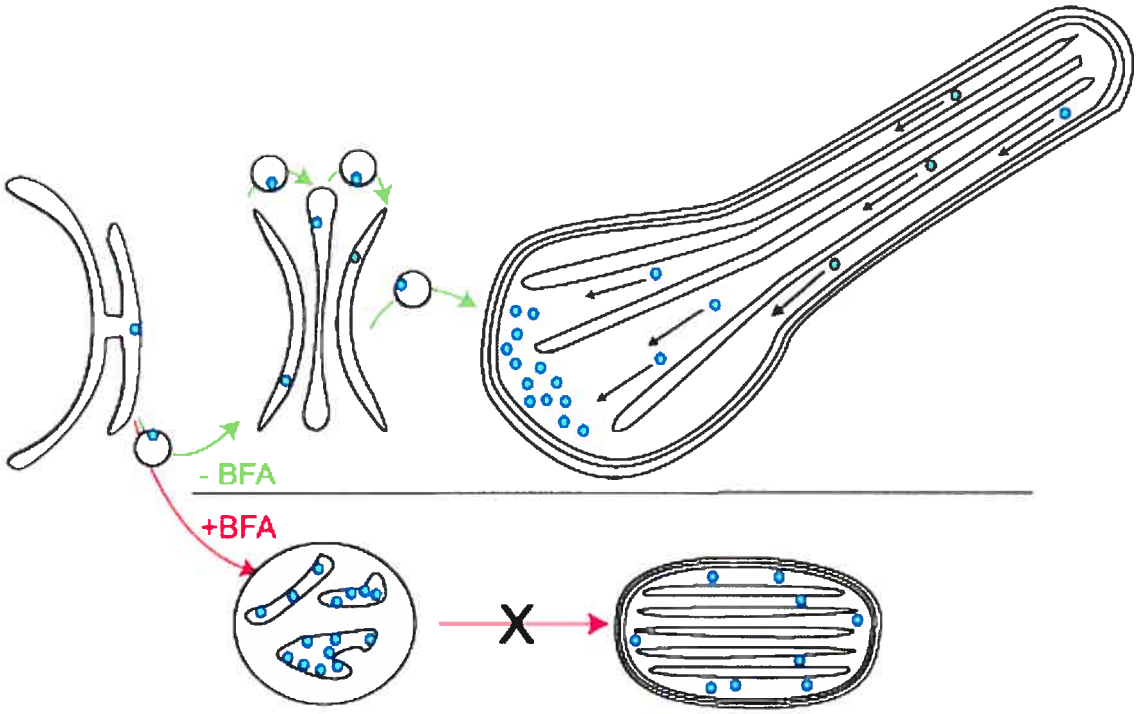
- BFA
+BFA
X

4.6. Acknowledgements

We thank Louise Pelletier for assistance with sample preparation for electron microscopy. We gratefully acknowledge the financial support of the National Science and Engineering Research Council of Canada

5. General Discussion

Dinoflagellates are an important part of the phytoplankton as they contribute significantly to the photosynthetic primary production of the marine ecosystem. Blooms of certain groups of dinoflagellates are responsible for the red tides that can be devastating to the fishery and the tourism industry since some of them are able to produce strong neurotoxins posing a significant health risk. Phylogenetically, dinoflagellates are related to the more well studied ciliates and apicomplexans. But above all studying dinoflagellates are fascinating because of their uniqueness and their extraordinary unexplored characteristics. Fossil evidence suggest that they have survived for approximately 400 million years yet they often present unusual solutions to ordinary biochemical processes that challenge our view of a "best solution" honed by evolution. This alone deserves study in order to understand their continued existence through evolution.

Perhaps one of the best examples of unusual biochemistry is the use of a form II Rubisco as the primary catalyst for the fixation of CO_2 in their Calvin cycle. The form II Rubisco, like its form I homologue, catalyzes the first oxygenation step in photorespiration, in addition to its carboxylation activity. Oxygen is thus a competitive inhibitor of CO_2 binding to both forms of Rubisco, and the relative specificity of RuBisCO (s_{rel}), which defines the ratio between the carboxylase and oxygenase activities at a particular $[CO_2]\backslash[O_2]$, is thus a central parameter to consider. The s_{rel} values for higher plants cluster around 100 while the form II Rubisco found in Rhodopseudomonas (a non-sulfur purple bacteria) has an s_{rel} value of 12 (Jordan et al 1981). Thus the rate of oxygenation is about 3 fold faster than that of carboxylation in natural conditions ($0.03\%CO_2$, $21\%O_2$). Such a nondiscriminatory Rubisco is satisfactory for an organism with an anaerobic lifestyle, but this is not the case in the dinoflagellate chloroplast where O_2 is evolved (Morse et al.1995).

One major question is where did this gene come from? One scheme is transfer of a form II Rubisco gene to the nucleus directly from a proteobacterium or indirectly from the dinoflagellate mitochondrion, which themselves evolved from a proteobacterium, followed by the loss of the original form I gene of the plastid origin (lateral gene transfer) (Palmer, 1995) . Recently it has been shown that in apicomplexans a minor component of

the apicoplast DNA is indeed originally from the mitochondrion, thus supporting the idea of inter-compartmental DNA traffic in the alveolate lineage (Obornik et al., 2002).

A second and more important issue is how the form II Rubisco copes with the O_2 dilemma and actually fixes carbon in *Gonyaulax*. Our observations show that *Gonyaulax* has developed a mechanism that enables it to compartmentalize its Rubisco in the pyrenoids, which is presumably an O_2 depleted microenvironment such as carboxysomes in cyanobacteria. Carboxysomes are small bodies containing Rubisco surrounded by proteinaceous shell, and pumps located in the plasmalemma deliver HCO_3^- to the cytoplasm which diffuses into the carboxysomes where carbonic anhydrase catalyzes its conversion to CO_2 that could then be used by Rubisco prior to its diffusion out of the carboxysomes (Price et al., 1998)

One major difference is that in *Gonyaulax* CO_2 concentrating elements are not thus far known to be present and pyrenoids are separated from the rest of the plastid by a molecular barrier rather than a physical one. In the dinoflagellate *Symbiodinium*, the energy required for the carbon concentrating mechanism (CCM) to move inorganic carbon into the cell is supplied by photosynthetic electron transport (Badger et al. 1998). However, in *Gonyaulax*, the CO_2 fixation rates rise to their peak when O_2 evolution rates are still at their nadir as observed in Figure 2.1. This ~6 hr difference between the onset of the two rhythms eliminates the possibility that the increase in carbon fixation rates could be due to an increase in photosynthetic electron transport. Certainly the existence of a CCM in *Gonyaulax* is not ruled out and further research for locating them is required. However, we hypothesized that the spatial separation of Rubisco and PCP could decrease the local oxygen tension in the pyrenoids hence reduce competition by oxygen for the active site of the form II enzyme and thus increase the rate of carbon fixation.

The basic theme of enzyme localization appears to be a conserved feature in regulation of circadian rhythms in some dinoflagellates. Previously it had been shown that in the dinoflagellate *Pyrocystis fusiformis* the level of luciferase is constant while its distribution undergoes a circadian change in phase with the onset of bioluminescence (Widder and Case 1982) hence protein localization is accountable for the rhythmic behavior. Of course our observation is at suborganelle level while in the aforementioned case, the changes are subcellular.

It is pertinent to mention that movement of Rubisco in and out of the pyrenoids (but always inside the plastid) has been previously reported in different algae (for example prior to plastid and cell division). The mechanism for this, however, remains unknown. It seems likely that when aggregates of Rubisco form in the pyrenoids, the added volume will push apart the thylakoids to form the easily recognized morphology, but what moves the Rubisco? One possibility is that thylakoid membranes are brought into close physical association in cortical regions of the plastid, which forces Rubisco down toward the cell center in a manner similar to the extrusion of toothpaste from a toothpaste tube. However, there is little day/night variation in the distance between thylakoids in cortical regions of the plastid (Rensing et al.,1980), suggesting that this possibility is unlikely. An alternative could involve active recruitment of Rubisco to a developing pyrenoid, perhaps using prokaryotic-type cytoskeletal elements such as FtsZ which are known to be present in plastids (Lutkenhaus and Addinall 1997; Osteryoung et al. 1998). However, motor proteins are not believed to be found in prokaryotes, and by extension, in organelles.

It is interesting that both Rubisco and PCP synthesis rates increase in parallel with rate increases in their respective photosynthetic rhythms, just as LBP synthesis occurs as bioluminescence emission is increasing in the cell. However, the synthesis of LBP stops before the rhythm has peaked, while for photosynthesis, protein synthesis continues for as long as the rhythm is at a maximum. This synchronization between the timing of synthesis and the observed activity indicates a plausible link which we tried to test by using BFA to block Rubisco transport (chapter 4, also see below).

We speculate that the newly synthesized Rubisco or another protein made at the same circadian time can act as a pyrenoid formation signal. Furthermore, as Rubisco enters the plastid close to the site of the developing pyrenoid, newly synthesized protein must rest in that region and contribute to the pyrneoid. But how does the previously synthesized Rubisco that moved to peripheral regions of the plastid when the CO_2 fixation rates were low, move back to the developing pyrenoid? Could the newly synthesized Rubisco have a self-aggregating nature that enables it to accumulate in one part of the chloroplast and attract previously synthesized protein? Alternatively, a "Rubisco binding protein" that can bind Rubisco, imported from the Golgi, could make Rubisco aggregate in the pyrenoids. For identifying proteins that might bind Rubisco and organize formation of

pyrenoids, a comparison of protein profiles of two-dimensional electrophoretic patterns by a proteomic approach could possibly pinpoint proteins whose amount or electrophoretic mobility changes between dusk and dawn which corresponds to times that pyrenoids appear and disappear.

Interestingly Rubisco in peridinin-containing dinoflagellates is synthesized as a polyprotein (Rowan 1996, Nassoury unpublished data). Polyproteins are mature proteins separated by roughly icosapeptide spacers that exhibit a bipartite structure with the N-terminal half being relatively hydrophobic and rich in Alanine while the C-terminal half is relatively polar (Houlne and Shantz 1993.). The spacer in *Gonyaulax* is AAAFVGAQART GRSTVVRRA while for Symbiodinium which has 3 aminoacids more is SAAAFVGAS VAPAKKENVVARQA. These sequences are very similar and a common peptidase might process both. It would be very interesting to discover this peptidase, and its localization (i.e., stromal or membrane-bound), as if they are stromal how would the thylakoid polyproteins (such as the light-harvesting protein) get processed and targeted to their proper suborganellar location?

It has been speculated that the triple-membrane structure around the plastid favor the organization of abundant nuclear-encoded chloroplast protein into precursor polyproteins Chan et al. 1990). Although this does not seem to be likely since in *Gonyaulax* the very abundant PCP is not synthesized as a polyprotein. However, one can not rule out a relationship between occurrence of nuclear-encoded polyprotein precursors and the three membrane-bound chloroplasts regardless of their abundance, given that polyproteins are unique to this group of secondary plastids. What is the evolutionary force behind it? If it is solely more economic for the plastid import machinery, why is it not more widespread in the other secondary plastids?

As previously mentioned above, the major light harvesting protein in some dinoflagellates is PCP. Remarkably, PCP has no sequence or structural homology to other light harvesting proteins known from other photosynthetic organisms (Norris & Miller 1994; Le 1997; Hofmann 1996). It is noteworthy to mention that the *Gonyaulax* PCP isoform results from a gene duplication followed by a fusion event (Norris and Miller 1994; Le 1997). In *Gonyaulax* there are roughly 5000 copies of the PCP gene found as tandem repeats which are separated by conserved 1-kb spacers (Le 1997). Could the PCP

gene duplication and the appearance of polyproteins be somehow related? Interestingly, luciferase is also a result of gene fusion (between three identical domains) and also occurs as tandem repeats (Okamoto et al. 2001).

We were interested in how nuclear-encoded plastid proteins get routed to the dinoflagellate plastids given their unusual structure. In order to examine this plastid import pathway we first compared the leader sequences used by the dinoflagellates, including that of PCP and other available sequences, with leader sequences directing import into other complex plastids. A hydrophobic N-terminal signal peptide and an internal plastid transit sequence are recognized in all plastids, and appear to be a consequence of the secondary endosymbiosis. However, unlike most other leader sequences, the dinoflagellate leaders contain a second hydrophobic region at their C-terminal end, a feature shared only by leader sequences of *Euglena*, (Fig. 3.4A). This second hydrophobic region acts as a stop transfer sequence after the plastid proteins begin co-translational translocation to the ER, so that the part of the plastid-directed protein corresponding to the mature processed protein actually remains in the cytoplasm (Sulli and Schwartzbach 1996; Nassoury 2003). Even though both *Euglena* and the dinoflagellates share the same plastid architecture, their evolutionary origin is different. We have thus proposed that this second hydrophobic sequence and the atypical protein topology that results from its insertion in the membrane of the transport vesicles, is requisite by the organelle's ultrastructure rather than the evolutionary origin of the plastid. It would be interesting to know why the second membrane-spanning region in the dinoflagellate leader has evolved and what requirement it fulfills. Could it be operating as a recovery mechanism so that if any of the plastid proteins were misdirected to the plasma membrane, they would not be secreted from the cell and thus irretrievably lost? Perhaps having the bulk of the protein in the cytoplasm may suggest that the proteins may lack the usual cytoplasmic sorting signals expected to associate with adaptors or coat recruitment proteins which charge the vesicles with the appropriate cargo . Alternatively, the appropriate vesicular targeting proteins (such as SNAREs) may not be present, perhaps permitting more promiscuous vesicle fusion events.

Another possible role may be to simply present the plastid transit sequence to the protein translocators in the inner (second) membranes. To prove this more data about the

localizations of the translocator proteins in the different membranes of the plastid, must be available.

Recently it has been shown that dinoflagellates encode the smallest number of plastid genes of any photosynthetic eukaryote and 15 genes that have always been reported to be in the plastid genome of other algae and plants have found their way to the nucleus in dinoflagellates (Hackett et al. 2004). Many of these are hydrophobic photosystem components, and perhaps the sedond hydrophobic regions required for plastid targeting is found naturally occurring in the sequence. This may allow these proteins to be correctly targeted to their destined organelle, and predicts that some may even lack the typical second hydrophobic region in the leader.

The difficult biology of dinoflagellates sometimes limits the use of tools and approaches that are common in other model systems. These limitations might occasionally push a researcher to take advantage of sometimes more eccentric tools in order to better dissect the mechanisms under study. The use to BFA to dissect the control over the photosynthetic carbon fixation rhythm is a case in point, as one would not normally expect carbon fixation to be sensitive to this type of drug.

The inhibition of the carbon fixation rhythm also helps shed some light on the basic circadian organization in *Gonyaulax*. As mentioned previously, bioluminescence and cell division are also rhythmic, and all these three rhythms are clock controlled. The fact that these other two rhythms continue to run normally, even after inhibition of the carbon fixation rhythm indicates there is no direct link between them and the output of photosynthesis rhythm. The photosynthetic rhythm thus reflects a hand of the circadian clock that can be taken off without affecting the clock itself or its ability to move the other hands.

As mentioned above, we have speculated that the newly synthesized Rubisco (or another protein made at the same circadian time) can act as a pyrenoid formation signal, as its synthesis rate increases at the same time as pyrenoid formation and the increase in carbon fixation rates. Using the fungi metabolite Brefeldin A (BFA) to block protein import into the plastids allows two major questions to be addressed: would pyrenoids form in absence of the newly synthesized Rubisco, and would the plastids without pyrenoids be able to fix carbon efficiently? By applying different concentrations of BFA we were able

to block the import of Rubisco into the plastids (Fig. 4.4) and the formation of pyrenoids (Fig. 4.2) in a dose dependant manner. It was interesting to see that lower doses or shorter treatment times reduced not only Rubisco enrichment in the pyrenoid but also the relative label density in the BFA body (Table 4.2). This confirms the dose dependent blockage of protein transport. More importantly, in agreement with our speculation of a correlation between the appearance of pyrenoids and the carbon fixation ability of the cells, by inhibiting the pyrenoid formation with BFA, the carbon fixation rhythm was noticeably affected (Fig. 4.1). This abolishment of the carbon fixation rhythm was not due to the effect of the BFA on the clock mechanism itself, since we were able to show that BFA treatment had no effect on either the bioluminescence or cell division rhythms (Fig. 4.7). The mechanism whereby newly synthesized protein acts as the functional signal for pyrenoid formation is not yet known. However, independent from the identity of the actual signaling molecule, it appears that it is the site of protein entry from the Golgi that defines the site of pyrenoid formation. Pyrenoids only form in regions of the plastid near the Golgi apparatus, through which the nuclear-encoded plastid directed proteins pass (Nassoury et al., 2003). To test if Rubisco itself is the signal for pyrenoid formation, one method would be to examine if by introducing Rubisco RNAi (by which synthesis of Rubisco should be inhibited), the cells would still form pyrenoids. This would provide a more specific tool for determining the role of new protein synthesis in the regulation of pyrenoid formation. To date, no studies have yet reported tests of RNAi in algae.

To summarize the case of *Gonyaulax* and its carbon fixation rhythm, it is the presence of Rubisco at the right circadian time at the right location of the cell that appears to have guaranteed its function and therefore the survival of the algae. Never has the epithet "Location, location, location" been more appropriate.

6. References

Abrahams, M., and L. Townsend. 1993. Bioluminescence in dinoflagellates: a test of the burglar alarm hypothesis. *Ecology,* 74:258-260.

Adams, K.L., D.O. Daley, Y.L. Qiu, J. Whelan and J.D. Palmer. 2000. Repeated, recent and diverse transfers of a mitochondrial gene to the nucleus in flowering plants. *Nature,* 408:354-7.

Apt, K.E., N.E. Hoffman and A.R. Grossman. 1993. The gamma subunit of R-phycoerythrin and its possible mode of transport into the plastid of red algae. *J. Biol. Chem.,* 268:16208-15.

Badger, M., T. Andrews, S. Whitney, M. Ludwig, D. Yellowlees, W. Leggat and G. Price. 1998. The diversity and coevolution of Rubisco, plastids, and chloroplast based CO2 concentrating mechanisms in algae. *Can. J. Bot.,* 76:1052-1071.

Baldauf, S.L., A.J. Roger, I. Wenk-Siefert and W.F. Doolittle. 2000. A kingdom-level phylogeny of eukaryotes based on combined protein data. *Science,* 290:972-7.

Barbrook, A.C., and C.J. Howe. 2000. Minicircular plastid DNA in the dinoflagellate Amphidinium operculatum. *Mol Gen Genet.,* 263:152-158.

Berks, B.C., F. Sargent and T. Palmer. 2000.The Tat protein export pathway. *Mol. Microbiol.,* 35:260-74.

Bhaud, Y., D. Guillebault, J. Lennon, H. Defacque, M.O. Soyer-Gobillard, and H. Moreau. 2000. Morphology and behaviour of dinoflagellate chromosomes during the cell cycle and mitosis. *J Cell Sci.,* 113:1231-1239.

Blobel, G. 1980. Intracellular protein topogenesis, *Proc. Natl. Acad. Sci. USA,* 77:496-500.

Bode, V.C., R. DeSa, and J.W. Hastings. 1963. Daily rhythm of luciferin activity in Gonyaulax polyedra. *Science,* 141:913-915.

Bogsch, E.G., F. Sargent, N.R. Stanley, B.C. Berks, C. Robinson and T. Palmer. 1998. An essential component of a novel bacterial protein export system with homologues in plastids and mitochondria. *J. Biol. Chem.,* 273:18003-6.

Bolter, B., J. Soll, A. Schulz, S. Hinnah and R. Wagner. 1998. Origin of a chloroplast protein importer. *Proc. Natl. Acad. Sci. USA,* 95:15831-6.

Broda, H., V.D. Gooch, W. Taylor, N. Aiuto, J.W. Hastings. 1986. Acquisition of circadian bioluminescence data in *Gonyaulax* and an effect of the measurement procedure on the period of the rhythm. *J. Biol. Rhythms,* 1:251-263.

Bruce, B.D. 1998. The role of lipids in plastid protein transport, *Plant Mol. Biol.,* 38:223-46.

Bruce, B.D. 2000. Chloroplast transit peptides: structure, function and evolution. *Trends Cell Biol.,* 10:440 -447.

Bush, K.J. and B.M. Sweeney. 1972. The activity of ribulose diphosphate carboxylase in extracts of Gonyaulax polyedra in the day and the night phases of the circadian rhythm of photosynthesis. *Plant Physiol.,* 50:446-451.

Caliebe, A., R. Grimm, G. Kaiser, J. Lubeck, J. Soll and L. Heins. 1997. The chloroplastic protein import machinery contains a Rieske-type iron-sulfur cluster and a mononuclear iron-binding protein. *Embo J.,* 16:7342-50.

Cavalier-Smith,T. 1982.The origins of plastids, *Biol. J. Linn. Soc.,* 17:289-306.

Cavalier-Smith, T. and J.J. Lee.1985. Protozoa as hosts for endosymbioses and the conversion of symbionts into organelles, *J. Protozool.,* 32:376-379.

Cavalier-Smith, T. 1987. The simultaneous symbiotic origin of mitochondria, chloroplasts, and microbodies, *Ann. N Y Acad. Sci.,* 503:55-71.

Cavalier-Smith, T. 1993. The origins, losses and gains of chloroplasts in (Lewin, R.A., ed.) Origin of plastids: symbiogenesis, prochlorophytes and the origins of chloroplasts., Chapman & Hall, pp. 291-348.

Cavalier-Smith, T. 1999. Principles of protein and lipid targeting in secondary symbiogenesis: euglenoid, dinoflagellate and sporozoan plastid origins and the eukaryotic family tree. *J. Euk. Microbiol.,* 46:347-366.

Cavalier-Smith, T. 2000. Membrane heredity and early chloroplast evolution. *Trends Plant Sci.,* 5:174-82

Cavalier-Smith, T., 2003. Genomic reduction and evolution of novel genetic membranes and protein-targeting machinery in eukaryote-eukaryote chimaeras (meta-algae). *Philos. Trans R. Soc. Lond. B. Biol. Sci.,* 358 :109-33; discussion 133-4.

Ceriani, M., T. Darlington, D. Staknis, P. Mas , A. Petti, C. Weitz and S. Kay.1999. Light-dependent sequestration of TIMELESS by CRYPTOCHROME. *Science,* 285:553-556.

Chan, R.L., M. Keller, J. Canaday, J. H. Weil and P. Imbault. 1990. Eight small subunits of *Euglena* ribulose 1-5 bisphosphate carboxykase/oxygenase are translated from a large mRNA as a polyproteins. *EMBO J.,* 9:333-338.

Chen, X. and D.J. Schnell. 1999. Protein import into chloroplasts. *Trends Cell. Biol.,* 9: 222-7.

Chen, X., M.D. Smith, L. Fitzpatrick and D.J. Schnell. 2002. In vivo analysis of the role of atTic20 in protein import into chloroplasts. *Plant Cell,* 14:641-54.

Colepicolo, P, V.C. Camarero and J.W. Hastings. 1992. A circadian rhythm in the activity of superoxide dismutase in the photosynthetic alga *Gonyualax polyedra. Chronobiol. Int.,* 9:266-268.

Colepicolo, P., T. Roenneberg, D. Morse, et al. 1993. The circadian bioluminescence of *Pyrocystis lunula. J. Phycol.,* 29:173-179.

Crosthwaite, S., J. Dunlap and J. Loros. 1997. Neurospora wc-1 and wc-2: Transcription, Photoresponses, and the origins of circadian rhythmicity. *Science,* 276:763-769.

Crutchfield, A.L.M., K.R. Diller and J.J. Brand. 1999. Cryopreservation of *Chlamydomonas reinhardtii* (Chlorophyta). *Eur. J. Phycol.,* 34:43-52.

Cullen, J.J. and S.G. Horrigan. 1981. Effect of nitrate on the diurnal vertical migration, carbon to nitrogen ratio, and the photosynthetic capacity of the dinoflagellate *Gymnodinium splendens. Mar. Biol.,* 62:81-89.

Dascher, C. and W.E. Balch. 1994. Dominant inhibitory mutants of ARF1 block endoplasmic reticulum to Golgi transport and trigger disassembly of the Golgi apparatus. *J Biol Chem.,* 269:1437-1448.

de Lanerolle, P. and A.B. Cole. 2002. Cytoskeletal proteins and gene regulation: form, function, and signal transduction in the nucleus. *Sci STKE.*, PE30.

Delwiche, C. and J. Palmer. 1996. Rampant horizontal transfer and duplication of rubisco genes in eubacteria and plasmids. *Mol. Biol. Evol.,* 13:873 -882.

Delwiche C.F. and J.D. Palmer. 1997. The origin of plastids and their spread via secondary endosymbiosis in (Bhattacharya, D., ed.) The origins of algae and their plastids., Springer-Verlag, Vienna pp. 53-86.

DeRocher, A., C.B. Hagen, J.E. Froehlich, J.E. Feagin and M. Parsons. 2000. Analysis of targeting sequences demonstrates that trafficking to the *Toxoplasma gondii* plastid branches off the secretory system. *J. Cell Sci.,* 113:3969 -3977.

Desjardins, M. and D. Morse. 1993. The polypeptide components of scintillons, the bioluminescence organelles of the dinoflagellate *Gonyaulax polyedra. Biochem. Cell Biol.,* 71:176-182.

Donaldson, J.G., D. Finazzi and R.D. Klausner. 1992. Brefeldin A inhibits Golgi membrane-catalysed exchange of guanine nucleotide onto ARF protein. *Nature,* 360:350-352.

Douglas, S., S. Zauner, M. Fraunholz, M. Beaton, S. Penny, L.T. Deng, X. Wu, M. Reith, T. Cavalier-Smith and U.G. Maier. 2001. The highly reduced genome of an enslaved algal nucleus. *Nature,* 410:1091-6.

Dunlap, J.C., W.R. Taylor and J.W. Hastings. 1980. The effects of protein synthesis inhibitors on the Gonyaulax clock I: Phase shifting effects of cycloheximide. *J. Comp. Physiol.,* 138:1-8.

Dunlap, J.C. and J.W. 1981. Hastings The biological clock in *Gonyaulax* controls luciferase activity by regulating turnover. *J. Biol. Chem.,* 256:10509-10518.

Dunlap, J.C. 1999. Molecular bases for circadian clocks. *Cell,* 96:271-290.

Dunlap, J.C. 1993. Genetic analysis of circadian clocks. *Annu. Rev. Physiol.,* 55:683-728.

Dyall, S.D., M.T. Brown and P.J. Johnson. 2004. Ancient invasions: from endosymbionts to organelles. *Science,* 304:253-7.

Eckert, R. 1965. Bioelectric control of Bioluminescence in the dinoflagellate *Noctiluca. Science,* 147:1140-1145.

Eckert, R. and T. Sibaoka. 1968. The flash triggering action potential of the luminescent dinoflagellate *Noctiluca. J. Gen. Physiol.,* 52:258-282.

Economou, A. and W. Wickner. 1994. SecA promotes preprotein translocation by undergoing ATP-driven cycles of membrane insertion and deinsertion. *Cell,* 78:835-843.

Edery, I., L. Zwiebel, M. Dembinska, M. Rosbash. 1994. Temporal phosphorylation of the drosophila period protein. *Proc. Natl. Acad. Sci. USA,* 91:2260-2264.

Edmunds, L.J., editor. 1984. Cell Cycle Clocks. New York: Marcel Dekker.

Eppley, R.W., O. Holm-Hansen and J.D.H. Strickland. 1968. Some observations on the vertical migration of dinoflagellates. *J. Phycol.,* 4:333-340.

Esaias, W. and H.J. Curl. 1972. Effect of dinoflagellate bioluminescence on copepod ingestion rates. *Limnol. Oceanogr.,* 17(zooplankton ecology): 901-906.

Fagan, T., D. Morse and J. Hastings.1999. Circadian synthesis of a nuclear encoded chloroplast Glyceraldehyde-3-phosphate dehydrogenase in the dinoflagellate *Gonyaulax polyedra* is translationally controlled. *Biochemistry,* 38:7689-7695.

Fagan, T., J. Hastings and D. Morse. 1998. Phylogeny of Glyceraldehyde-3-phosphate dehydrogenase indicates lateral gene transfer from cryptomonads to dinoflagellates. *J. Mol. Evol.,* 47:633 -639.

Fast, N.M., J.C. Kissinger, D.S. Roos and P.J. Keeling. 2001. Nuclear-encoded, plastid-targeted genes suggest a single common origin for apicomplexan and dinoflagellate plastids. *Mol. Biol. Evol.,* 18:418 -426.

Fast, N.M., L. Xue, S. Bingham and P.J. Keeling. 2002. Re-examining alveolate evolution using multiple protein molecular phylogenies. *J. Eukaryot. Microbiol.,* 49:30-37.

Field, C.B., M. J. Behrenfeld, J.T. Randerson and P. Falkowski. 1998. Primary production of the biosphere: integrating terrestrial and oceanic components. *Science,* 281:237-240.

Fogel, M. and J.W. Hastings. 1972. Bioluminescence: mechanism and mode of control of scintillon activity. *Proc. Natl. Acad. Sci. USA,* 69:690-693.

Foth, B.J., S.A. Ralph, C.J. Tonkin, N.S. Struck, M. Fraunholz, D.S. Roos, A.F. Cowman and G.I. McFadden. 2003. Dissecting apicoplast targeting in the malaria parasite *Plasmodium falciparum. Science,* 299:705 -708.

Friesen, W.O., G.D. Block and C.G. Hocker. 1993. Formal approaches to understanding biological oscillators. *Annu. Rev. Physiol.,* 55:661-681.

Fritz, L. and R.E. Treimer. 1983. An ultrastructural study of mitosis in a marine dinoflagellate Prorocentrum minimum. *J. Protozool.,* 30:437-444.

Fritz, L., D. Morse and J.W. Hastings. 1990. The circadian bioluminescence rhythm of *Gonyaulax* is related to daily variations in the number of light-emitting organelles *J. Cell Sci.,* 95:321-328.

Fritz, L., P.M. Milos, D. Morse and J.W. Hastings. 1991. In situ hybridization of luciferin binding protein antisense RNA to thin sections of the bioluminescence dinoflagellate *Gonyaulax polyedra. J. Phycol.,* 27:436-441.

Fritz, L., C.G. Stringher and P. Colepicolo. 1996. Imaging oscillations in *Gonyaulax*: a chloroplast rhythm of nitrate reductase visualized by immunocytochemistry. *Braz. J. Med. Biol. Res.,* 29:111-117.

Funes, S., E. Davidson, A. Reyes-Prieto, S. Magallon, P. Herion, M.P. King and Gonzalez-Halphen, D. 2002. A green algal apicoplast ancestor. *Science,* 298:2155-2161.

Gastel, J., P. Roseboom, P. Rinaldi, J. Weller and D. Klein. 1998. Melatonin production: proteasomal proteolysis in seratonin N-acetyltransferase regulation. *Science,* 279:1358-1360.

Gentle, I., K. Gabriel, P. Beech, R. Waller and T. Lithgow. 2004. The Omp85 family of proteins is essential for outer membrane biogenesis in mitochondria and bacteria. *J. Cell Biol.,* 164:19-24.

Gibbs, S.1978. The chloroplasts of *Euglena* may have evolved from symbiotic green algae, *Can. J. Bot.,* 56:2883-2889.

Gibbs, S.P.,1979. The route of entry of cytoplasmically synthesized proteins into chloroplasts of algae possessing chloroplast ER. *J. Cell Sci.,* 35:253-66.

Gibbs, S. 1981. The chloroplasts of some algal groups may have evolved from endosymbiotic eukaryotic algae. *Ann. N.Y. Acad. Sci.,* 361:193-208.

Gilson, P.R. and G.I. McFadden. 1997. Good things in small packages: the tiny genomes of chlorarachniophyte endosymbionts. *Bioessays,* 19:167-73.

Gilson P.R. and G.I. McFadden. 2002. Jam packed genomes--a preliminary, comparative analysis of nucleomorphs. *Genetica,* 115:13-28.

Gliwicz, M. Z. 1986. Predation and the evolution of vertical migration in zooplankton. *Nature,* 320:746-748.

Govindjee, B., D. Wong, B. Prezelin and B. Sweeney. 1979. Chlorophyll a fluorescence of Gonyaulax polyedra grown on a light-dark cycle and after transfer to constant light. *Photochem. Photobiol.,* 30:405-411.

Guillard, R.R.L. and J.H. Ryther.1962.Studies on marine planktonic diatoms: *Cyclotella nana* Hufstedt and *Denotula confervacea* (Cleve) Gran. *Can. J. Microbiol.*, 8:229-239.

Hackett, J.D., H.S. Yoon, M.B. Soares, M.F. Bonaldo, T.L. Casavant, T.E. Scheetz, T. Nosenko and D. Bhattacharya. 2004. Migration of the plastid genome to the nucleus in a peridinin dinoflagellate. *Curr. Biol.*, 14:213-218.

Harmer, S.L., S. Panda, S.A. Kay. 2001. Molecular bases of circadian rhythms. *Annu. Rev. Cell Dev. Biol.,* 17:215-253.

Harper, J.T. and P.J. Keeling. 2003. Nucleus-encoded, plastid-targeted glyceraldehyde-3-phosphate dehydrogenase (GAPDH) indicates a single origin for chromalveolate plastids. *Mol. Biol. Evol.,* 20:1730-5.

Harrison W.G. 1976. Nitrate metabolism of the red tide dinoflagellate *Gonyaulax polyedra. J. Exp. Mar. Biol. Ecol.,* 21:199-209.

Hartman, F. and M. Harpel. 1994. Structure, function, regulation and assembly of D-ribulose-1,5-bisphosphate carboxylase/oxygenase. *Annu. Rev. Biochem.,* 63:197-234.

Hastings, J.W. and B.M. Sweeney. 1957. On the mechanism of temperature independence in a biological clock. *Proc. Nat. Acad. Sci. USA,* 43:804-811.

Hastings, J.W. and B.M. Sweeney. 1958. A persistent diurnal rhythm of luminescence in *Gonyaulax polyedra*. *Biol. Bull.,* 115:440-458.

Hastings, J.W. 1960. Biochemical aspects of rhythms: phase shifting by chemicals. Cold Spring Harbr. *Symp. Quant. Biol.,* 25:131-148.

Hastings, J.W., L. Astrachan, B.M. Sweeney. 1961. A persistent daily rhythm in photosynthesis. *J. Gen. Physiol.,* 45:69-76.

Hastings, J.W. 2001. Cellular and molecular mechanisms of circadian regulation in the unicellular dinoflagellate *Gonyaulax polyedra*. In: Takahashi JS, Turek F, Moore RY, editors. Handbood of Behavioral Neurobiology. New York N.Y.: Plenum Press; p. 321-334.

Heaney, S.I. and R.W. Eppley. 1981. Light, temperature and nitrogen as interacting factors affecting diel vertical migrations of dinoflagellates in culture. *J.Plankton Res.,* 3:331-344.

Heins, L. and J. Soll. 1998. Chloroplast biogenesis: mixing the prokaryotic and the eukaryotic? *Curr. Biol.,* 8:215-7.

Heins, L., A. Mehrle, R. Hemmler, R. Wagner, M. Kuchler, F. Hormann, D. Sveshnikov and J. Soll. 2002. The preprotein conducting channel at the inner envelope membrane of plastids. *Embo J.,* 21:2616-25.

Helms, J.B. and J.E. Rothman. 1992. Inhibition by brefeldin A of a Golgi membrane enzyme that catalyses exchange of guanine nucleotide bound to ARF. *Nature,* 360:352-354.

Henze, K., A. Badr, M. Wettern, R. Cerff and W. Martin. 1995. A nuclear gene of eubacterial origin in Euglena gracilis reflects cryptic endosymbioses during protist evolution. *Proc. Natl. Acad. Sci. USA,* 92:9122 -9126.

Herman, E.M. and B.M. Sweeney. 1975. Circadian rhythm of chloroplast ultrastructure in *Gonyaulax polyedra*, concentric organization around a central cluster of ribosomes. *J. Ultrastruct. Res.,* 50:347-354.

Hiltbrunner, A., J. Bauer, P.A. Vidi, S. Infanger, P. Weibel, M. Hohwy and F. Kessler. 2001. Targeting of an abundant cytosolic form of the protein import receptor at Toc159 to the outer chloroplast membrane, *J. Cell Biol.,* 154:309-16.

Hinnah, S.C., R. Wagner, N. Sveshnikova, R. Harrer and J. Soll. 2002. The chloroplast protein import channel Toc75: pore properties and interaction with transit peptides. *Biophys. J.,* 83:899-911.

Hirsch, S., E. Muckel, F. Heemeyer, G. von Heijne and J. Soll. 1994. A receptor component of the chloroplast protein translocation machinery. *Science,* 266:1989-92.

Hofmann, E., P.M. Wrench, F.P. Sharples, R.G. Hiller, W. Welte and K. Diedrichs. 1996. Structural basis of light harvesting by carotenoids: peridinin- chlorophyll-protein from *Amphidinium carterae. Science,* 272:1788-1791.

Hollnagel, H.C., E. Pinto, D. Morse and P. Colepicolo. 2002. The oscillation of photosynthetic capacity in *Gonyaulax polyedra* is not related to differences in Rubisco, peridinin or chlorophyll *a* amounts. *Biol. Rhythms Res.,* 33:443-458.

Holm-Hansen, O. 1969. Algae: amounts of DNA and carbon in single cells. *Science,* 163:87-88.

Homma, K. and J.W. Hastings. 1988. Cell cycle-synchronization of *Gonyaulax polyedra* by filtration: quantized generation times. *J. Biol. Rhythms,* 3:49-58.

Homma, K and J.W. Hastings. 1989a. The S phase is discrete and is controlled by the circadian clock in the marine dinoflagellate *Gonyaulax polyedra. Exp. Cell. Res.,* 182:635-644.

Homma, K. and J.W. Hastings. 1989b. Cell growth kinetics, division asymetry, and volume control at division in the marine dinoflagellate *Gonyaulax polyedra*: a model of circadian clock control of the cell cycle. *J. Cell Sci.,* 92:303-318.

Houlne, G. and R. Shantz. 1993. Expression of polyproteins in *Euglena. Crit. Rev. Plant Sci.,* 12:1-17.

Huang, C.Y., M.A. Ayliffe and J.N. Timmis. 2003. Direct measurement of the transfer rate of chloroplast DNA into the nucleus. *Nature,* 422:72-6.

Ishida, K., Y. Cao, M. Hasegawa, N. Okada and Y. Hara.1997. The origin of chlorarachniophyte plastids, as inferred from phylogenetic comparisons of amino acid sequences of EF-Tu. *J. Mol. Evol.,* 45:682-7.

Ishida, K., T. Cavalier-Smith and B.R. Green. 2000. Endomembrane structure and the chloroplast protein targeting pathway in *Heterosigma akashiwo* (Raphidophyceae, Chromista). *J. Phycol.,* 36:1135-1144.

Jakowitsch, J., C. Neumann-Spallart, Y. Ma, J. Steiner, H.E. Schenk, H.J. Bohnert and W. Loffelhardt. 1996. In vitro import of pre-ferredoxin-NADP+-oxidoreductase from Cyanophora paradoxa into cyanelles and into pea chloroplasts. *FEBS Lett.,* 381:153-5.

Jarvis, P. and J. Soll. 2002. Toc, tic, and chloroplast protein import. *Biochim. Biophys. Acta,* 1590:177-89.

Jeffrey, S., M. Seilicki and F. Haxo. 1975. Chloroplast pigment patterns in dinoflagellates. *J. Phycol.,* 11:374-384.

Jenks, A. and S. Gibbs. 2000. Immunolocalization and distribution of form II Rubisco in the pyrenoid and chloroplast stroma of Amphidinium carterae and form I Rubisco in the symbiont derived plastids of Peridinium foliaceum (dinophyceae). *J. Phycol.,* 36:127-138.

Jin, X., L. Shearman, D.Weaver, M. Zylka, G. De Vries and S. Reppert. 1999. A molecular mechanism regulating rhythmic output from the suprachiasmatic circadian clock. *Cell,* 96:57-68.

Johnson, C.H., J. F. Roeber and J.W. Hastings. 1984. Changes in luciferase amount account for the circadian bioluminescece rhythm in Gonyaulax. *Science,* 1428-1430.

Johnson, C.H., S. Inoue, A. Flint and J.W. Hastings. 1985. Compartmentalization of algal bioluminescence: Auto fluorescence of bioluminescenct particles in the dinoflagellate *Gonyaulax* as studied with image-intensified video microscopy and flow cytometry. *J. Cell Biol.,* 100:1435-1446.

Joiner K.A. and D.S. Roos. 2002. Secretory traffic in the eukaryotic parasite *Toxoplasma gondii:* less is more. *J. Cell Biol.,* 157:557-63.

Jordan, D. and W. Ogren. 1981. Species variation in the specificity of ribulose biphosphate carboxylase/oxygenase. *Nature,* 291:513-515.

Joyard, J., A. Billecocq, S.G. Bartlett, M.A. Block, N.H. Chua and R. Douce. 1983. Localization of polypeptides to the cytosolic side of the outer envelope membrane of spinach chloroplasts. *J. Biol. Chem.,* 258:10000-6.

Joyard, J., E. Teyssier, C. Miege, D. Berny-Seigneurin, E. Marechal, M.A. Block, A.J. Dorne, N. Rolland, G. Ajlani and R. Douce. 1998. The biochemical machinery of plastid envelope membranes. *Plant Physiol.,* 118:715-23.

Keegstra, K. 1989. Transport and routing of proteins into chloroplasts. *Cell,* 56:247-53.

Keegstra, K. and J.E. Froehlich. 1999 Protein import into chloroplasts. *Curr. Opin. Plant Biol.,* 2:471-6.

Kessler, F., G. Blobel, H.A. Patel and D.J. Schnell. 1994. Identification of two GTP-binding proteins in the chloroplast protein import machinery. *Science,* 266:1035-9.

Kessler, F., and G. Blobel. 1996. Interaction of the protein import and folding machineries of the chloroplast. *Proc. Natl. Acad. Sci. USA,* 93:7684-9.

Killian, O. and P.G. Kroth. 2003. Evolution of protein targeting into "complex" plastids: the "secretory transport hypothesis". *Plant Biol.,* 5:350-358.

Kirchhausen, T., J.S. Bonifacino and H. Riezman. 1997. Linking cargo to vesicle formation: receptor tail interactions with coat proteins. *Curr. Opin. Cell Biol.,* 9:488-95.

Kishore, R., U.S. Muchhal and S.D. Schwartzbach. 1993. The presequence of Euglena LHCPII, a cytoplasmically synthesized chloroplast protein, contains a functional endoplasmic reticulum-targeting domain. *Proc. Natl. Acad. Sci. USA,* 90:11845-11849.

Knaust, R., T. Urbig, L. Li, W. Taylor and J. Hastings. 1998. The circadian rhythm of bioluminescence in *Pyrocystis* is not due to differences in the amount of luciferase: a comparitive study of three bioluminescenct marine dinoflagellates. *J. Phycol.,* 34:167-172.

Knoetzel, J. and L.Rensing. 1990. Characterization of the photosynthetic apparatus from the marine dinoflagellate *Gonyaulax polyedra*. II. Circadian rhythmicity of photosynthesis and the supramolecular organization of pigment-protein complexes. *J. Plant Physiol.,* 136:280-288.

Kohler, S., C.F. Delwiche, P.W. Denny, L.G. Tilney, P. Webster, R. J. Wilson, J.D. Palmer and Roos, D. S. 1997. A plastid of probable green algal origin in Apicomplexan parasites. *Science,* 275:1485 -1489.

Krasnow, R., J.C. Dunlap, W. Taylor, J.W. Hastings, W. Vetterling and V. Gooch. 1980. Circadian spontaneous bioluminescent glow and flashing of *Gonyaulax polyedra*. *J. Comp. Physiol.,* 138:19-26.

Krasnow R, J. Dunlap, W. Taylor, et al. 1981. Measurements of *Gonyaulax* bioluminescence, including that of single cells. In: Nealson KH, editor. Bioluminescence: Current perspectives: Burgess Publishing Co.

Kreis, T.E., M. Lowe and R. Pepperkok. 1995. COPs regulating membrane traffic. *Annu. Rev. Cell Dev. Biol.,* 11:677-706.

Kronauer, R.E., C.A. Czeisler, S.F. Pilato, M.C. Moor-Ede and E.D. Weitzman. 1982. Mathematical model of the human circadian system with two interacting oscillators. *Am. J. Physiol.,* 11:R3-R17.

Kronauer, R., M.E. Jewett and C.A. Czeisler. 1991. Human circadian rhythms. *Nature,* 351:193.

Kroth, P.G. 2002. Protein transport into secondary plastids and the evolution of primary and secondary plastids. *Int. Rev. Cytol.,* 221:191-255.

Kouranov, A., X. Chen, B. Fuks and D.J. Schnell. 1998. Tic20 and Tic22 are new components of the protein import apparatus at the chloroplast inner envelope membrane. *J. Cell. Biol.,* 143:991-1002.

Kubo, N., K. Harada, A. Hirai and K. Kadowaki. 1999. A single nuclear transcript encoding mitochondrial RPS14 and SDHB of rice is processed by alternative splicing: common use of the same mitochondrial targeting signal for different proteins. *Proc. Natl. Acad. Sci. USA,* 96:9207-11.

Kuhn, A., R. Stuart, R. Henry and R.E. Dalbey. 2003. The Alb3/Oxa1/YidC protein family: membrane-localized chaperones facilitating membrane protein insertion? *Trends Cell. Biol.,* 13:510-6.

Lang, M., K.E. Apt and P.G. Kroth. 1998. Protein transport into "complex" diatom plastids utilizes two different targeting signals. *J. Biol. Chem.,* 273:30973-8.

Lang, B.F., M.W. Gray and G. Burger.1999. Mitochondrial genome evolution and the origin of eukaryotes, *Annu Rev Genet.,* 33:351-97.

Le, Q.H., P. Markovic, R. Jovine, J. Hastings and D. Morse. 1997. Sequence and genomic organization of the peridinin-chlorophyll a-protein from *Gonyaulax polyedra. Mol. Gen. Genet.,* 255:595 -604.

Le, Q., R. Jovine, P. Markovic and D. Morse. 2001. PCP is not implicated in the photosynthesis rhythm of Gonyaulax despite circadian regulation of its translation. *Biol. Rhythm Research,* 32:579-594.

Lee, D.H., M. Mittag, S. Sczekan, D. Morse and J.W. Hastings.1993. Molecular cloning and genomic organization of a gene for luciferin binding protein from the dinoflagellate *Gonyaulax polyedra. J. Biol. Chem.,* 268:8842-8850.

Lippincott-Schwartz, J., T.H. Roberts and K. Hirschberg. 2000. Secretory protein trafficking and organelle dynamics in living cells. *Annu. Rev. Cell Dev. Biol.,* 16:557-589.

Liu, Y., M. Merrow, J. Loros and J. Dunlap. 1998. How temperature changes reset a circadian oscillator *Science,* 281:825-829.

Long, M., S.J. de Souza, C. Rosenberg and W. Gilbert. 1996. Exon shuffling and the origin of the mitochondrial targeting function in plant cytochrome c1 precursor. *Proc. Natl. Acad. Sci. USA,* 93:7727-31.

Loros, J.J. and J.C. Dunlap. 1991. *Neurospora crassa* clock-controlled genes are regulated at the level of transcription. *Mol. Cell. Biol.,* 11:558-563.

Lutkenhaus, J. and S. Addinall. 1997. Bacterial cell division and the Z ring. *Annu. Rev. Biochem.,* 66:93-116.

Markovic, P., T. Roenneberg and D. Morse. 1996. Phased protein synthesis at several circadian times does not change protein levels in Gonyaulax. *J. Biol. Rhythms,* 11:57 -67.

Martin, W., C. Somerville and S. Loiseaux-de Goër.1992. Molecular phylogenies of plastid origins and algal evolution, *J. Mol. Evol.,* 35:385-404.

Martin, W. and C. Schnarrenberger. 1997. The evolution of the Calvin cycle from prokaryotic to eukaryotic chromosomes: a case study of functional redundancy in ancient pathways through endosymbiosis. *Curr. Genet.,* 32:1 -18.

Martin, W.and R.G. Herrmann.1998. Gene transfer from organelles to the nucleus: how much, what happens, and Why? *Plant Physiol.,* 118:9-17.

Martin, W., B. Stoebe, V. Goremykin, S. Hapsmann, M.Hasegawa and K. V. Kowallik. 1998. Gene transfer to the nucleus and the evolution of chloroplasts. *Annu. Rev. Genet.,* 393:162 -165.

Matthys-Rochon, E. 1979. Evolution d'un dinoflagellé libre au cours d'un cycle cellulaire. *Biol. Cell.,* 35:313-320.

Matton, D. P., O. Maes, G. Laublin, Q. Xike, C. Bertrand, D.Morse, and M. Cappadocia. 1997. Hypervariable domains of self-incompatibility RNases mediate allele-specific pollen recognition. *Plant Cell,* 9:1757-1766.

McDougall, C. 2002. Bioluminescence and the actin cytoskeleton in the dinoflagellate *Pyrocystis fusiformis*: an examination of organelle transport and mechanotransduction. *In* Biology. University of California, Santa Barbara. 121.

McMurry, L. and J.W. Hastings. 1972. No desynchronization among the four circadian rhythms in the unicellular alga, *Gonyaulax polyedra. Science,* 175:1137-1139.

McFadden, G.I., M.E. Reith, J. Munholland and N. Lang-Unnasch. 1996. Plastid in human parasites. *Nature,* 381:482.

McFadden, G. I. 1999. Plastids and protein targeting. *J. Eukaryot. Microbiol.,* 46:339 - 346.

McKay, R. and S. Gibbs. 1991. Composition and function of pyrenoids: cytochemical and immunocytochemical approaches. *Can. J. Bot.*, 69:1040-1052.

Michael T.P., P.A. Salome and C.R. McClung. 2003. Two Arabidopsis circadian oscillators can be distinguished by differential temperature sensitivity. *Proc. Natl. Acad. Sci. USA,* 100:6878-68783.

Milos, P., D. Morse and J.W. Hastings. 1990. Circadian control over synthesis of many *Gonyaulax* proteins is at a translational level. *Naturwiss*, 77:87-89.

Mittag, M., D-H. Lee and J.W. Hastings. 1994. Circadian expression of the luciferin-binding protein correlates with the binding of a protein to the 3' untranslated region of its mRNA. *Proc. Natl. Acad. Sci. USA,* 91:5257-5261.

Mittag, M. 1996. Conserved circadian elements in phylogenetically diverse algae. *Proc. Natl. Acad. Sci. USA,* 93:14401-14404.

Mittag, M., C. Eckerskorn, K. Strupat and J.W. Hastings. 1997. Differential translational initiation of lbp mRNA is caused by a 5' upstream open reading frame. *FEBS Lett.,* 411:245-250.

Mittag, M., L. Li and J.W.Hastings. 1998. The mRNA level of the circadian regulated *Gonyaulax* luciferase remains constant over the cycle. *Chronobiol. Int.,* 15:93-98.

Morden, C., C. Delwiche, M. Kuhsel and J. Palmer. 1992. Gene phylogenies and the endosymbiotic origin of plastids. *Biosystems,* 28:75-90.

Morse, D., P.M. Milos, E. Roux and J.W. Hastings. 1989a. Circadian regulation of bioluminescence in Gonyaulax involves translational control. *Proc Natl. Acad. Sci. USA,* 86:172-176.

Morse, D., A.M.J. Pappenheimer and J.W. Hastings. 1989b. Role of a luciferin-binding protein in the circadian bioluminescent reaction of *Gonyaulax polyedra. J. Biol. Chem.,* 264:11822-11826.

Morse, D.S., L. Fritz and J.W. Hastings. 1990. What is the clock? Translational regulation of circadian bioluminescence. *Trends Biochem. Sci.,* 15:262-265.

Morse D, J.W. Hastings and T. Roenneberg. 1994. Different phase responses of the two circadian oscillators in *Gonyaulax. J. Biol. Rhythms*, 9:263-274.

Morse, D., P. Salois, P. Markovic and J.W. Hastings. 1995. A nuclear encoded form II rubisco in dinoflagellates. *Science,* 268:1622-1624.

Morse, D. and P. Sassone-Corsi. 2002. Time after time: inputs to and outputs from the mammalian circadian oscillators. *Trends Neurosci.,* 25:632-637.

Moss, J. and M. Vaughan. 1999. Activation of toxin ADP-ribosyltransferases by eukaryotic ADP-ribosylation factors. *Mol Cell Biochem.,* 193:153-157.

Mossessova, E., R.A. Corpina and J. Goldberg. 2003. Crystal structure of ARF1*Sec7 complexed with Brefeldin A and its implications for the guanine nucleotide exchange mechanism. *Mol Cell.,* 12:1403-1411.

Nakamura, H., Y. Kishi, O. Shimomura, D. Morse and J.W. Hastings. 1989. Structure of dinoflagellate luciferin and its enzymatic and non-enzymatic air oxidation products. *J. Am. Chem. Soc.,* 111:7607-7611.

Narang, F., L. McIntosh and C. Somerville. 1984. Nucleotide sequence of the ribulose bisphosphate carboxylase gene from *Rhodospirillum rubrum. Mol. Gen. Genet.,* 193:220-224.

Nassoury, N., L. Fritz and D. Morse. 2001. Circadian changes in ribulose-1,5-bisphosphate carboxylase/oxygenase distribution inside individual chloroplasts can account for the rhythm in dinoflagellate carbon fixation. *Plant Cell,* 13:923-934.

Nassoury, N., M. Cappadocia and D. Morse. 2003. Plastid ultrastructure defines the protein import pathway in dinoflagellates. *J. Cell Sci.,* 116:2867-2874.

Nicolas, M.T., G. Nicolas, C.H. Johnson, J.M. Bassot and J.W. Hastings. 1987. Characterization of the bioluminescent organelles in *Gonyaulax polyedra* (dinoflagellates) after fast-freeze fixation and antiluciferase immunogold staining. *J. Cell Biol.,* 105:723-35.

Nicolas, M.T., D. Morse, J.M. Bassot and J.W. Hastings. 1991. Colocalization of luciferin binding protein and luciferase to the scintillons of *Gonyaulax polyedra* revealed by double immunolabeling after fast freeze fixation. *Protoplasma,* 160:159-166.

Nimmo, G., H. Nimmo, C. Fewson and M. Wilkins. 1984. Diurnal changes in the properties of phosphoenolpyruvate carboxylase in Bryophyllum leaves: a possible covalent modification. *FEBS letters,* 178:199-203.

Nikaido, S.S. and C.H. Johnson. 2000. Daily and circadian variation in survival from ultraviolet radiation in *Chlamydomonas reinhardtii. Photochem. Photobiol.,* 71:758-765.

Njus, D., V.Gooch and J.W. Hastings. 1981. Precision of the *Gonyaulax* clock. *Cell Biophys.,* 3:221-231.

Norris, B. and D. Miller. 1994. Nucleotide sequence of a cDNA clone encoding the precursor of the peridinin-chlorophyll a-binding protein from the dinoflagellate Symbiodinium. *Plant Mol. Biol.,* 24:673-677.

Obornik, M., Y. Van de Peer, V. Hypsa, T. Frickey, J.R. Slapeta, A. Meyer and J. Lukes. 2002. Phylogenetic analyses suggest lateral gene transfer from the mitochondrion to the apicoplast. *Gene,* 285:109-118.

Okamoto, O.K., L. Liu, D.L. Robertson and J.W. Hastings. 2001. Members of a dinoflagellate luciferase gene family differ in synonymous substitution rates. *Biochemistry,* 40:15862-15868.

Okamoto, O.K., D.L. Robertson, T.F. Fagan, J.W. Hastings and P. Colepicolo. 2001. Different regulatory mechanisms modulate the expression of a dinoflagellate iron-superoxide dismutase. *J. Biol. Chem.,* 276:19989-19993.

Okamoto, O.K. and J.W. Hastings. 2003. Novel dinoflagellate circadian-clock genes identified through microarray analysis of a phase shifted clock. *J. Phycology,* 39:1-9.

Olson, R.J. and S.W. Chisholm. 1986. Effects of light and nitrogen limitation on the cell cycle of the dinoflagellate *Amphidinium carterae. J. Plankton Res.,* 8:785-793.

Orci, L., A. Perrelet, M. Ravazzola, F.T. Wieland, R. Schekman and J.E. Rothman. 1993. "BFA bodies": a subcompartment of the endoplasmic reticulum. *Proc, Natl, Acad, Sci, USA,* 90:11089-11093.

Osafune, T., A.Yokota, S. Sumida and E. Hase. 1990. Immunogold localization of Ribulose-1,5-bisphosphate Carboxylase with reference to pyrenoid morphology in chloroplasts of synchronized Euglena gracilis cells. *Plant Physiol.,* 92:802-808.

Osteryoung, K., K. Stokes, S. Rutherford, A. Percival and W. Lee. 1998.Chloroplast division in higher plants requires members of two functionally divergent gene families with homology to bacterial ftsZ. *Plant Cell,* 10:1991-2004.

Paasche, E., I. Bryceson, K. Tangen. 1984. Interspecific variation in dark nitrogen uptake by dinoflagellates. *J. Phycology,* 20:394-401.

Palmer, J.D. 1995. Rubisco rules fall; gene transfer triumphs. *Bioessays,* 17:1005-1008.

Palmer, J. D. and C. F. Delwiche. 1996. Second-hand chloroplasts and the case of the disappearing nucleus. *Proc. Natl. Acad. Sci. USA,* 93:7432 -7435.

Palmer, J.D. 2003. The symbiotic birth and spread of plastids: how many times and whodunit? *J. Phycol.,* 39:4-11.

Perret, E., J. Davoust, M. Albert, L. Besseau and M.O. Soyer-Gobillard. 1993. Microtubule organization during the cell cycle of the primitive eukaryote dinoflagellate *Crypthecodinium cohnii. J. Cell Sci.,* 104:639-651.

Peyroche, A., B. Antonny, S. Robineau, J. Acker, J. Cherfils and C.L. Jackson. 1999. Brefeldin A acts to stabilize an abortive ARF-GDP-Sec7 domain protein complex: involvement of specific residues of the Sec7 domain. *Mol. Cell.,* 3:275-285.

Pierce, J., T. Carlson and Williams, J. 1989. A cyanobacterial mutant requiring the expression of ribulose bisphosphate carboxylase from a photosynthetic anaerobe. *Proc. Natl. Acad. Sci. USA,* 86:5753-5757.

Pittendrigh, C.S. 1993.Temporal organization: reflections of a Darwinian clock-watcher. *Annu. Rev. Physiol.,* 55:16-54.

Pöggler, B., I. Balzer and R. Hardeland. 1991. Pineal hormone melatonin oscillates also in the dinoflagellate *Gonyaulax polyedra. Naturwissenschaften,* 78:268-269.

Prezelin, B. B., B.W. Meeson and B.M. Sweeney. 1977. Characterization of photosynthetic rhythms in marine dinoflagellates. *I. Pigmentation, photosynthetic capacity and respiration,* 60:384-687.

Presley, J.F., T.H. Ward, A.C. Pfeifer, E.D. Siggia, R.D. Phair and J. Lippincott-Schwartz. 2002. Dissection of COPI and Arf1 dynamics in vivo and role in Golgi membrane transport. *Nature,* 417:187-193.

Price, G.D., D. Sultemeyer, B. Klughammer, M. Ludwig and M.R. Badger. 1998. The functioning of the CO_2 concentrating mechanism in several cyanobacterial strains: a review of general physiological charachteristics, genes, proteins, and recent advances. *Can. J. Botany,* 76:973-1002.

Ramalho, C.B., J.W. Hastings, P. Colepicolo. 1995. Circadian oscillation of nitrate reductase activity in *Gonyaulax polyedra* is due to changes in cellular protein levels. *Plant Physiol.,* 107:225-231.

Raven, P. 1970. A multiple origin for plastids and mitochondria. *Science,* 169:641-646.

Rapoport, B. Jungnickel and U. Kutay. 1996. Protein transport across the eukaryotic endoplasmic reticulum and bacterial inner membranes, *Annu. Rev. Biochem.,* 65:271-303.

Renaud, F., E. Parisi, A. Capasso and P. D. Prisco. 1983. On the pole of serotonin and 5-methoxy-tryptamine in the regulation of cell division in sea urchin eggs. *Cortex Extracts*, 98:37-46.

Renn, S., J. Park, M. Rosbash, J. Hall and P.Taghert. 1999. A pdf neuropeptide gene mutation and ablation of pdf neurons each cause severe abnormalities of behavioral circadian rhythms in Drosophila. *Cell,* 99:791-802.

Rensing, L., W.R. Taylor, J. Dunlap and J.W. Hastings. 1980. The effects of protein synthesis inhibitors on the *Gonyaulax* clock II: the effect of cycloheximide on ultrastructural parameters *J. Comp. Physiol.,* 138:9-18.

Reumann, S., J. Davila-Aponte and K. Keegstra. 1999. The evolutionary origin of the protein-translocating channel of chloroplastic envelope membranes: identification of a cyanobacterial homolog. *Proc. Natl. Acad. Sci. USA,* 96:784-9.

Reumann, S. and K. Keegstra. 1999. The endosymbiotic origin of the protein import machinery of chloroplastic envelope membranes. *Trends Plant Sci.,* 4:302-307.

Ritzenthaler, C., A. Nebenfuhr, A. Movafeghi, C. Stussi-Garaud, L. Behnia, P. Pimpl, L.A. Staehelin and D.G. Robinson. 2002. Reevaluation of the effects of brefeldin A on plant cells using tobacco Bright Yellow 2 cells expressing Golgi-targeted green fluorescent protein and COPI antisera. *Plant Cell,* 14:237-61.

Rizzo, P. 1991. The enigma of the dinoflagellate chromosome. *J. Protozool.,* 38:246-252.

Roenneberg, T., G.N. Colfax and J.W. Hastings. 1989. A circadian rhythm of population behavior in *Gonyaulax polyedra. J. Biol. Rhythms,* 4:201-216.

Roenneberg, T. and J. Hastings. 1992. Cell movement and pattern formation in *Gonyaulax polyedra*. In: Rensing L, editor. *Oscillations and Morphogenesis*. New York: Marcel Dekker.

Roenneberg, T. and D. Morse. 1993. Two circadian clocks in a single cell. *Nature,* 362:362-364.

Roenneberg, T. and J. Rehman. 1996. Nitrate, a nonphotic signal for the circadian system. *FASEB J.*, 10:1443-1447.

Roenneberg, T. and M. Mittag. 1996. The circadian program of algae. *Cell Dev. Biol.,* 7:753-763.

Roenneberg, T. and R.G. Foster. 1997. Twilight times: light and the circadian system. *Photochem. Photobiol.,* 66:549-561.

Roenneberg, T. and M. Merrow. 2001. Circadian systems: different levels of complexity. *Philos. Trans. R. Soc. Lond B. Biol. Sci.,* 356:1687-1696.

Rossini, C., W. Taylor, T. Fagan and J.W. Hastings. 2003. Lifetimes of mRNAs for clock regulated proteins in a dinoflagellate. *Chronobiol. Int.,* 20:963-976.

Rowan, R., S.M. Whitney, A. Fowler and D. Yellowlees. 1996. Rubisco in marine symbiotic dinoflagellates: form II enzymes in eukaryotic oxygenic phototrophs encoded by a nuclear multigene family. *Plant Cell,* 8:539-553.

Saba-El-Leil, M., S. Rivard, D. Morse and M. Cappadocia. 1994. The S11 and S13 self incompatibility alleles in *Solanum chacoense* Bitt. are remarkably similar. *Plant Mol. Biol.,* 24:571-583.

Samuelsson, G., B. M. Sweeney, H. A. Matlick and B. B. Prezelin. 1983. Changes in photosystem II account for the circadian rhythm in photosynthesis in *Gonyaulax polyedra. Plant Physiol.,* 73:329-331.

Schekman, R. and L. Orci. 1996. Coat proteins and vesicle budding. *Science,* 271:1526-1533.

Scheving, L.E. and F. Halberg. 1980. Chronobiology: Principles and applications to shifts in schedules. Sijthoff & Nordhoff, Netherlands.

Schnell D.J. and G. Blobel. 1993. Identification of intermediates in the pathway of protein import into chloroplasts and their localization to envelope contact sites. *J. Cell Biol.,* 120:103-15.

Schnell, D.J., F. Kessler and G. Blobel. 1994. Isolation of components of the chloroplast protein import machinery. *Science,* 266: 1007-12.

Schnell, D.J. and D.N. Hebert. 2003. Protein translocons: multifunctional mediators of protein translocation across membranes. *Cell,* 112:491-505.

Schiff, J.A., S.D. Schwartzbach, T. Osafune and E. Hase. 1991. Photocontrol and processing of LHCP II apoprotein in Euglena: possible role of Golgi and other cytoplasmic sites. *J. Photochem. Photobiol. B.,* 11:219 -236.

Schmitter, R. 1971. The fine structure of *Gonyaulax polyedra*, a bioluminescent marine dinoflagellate. *J. Cell Sci.,* 9:147-173.

Schopf J.W.1993. Microfossils of the Early Archean Apex chert: new evidence of the antiquity of life, *Science,* 260:640-6.

Schwartzbach, S.D., T. Osafune and W. Loffelhardt. 1998. Protein import into cyanelles and complex chloroplasts. *Plant Mol. Biol.,* 38:247-63.

Seliger, H.H., W.H. Biggley and E. Swift. 1969. Absolute values of photon emission from the marine dinoflagellates *Pyrodinium bahamense*, *Gonyaulax polyedra* and *Pyrocystis lunula*. *Photochem. Photobiol.,* 10:227-232.

Serafini, T., L. Orci, M. Amherdt, M. Brunner, R.A. Kahn and J.E. Rothman. 1991. ADP-ribosylation factor is a subunit of the coat of Golgi-derived COP-coated vesicles: a novel role for a GTP-binding protein. *Cell,* 67:239-53.

Sharples, F., P. Wrench, K. Ou and R. Hiller. 1996. Two distinct forms of the peridinin-chlorophyll a-protein from Amphidinium carterae. *Biochim. Biophys. Acta,* 1276:117-123.

Shearman, L., S. Sriram, D. Weaver, E. Maywood, I. Chaves, B. Zheng, K. Kume, C.Lee, G. van der Horst, M. Hastings and S. Reppert. 2000. Interacting molecular loops in the mammalian circadian clock. *Science,* 288:1013-1019.

Skop, A.R., D. Bergmann, W.A. Mohler and J.G. White. 2001. Completion of cytokinesis in C. elegans requires a brefeldin A-sensitive membrane accumulation at the cleavage furrow apex. *Curr Biol.,* 11:735-746.

Sogin, M.L., H.G. Morrison, G. Hinkle and J.D. Silberman. 1996. Ancestral relationships of the major eukaryotic lineages. *Microbiologia,* 12:17-28.

Soll, J. 2002. Protein import into chloroplasts. *Curr. Opin. Plant Biol.,* 5:529-35.

Spector, D., A. Vasconcelos and R. Triemer. 1981. DNA duplication and chromosome structure in the dinoflagellates. *Protoplasma.,* 105:185-195.

Spector, D., editor. 1984. *Dinoflagellates*. New York: Academic Press;

Stiller, J.W. and B.D. Hall.1998. Sequences of the largest subunit of RNA polymerase II from two red algae and their implications for rhodophyte evolution, *J. Phycol.,* 34:857-864.

Stiller, J.W., D.C. Reel and J.C. Johnson. 2003. A single origin of plastids revisited: convergent evolution in organellar genome content. *J. Phycol.,* 39:95-105.

Strub, A., J.H. Lim, N. Pfanner and W. Voos. 2000. The mitochondrial protein import motor. *Biol. Chem.,* 381:943 -949.

Sulli, C. and S.D. Schwartzbach. 1996. A soluble protein is imported into *Euglena* chloroplasts as a membrane-bound precursor. *Plant Cell,* 8:43 -53.

Sulli, C., Z. Fang, U. Muchhal and S.D. Schwartzbach. 1999. Topology of Euglena chloroplast protein precursors within endoplasmic reticulum to Golgi to chloroplast transport vesicles. *J. Biol. Chem.,* 274:457 -463.

Summer, E.J. and K. Cline. 1999. Red bell pepper chromoplasts exhibit in vitro import competency and membrane targeting of passenger proteins from the thylakoidal sec and

DeltapH pathways but not the chloroplast signal recognition particle pathway. *Plant Physiol.,* 119:575-84.

Sweeney, B.M. and J.W. Hastings. 1957. Characteristics of the diurnal rhythm of luminescence in *Gonyaulax polyedra. J. Cellular Comp. Physiol.,* 49:115-128.

Sweeney, B.M. and J.W. Hastings. 1958. Rhythmic cell division in populations of *Gonyaulax polyedra. J. Protozool.,* 5:217-224.

Sweeney, B.M. 1960.The photosynthetic rhythm in single cells of *Gonyaulax polyedra. Cold Spring Harbor Symp. Quan. Biol.,* 25:145-148.

Sweeney B.M. and J.W. Hastings, editors. 1961. Diurnal, tidal and lunar rhythms in the algae. N.Y.: Academic Press.

Sweeney B.M. and S.I. Folli. 1984. Nitrate deficiency shortens the circadian period in *Gonyaulax. Plant Physiol.,* 75:242-245.

Tarricone, C., B. Xiao, N. Justin, P.A. Walker, K. Rittinger, S.J. Gamblin and S.J. Smerdon. 2001. The structural basis of Arfaptin-mediated cross-talk between Rac and Arf signalling pathways. *Nature,* 411:215-219.

Taylor, W., T. Krasnow, J.C. Dunlap, H. Broda, and J.W. Hastings. 1982a. Critical pulses of anisomycin drive the circadian oscillator in Gonyaulax towards its singularity. *J. Comp. Physiol B.,* 148:11-25.

Taylor, W., S. Wilson, R.P. Presswood and J.W. Hastings.1982b. Circadian rhythm data collection with the Apple II microcomputer. *J. Interdiscipl. Cycle Res.,* 13:71-79.

Takahashi, J.S., J.M. Kornhauser, C. Koumenis and A. Eskin. 1993. Molecular approaches to understanding circadian oscillations. *Annu. Rev. Physiol.,* 55:729-753.

Techel, D., E. Chuang, D.H. Lee, J. Comolli and J.W. Hastings. 1996. Changes in the ultrastructural localization of mRNA for a circadian regulated protein. *Mol. Mar. Biol. Biotechnol.,* 5:241-248.

Thorsness P.E. and T.D. Fox. 1990. Escape of DNA from mitochondria to the nucleus in Saccharomyces cerevisiae. *Nature,* 346:376-9.

Tomitani, A., K. Okada, H. Miyashita, H.C. Matthijs, T. Ohno and A. Tanaka.1999. Chlorophyll b and phycobilins in the common ancestor of cyanobacteria and chloroplasts, *Nature,* 400:159-62.

Triemer, R. and L. Fritz, editors. 1984. *Cell cycle and mitosis.*

van Dooren, G.G., R.F. Waller, K.A. Joiner, D.S. Roos and G.I. McFadden. 2000. Traffic jams: protein transport in *Plasmodium falciparum*. *Parasitol Today,* 16:421-7.

van Dooren, G.G., S.D. Schwartzbach, T. Osafune and G. I. McFadden. 2001. Translocation of proteins across the multiple membranes of complex plastids. *Biochim. Biophys. Acta.,* 1541:34 -53.

Van de Peer, Y., S.A. Rensing, U.G. Maier and R. De Wachter. 1996. Substitution rate calibration of small subunit ribosomal RNA identifies chlorarachniophyte endosymbionts as remnants of green algae. *Proc. Natl. Acad. Sci. USA,* 93:7732-6.

Van de Peer, Y., S.L. Baldauf, W.F. Doolittle and A. Meyer. 2000. An updated and comprehensive rRNA phylogeny of (crown) eukaryotes based on rate-calibrated evolutionary distances. *J Mol Evol.,* 51:565-76.

Van den Berg, B., W.M. Clemons, Jr., I. Collinson, Y. Modis, E. Hartmann, S.C. Harrison and T.A. Rapoport . 2004. X-ray structure of a protein-conducting channel. *Nature,* 427:36-44

Voelker, R. and A. Barkan. 1995. Two nuclear mutations disrupt distinct pathways for targeting proteins to the chloroplast thylakoid. *Embo J.,* 14:3905-14.

Vogel, H., S. Fischer and K. Valentin. 1996. A model for the evolution of the plastid sec apparatus inferred from secY gene phylogeny. *Plant Mol. Biol.,* 32:685-692.

von der Heyde, F., A. Wilkens and L. Rensing. 1992. The effects of temperature on the circadian rhythms of flashing and glow in *Gonyaulax polyedra*: are the two rhythms controlled by two oscillators? *J. Biol. Rhythms,* 7:115-123.

Vothknecht, U. C. and J. Soll. 2000. Protein import: the hitchhikers guide into chloroplasts. *Biol. Chem.,* 381:887-897.

Walker, M.B., L.M. Roy, E. Coleman, R. Voelker and A. Barkan. 1999. The maize tha4 gene functions in sec-independent protein transport in chloroplasts and is related to hcf106, tatA, and tatB. *J. Cell Biol.,* 147:267-76.

Wallas, T.R., M.D. Smith, S. Sanchez-Nieto and D.J. Schnell. 2003. The roles of toc34 and toc75 in targeting the toc159 preprotein receptor to chloroplasts. *J. Biol. Chem.,* 278: 44289-97.

Waller, R.F., P.J. Keeling, R.G. Donald, B. Striepen, E. Handman, N. Lang-Unnasch, A.F. Cowman, G.S. Besra, D.S. Roos and G.I. McFadden. 1998. Nuclear-encoded proteins target to the plastid in *Toxoplasma gondii* and *Plasmodium falciparum*. *Proc. Natl. Acad. Sci. USA,* 95:12352-7.

Waller, R.F., M.B. Reed, A.F. Cowman and G.I. McFadden. 2000. Protein trafficking to the plastid of *Plasmodium falciparum* is via the secretory pathway. *EMBO J.,* 19:1794 - 1802.

Wastl, J. and U.G. Maier. 2000. Transport of proteins into cryptomonads complex plastids. *J. Biol. Chem.,* 275:23194 -23198.

Wever, R. 1979. *The circadian System of man.* Berlin Heidelberg New York: Springer;

Whitney, S. and T. Andrews. 1998. The CO2/O2 specificity of single-subunit ribulose-bisphosphate carboxylase from the dinoflagellate *Amphidinium carterae. Aust. J. Plant Physiol.,* 25:131-138.

Whitney, S. and D.Yellowlees. 1995. Preliminary investigations into the structure and activity of ribulose bisphosphate carboxylase from two photosynthetic dinoflagellates. *J. Phycol.,* 31:138-146.

Widder, E. and J. Case. 1982. Distribution of subcellular bioluminescence sources in a dinoflagellate *Pyrocystis fusiformis. Biol. Bull.,* 162:423-428.

Widder, E.A. and J.F.Case. 1982. Luminescent microsource activity in bioluminescence of the dinoflagellate, *Pyrocystis fusiformis. J. Comp. Physiol.,* 145:517-527.

Wilson, R.J., P.W. Denny, P.R. Preiser, K. Rangachari, K. Roberts, A. Roy, A. Whyte, M. Strath, D.J. Moore, P.W. Moore, et al. . 1996. Complete gene map of the plastid-like DNA of the malaria parasite *Plasmodium falciparum. J. Mol. Biol.,* 261:155 -172.

Wilson, T. and J.W. Hastings. 1998. Bioluminescence. *Annu. Rev. Cell Dev. Biol.,* 14:197-230.

Wolter, F.P., C.C. Fritz, L. Willmitzer, J. Schell and P.H. Schreier. 1988. rbcS genes in Solanum tuberosum: conservation of transit peptide and exon shuffling during evolution. *Proc. Natl. Acad. Sci. USA,* 85:846-50.

Yamazaki, A.K. and D. Kamykowski. 2000. A dinoflagellate adaptive behavior model: response to internal biochemical cues. *Ecological Modelling,* 134:59-72.

Yoon, H.S., J.D. Hackett and D. Bhattacharya. 2002. A single origin of the peridinin- and fucoxanthin-containing plastids in dinoflagellates through tertiary endosymbiosis. *Proc. Natl. Acad. Sci. USA,* 99:11724 -11729.

Yoon, H.S., J.D. Hackett, C. Ciniglia, G. Pinto and D. Bhattacharya. 2004. A molecular timeline for the origin of photosynthetic eukaryotes. *Mol. Biol. Evol.*, 21:809-18.

Zaslavskaia, L.A., J.C. Lippmeier, P.G. Kroth, A.R. Grossman and K.E. Apt. 2000. Transformation of the diatom *Phaeodactylum tricornum* (Bacillariophyceae) with a variety of selectable marker and reporter genes. *J. Phycol.,* 36:79-386.

Zhang, Z., B.R. Green and T. Cavalier-Smith. 1999. Single gene circles in dinoflagellate chloroplast genomes. *Nature,* 400:155-159.

Zhang, Z., B.R. Green and T. Cavalier-Smith. 2000. Phylogeny of ultrarapidly evolving dinoflagellate chloroplast genes: a possible common origin for sporozoan and dinoflagellate plastids. *J. Mol. Evol.,* 51:26-40.

Zhang, H. and S. Lin. 2003. Complex gene structure of the form II Rubisco in the dinoflagellate *Prorocentrum minimum* (Dinophyceae). *J. Phycol.,* 39:1160-1171.

Zhao, B., C. Schneid, D. Iliev, E.M. Schmidt, V. Wagner, F. Wollnik and M. Mittag. 2004. The circadian RNA-binding protein CHLAMY1 represents a novel type heteromer of RRM and KH-containing subunits. *Eukaryotic Cell,* 3:815-825.